University of West Bohemia
Faculty of Electrical Engineering

DISSERTATION

Cooperative Reception of Small Satellites' Signals Based on Diversity Combining

Mr. Haidar Al-Anbagi **Pilsen, 2023**

FACULTY OF ELECTRICAL
ENGINEERING
UNIVERSITY OF WEST BOHEMIA

Dissertation

to earn the academic degree Ph.D. in the field

Electrical Engineering

Mr. Haidar Al-Anbagi

Optimization of New Generations Communication, Broadcasting, and IoT Networks

Supervisor: Ing. Ivo Veřtát, Ph.D.

Date of the state doctoral examination: 30/06/2022
Date of submission of work: 27/10/2023

Declaration

I declare that I have elaborated the dissertation thesis individually and have used sources which I cite and list in the bibliography. In the submitted scientific work, the usual scientific procedures are used.

Pilsen, 27/10/2023

signature

Mr. Haidar Al-Anbagi

Acknowledgments

I would like to express my gratitude to the creator of this universe for the way we live together, love each other, and continuously learn from others. To live and enjoy my study life no matter how difficult the obstacles were, was indeed a reflection of the great support of kind people to reach my goals. My Ph.D. journey started with an eagerness to learn and achieve what I was hoping for. Without the guidance and worthy support of my supervisor, the love and prayers of my family and friends, and the great learning environment at the University of West Bohemia, this journey could not have gone this far.

I would like to deeply acknowledge my supervisor, Dr. Ivo Veřtát, for his kind and sincere academic guidance with endless support during my study. I admire his knowledge and supervision style throughout this work. His valuable comments and suggestions were very fruitful in enriching the work's scientific contribution, broadening my vision, and making my goals reachable. My gratitude also extends to all the professors whom I have had the pleasure to study and learn from during my study.

I am truly grateful to Prof. Susanne Hipp for her thoughtful comments and recommendations on this dissertation during my internship at OTH Regensburg, Germany.

My extreme gratitude goes to the kindest mother and father, most supportive and lovely wife and daughters, most sincere siblings, and my lovely American family. Your prayers and support were deeply felt and appreciated.

To my best friends, the cooperative faculty staff, and the great people whom I met here in Pilsen, your role in this study journey is invaluable. My family and I are thankful for the help and support we have received from this great community.

My last appreciation goes to the great people in healthcare field for their sacrifices while being in the front lines against Covid-19 pandemic. Their duties in curing patients, preventing others from infection, and developing vaccines and related research were priceless. The contributions of such heroes helped the community remain united despite how severe and devastating the consequences of the pandemic were.

Project leader's statement

I declare that within the SGS-2021-005: Research, development, and implementation of modern electronic and information systems project, in which this dissertation thesis was elaborated, presented results were achieved. The student participated in these results by 100%.

Pilsen, date

……
signature

Abstract

Internet of Things (IoT) networks connect countless devices in endless daily life applications. However, current IoT coverage is not yet ubiquitous to the less inhabited and harsh environments such as oceans, forests, mountains, poles, and deserts. Accordingly, for an omnipresent coverage of the future Sixth Generation (6G), satellites must be integrated into terrestrial IoT networks. Small satellites in the Low Earth Orbit (LEO) are very popular nowadays and have already attracted attention towards such integration. However, the size constraints of small satellites impose limited transmitting power and tiny antennas onboard. Consequently, weak signals and higher outages are more probable at the receiving Ground Station (GS). Therefore, the GS must utilize high gain directive antennas with complex and expensive steering resources to collect such weak signals via a single radio link. This traditional communication scheme can track only one satellite at a time with more vulnerability to outages resulting from possible severe signal degradations or from sudden steering engine failures. To contribute to a successful integration of the popular but restricted small satellites into the future 6G ubiquitous IoT networks, this work presents a GS-based solution through a cooperative reception scheme in which diversity combining is utilized. The theoretical part of this work structured, modeled, and simulated the suggested cooperative scheme and developed a simple yet efficient combining method. The results of the simulated model revealed a significant reduction in the Bit Error Rate (BER) for a group of GSs when working in a diversity mode compared to the conventional single site mode. To validate the proposed concept, this dissertation carried out a real deployment of the cooperative reception scheme in combining real small satellites' signals. According to the experimental findings, if multiple GSs worked cooperatively in a diversity mode and shared their received streams, they could generate a combined version that was always better than any other individually received stream. Indeed, the endorsed cooperative reception assured a significant reduction in BER, decreased probability of outages, and meanwhile enabled the simultaneous tracking of multiple satellites. The achieved diversity gain is promising enough to even trigger the idea of replacing the current expensive directive receiving antennas and their complex steering resources with much more affordable omnidirectional ones.

Keywords

Cooperative reception, Diversity combining, Receive diversity, Software defined radio (SDR), SIMO, Satellite Internet of Things (SIoT), Small satellites, Virtual ground station.

Abbreviations

Abbreviation	Full Text
6G	Sixth Generation
AFCS	Analog Feedback Communication System
ARQ	Automatic Repeat Request
AWGN	Additive White Gaussian Noise
BER	Bit Error Rate
BFSK	Binary Frequency Shift Keying
BCH	Bose–Chaudhuri–Hocquenghem
BPSK	Binary Phase Shift Keying
CRC	Cyclic Redundancy Check
ED	Euclidean Distance
EGC	Equal Gain Combining
EIRP	Effective Isotropic Radiated Power
FEC	Forward Error Correction
FSO	Free Space Optical
GEO	Geostationary Earth Orbit
GS/GSs	Ground Station/Ground Stations
IoT/ SIoT	Internet of Things/ Satellite Internet of Things
LEO	Low Earth Orbit
LDPC	Low-density Parity Check
LNA	Low Noise Amplifiers
MEO	Medium Earth Orbit
MIMO/MU-MIMO	Multiple-input Multiple-output/ Multi-user Multiple-input Multiple-output
MISO	Multiple-input Single-output
ML	Maximum Likelihood
MRC	Maximal Ratio Combining
NVIS	Near Vertical Incidence Skywave
NOE/ NOEs	Number of Error/ Number of Errors
NOMA	Non-orthogonal Multiple Access
NORAD	North American Aerospace Defense Command
OBP	Onboard Processing
OFDM	Orthogonal Frequency Division Multiplexing
PDF/ PMF	Probability Density Function/ Probability Mass Function
QoS	Quality of Service
Rx/Tx	Receiver/Transmitter
SatNOGS	Satellite Networked Open Ground Station
SC	Selection Combining
SP	Signal Processing
SINR/ SIR	Signal-to-interference Plus Noise Ratio/ Signal to Interference Ratio
SNR	Signal to Noise Ratio
SDR	Software Defined Radio
SIMO	Single-input Multiple-output
SISO	Single-input Single-output
TLE	Two-line-element
UHF	Ultra-High Frequency
VHF	Very High Frequency
UWA	Underwater Acoustic
UWOC	Underwater Optical Communication
VGS	Virtual Ground Station

Appendixes

Appendix A: MATLAB script to simulate a reception system based on a conventional SISO structure and analyze its performance versus E_b/N_o and bit rate.

Appendix B: MATLAB script to simulate a reception system based on a SIMO structure and apply the developed post-detection combining.

Appendix C: MATLAB script to simulate a reception system based on a SIMO structure and apply the developed post-detection combining along with suggested further improvement techniques.

Appendix D: MATLAB script to simulate a reception system based on a SIMO structure and apply the developed pre-detection combining.

Appendix E: MATLAB script to implement **Experiment A** to combine the best detected match of each identifier from five observations.

Appendix F: MATLAB script to implement **Experiment B** to combine all detected Sync-Word from five observations in a time manner.

Appendix G: MATLAB script to visualize the received obdervations in a time manner and identify the earliest and the latest ones as well as the total satellite visibility time to all GSs.

Appendix H: MATLAB script to implement **Experiments C** and **D** to combine all detected identifiers from six and nine observations in a time manner.

Content

1 Introduction

Internet of Things (IoT) networks have witnessed rapid developments in a wide range of daily life applications and services. In parallel, miniaturized satellites have also developed recently to become much more affordable to manufacture, launch, and deploy creating cost-effective means to access and explore space. These concurrent developments could be exploited towards a future ubiquitous IoT coverage from space by miniaturized satellites to accommodate all areas including uninhabited and harsh environments. The core of this dissertation aims to deal with improving the reception quality of the collected, stored, and retransmitted sensors data from these popular but restricted small satellites by the relevant Ground Station (GSs). The efficient offloading of onboard data by GSs will therefore contribute to a successful integration of the small satellites into the future IoT networks.

Section 1.1 introduces the current terrestrial IoT networks, where they lack coverage, why future IoT networks must embrace satellites, and finally why the popular but restricted small satellites already attracted the attention in this future integration. In addition, **Section 1.2** and **Section 1.3** respectively provide general descriptions about small satellites and their relevant GSs.

1.1 Current terrestrial IoT networks and future satellite IoT

Current terrestrial IoT networks provide a variety of convenient services to countless users in urban and suburban areas. Billions of physical devices are massively interconnected through terrestrial IoT gateways to maintain such services. Examples of offered IoT employments are smart transportation [1, 2], automated agile agriculture [3], intelligent traffic flow estimation [4], and smart healthcare monitoring [5, 6]. However, the present IoT coverage does not yet include less inhabited and harsh environments like deserts, oceans, forests, mountains, and poles [7]. Meanwhile, these uncovered areas are still fertile ground for many investigations, environmental observations, a home for many inhabitants, and a part of the whole universe in case of natural disasters. This just emphasizes how vital the aimed inclusive IoT coverage is in accommodating these harsh but rich environments. From economic and practical perspectives, it may sound infeasible for the IoT service providers to cover such isolated areas by conventional terrestrial infrastructures. However, the need for these isolated areas to be explored, researched, monitored, and immediately responded to in case of supernatural events are encouraging reasons on why such inclusion in the IoT connectivity is deemed crucial. Consequently, the necessity of globally ubiquitous IoT

coverage has drawn the attention of service providers and researchers towards the satellites' engagement, giving a birth to the area named Satellite Internet of Things (SIoT) [7]. SIoT is full of promise to provide universal coverage with stable, consistent, and reliable services with no geographical limitations [8].

The architecture of a terrestrial IoT network for offloading sensors' data can be configured as depicted in **Figure 1** while the architecture of an SIoT network for offloading onboard sensors' data can be configured as in **Figure 2**. Observing both architectures, gives an insight into the idea that small satellites can function as gateways for the offloaded data from sensors in an SIoT network.

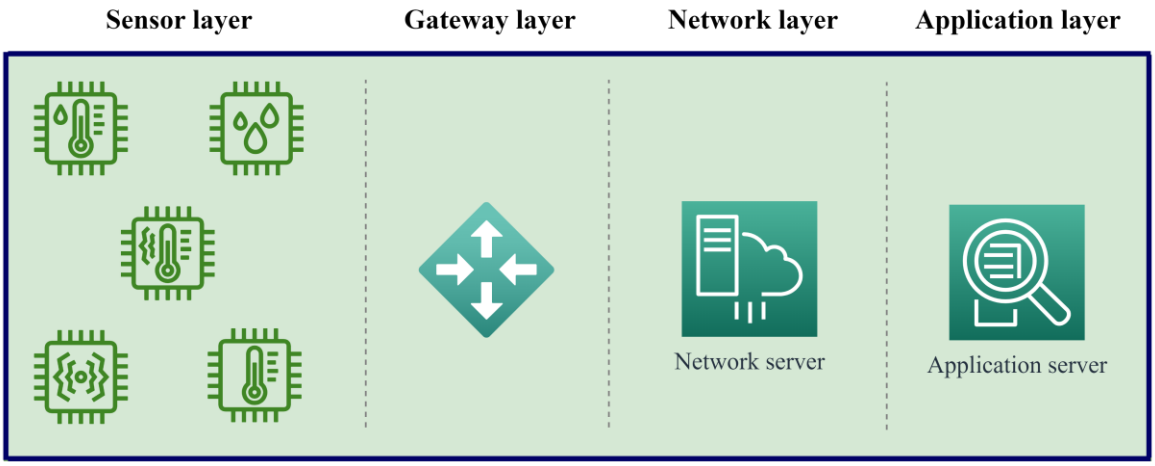

Figure 1. Terrestrial IoT network architecture.

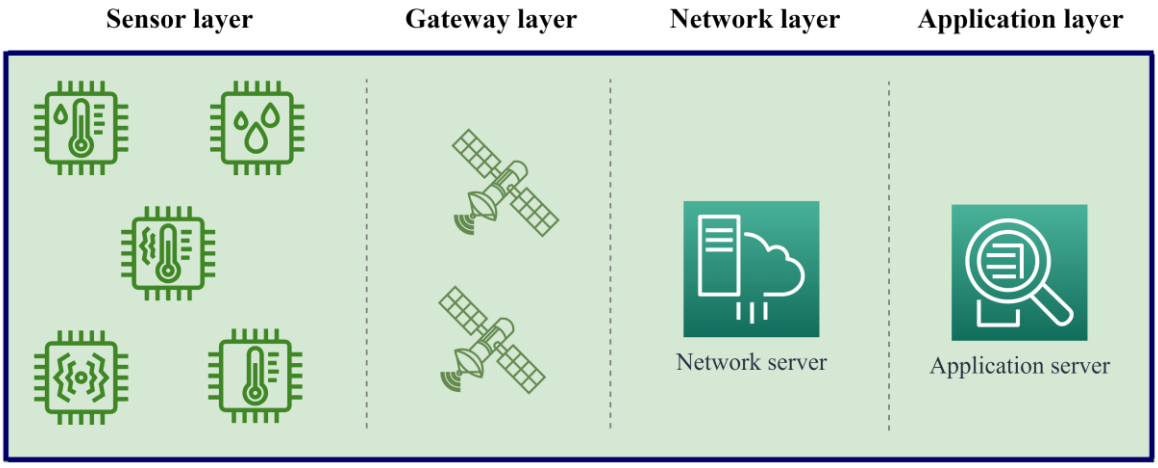

Figure 2. SIoT network architecture.

Apart from Medium Earth Orbit (MEO) and Geostationary Earth Orbit (GEO) satellites, Low Earth Orbit (LEO) satellites have received the attention of SIoT developers due to their attractive aspects [9]. LEO satellites have low altitudes, short latency, and low predictable path losses [10].

It is noteworthy that most of the recently launched LEO satellites are small ones designed with light weight, compact size, and most importantly they are more affordable to design, launch, and operate. The builders of small satellites have developed relatively fast manufacturing process providing a great opportunity for research groups and educational institutes to establish cost-effective private space missions. Concurrently, the recent development of ride-sharing launchers and reusable rockets has significantly reduced the cost to launch and deploy these small satellites. As a result, such attractive aspects of small satellites have made them very popular nowadays and hence future Sixth Generation (6G) systems seek the aimed ubiquitous IoT coverage through the integration of the popular but restricted small satellites into the terrestrial IoT networks.

1.2 General description of small satellites

Small satellites, which usually weight under 300 Kg, are sub-categorized into Micro, Nano, and Pico satellites ranging between 10-100 Kg, 1-10 Kg, and about 1 Kg, respectively. Besides weight, some other control factors, such as shape and size, can intervene to categorize a satellite. For instance, a cube-based shape of CubeSat platform is currently dominating in pico-, nano-, and microsatellite categories [11]. CubeSats were proposed for the first time in 1999 with a size of multiple U units, where 1U CubeSat is a cube of 10 cm a side, to help universities have their affordable and private space programs. This proposal has done so because many universities from all over the world currently have their space agendas running through CubeSats [12]. Examples of CubeSats configured based on different U units are illustrated in **Figure 3**.

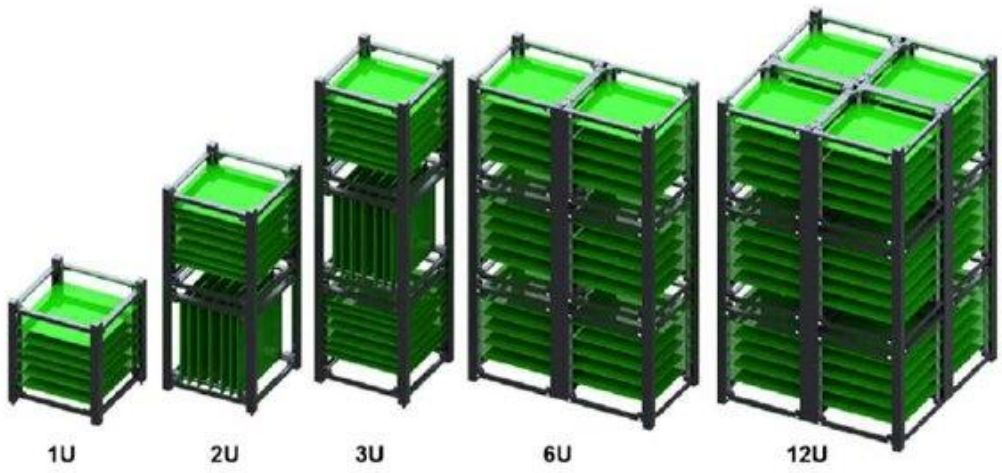

Figure 3. Different configurations of CubeSats [13].

Figure 4 shows the prototype of 1U CubeSat for the real satellite PilsenCUBE presented at the University of West Bohemia (UWB) in Pilsen, Czech Republic, while **Figure 5** and **Figure 6** respectively depict the Czech CubeSats VZLUSAT-1 and VZLUSAT-2. VZLUSAT-2 is a 3U CubeSat which was launched into space on the 26th of January 2022, whereas VZLUSAT-1 is a 2U CubeSat which was successfully launched on the 23rd of June 2017 [14].

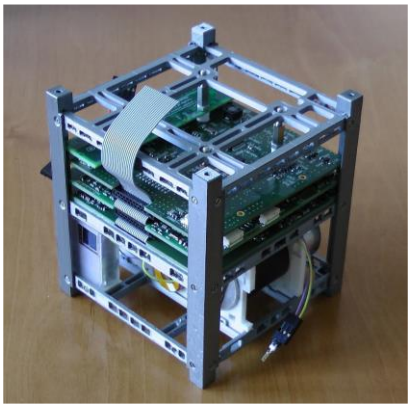

Figure 4. A prototype of the 1U Czech satellite PilsenCUBE.

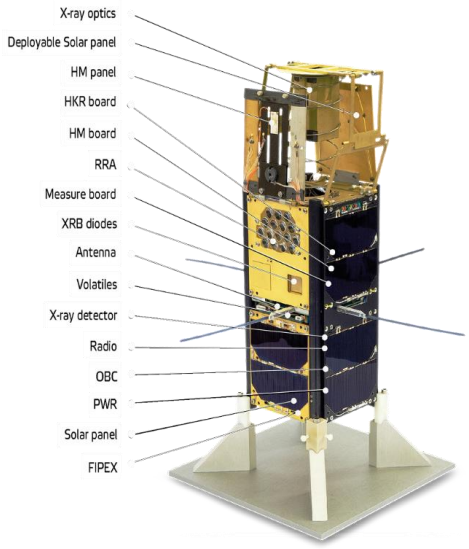

Figure 5. A prototype of the 2U CubeSat Czech satellite VZLUSAT-1.

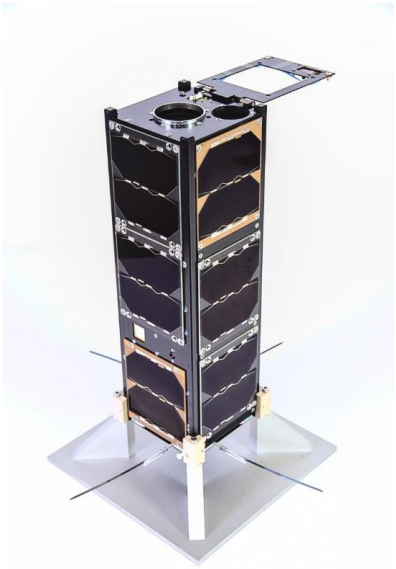

Figure 6. A prototype of the 3U CubeSat Czech satellite VZLUSAT-2.

The size restriction of such small satellites, however, implies the following limitations:

- Limited transmitted power of about 1 watt because of the limited surface area for solar panels and the cooling issue of the transmitters in vacuum condition.
- Limited data rates to few Kbps due to the link budget with limited antenna gains and transmission power.

- Low-gain antenna of about (2-3) dBi because of the dimension restrictions and in most cases of small satellites also due to the absence of precise attitude control system for pointing onboard antenna.
- High orbital speed so that the satellite orbits the earth several times a day which is attributed to the fact that small satellites are deployed in the LEO.
- High Doppler effect resulting from the high orbital speed in the LEO.
- Short communication window with the GS for the same previous reason.

Consequently, these limitations create a challenging reception task at the relevant GSs to collect and decode such anticipated weak signals.

1.3 General description of related ground stations

As a result of the limitations of small satellites, the receiving ground terminals experience higher levels of attenuations at the received signals with higher probability of communication outages. Therefore, the GSs of such small satellites from CubeSat category must deploy complex and expensive steering engines to precisely orient a high-gain directive antenna towards the satellite to establish a reliable single radio link, collect such weak signals, and demodulate the received data. This traditional single RF scheme, also known in the literature as Single-input Single-output (SISO), is highly vulnerable to outages when having severe signal degradations or with steering engine failures. In addition to the outages susceptibility, such system allows the tracking of only one satellite at a time. The operation frequency bands for these GSs are Ultra High Frequency (UHF), Very High Frequency (VHF), and S-band. These bands are highly affected by noise in certain regions compared to others as shown in **Figure 7**.

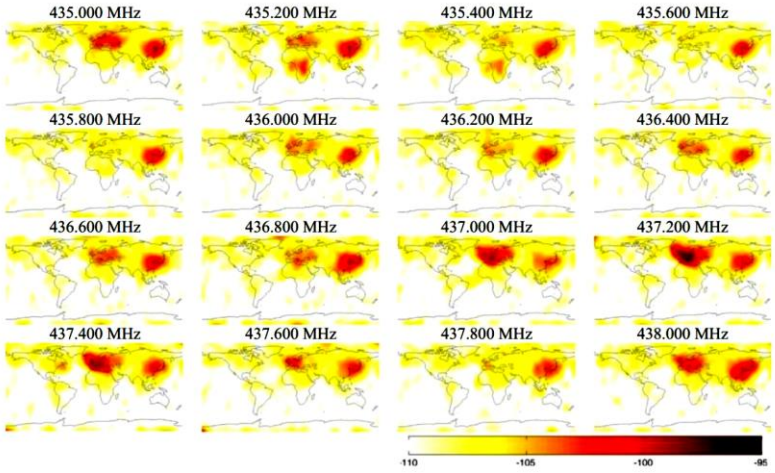

Figure 7. The frequency range (435-438) MHz has more levels of jamming in LEO orbits above certain areas than others [15]

To overcome the strong interference in the LEO, especially in the UHF and VHF bands, the GSs must afford an output power which generally ranges between a few tens of watts to several hundred watts.

When it comes to the antenna system of such GSs, complex and expensive mechanism for antenna steering is utilized for precisely orienting the receiving antenna towards the satellite. In addition to the outdoor rotation engine, other indoor steering equipment include rotator controller, rotator power supply, computer control, overload protection, remote diagnostics, and camera surveillance system. **Figure 8** demonstrates the outdoor steering engine mounted on a steel antenna mast while the indoor resources are depicted in **Figure 9**. **Figure 10** demonstrates the real antenna system of Pilsen's GS.

Figure 8. The outdoor steering engine mounted on antenna mast.

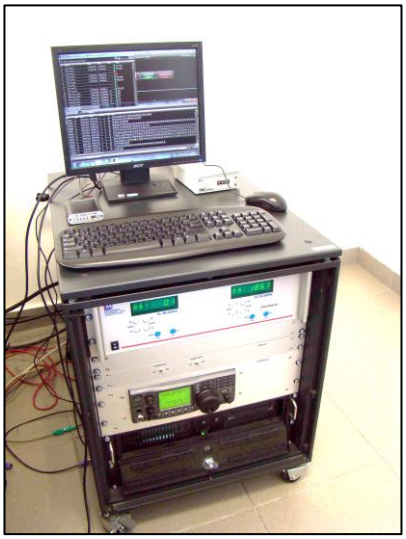

Figure 9. The complex and expensive indoor steering equipment [16].

Figure 10. The antenna system of Pilsen's GS, located at the University of West Bohemia.

Based on the description of the conventional GSs, they are considered complex ones with costly installation and maintenance processes. Good illustrative pictures in this context are presented in **Figures 11** and **12**.

Figure 11. An installation picture of the new Cal Poly's GS named "Friss" with four phased Yagi antenna to track LEO satellites at 437 MHz [17].

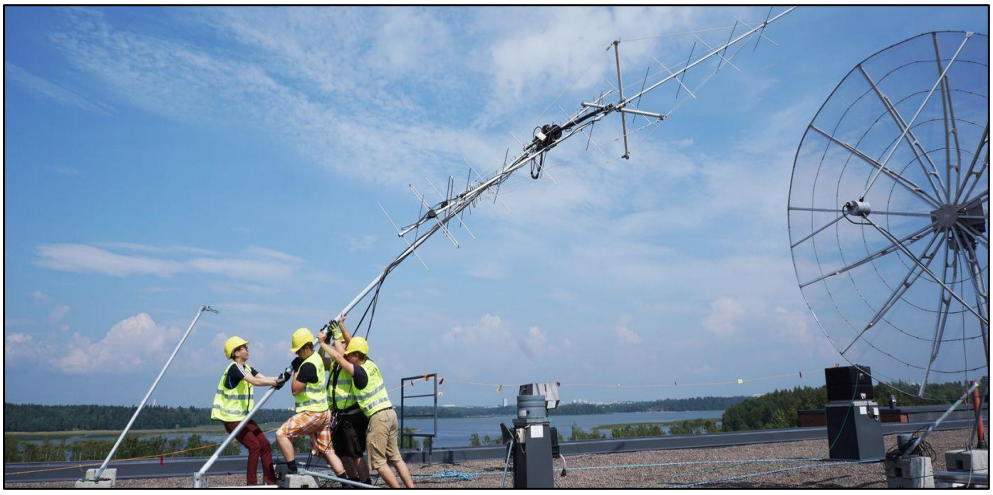

Figure 12. An illustrative installation picture posted by the operators of Aalto GS located on the roof of a campus building at Aalto University, Finland [18].

To contribute to a successful integration of the popular small satellites into the future IoT networks and to adopt a GS-based cheap solution, this work validates the concept of diversity combining in improving the reception quality of small satellites signals. The presented solution utilizes one of the available simple and public Software-defined Radios (SDR) GSs networks with predominant omnidirectional antennas to receive small satellites signals.

These public GSs networks such as **Sat**ellite **N**etworked **O**pen **G**round **S**tation (SatNOGS), SpyServer, OpenWebRx, and WebSDR do not yet work in a coordinated manner and do not perform any form of receive diversity combining. An example on how widely available these simple SDR-based GSs networks are, **Figure 13** depicts SatNOGS's network of the registered GSs around the world especially in Europe, United States of America, and Canada.

Figure 13. A global SatNOGS community of small GSs [19].

Simple omnidirectional GSs, like the one of SatNOGS's shown in **Figure 14**, offer multiple advantages such as low configuration and maintenance costs, simultaneous tracking of multiple satellites due to the omnidirectional pattern of the utilized antenna, wide digitized bandwidth by SDR, and the availability of large number of existing public receivers in networks like SatNOGS, AirSpy, and OpenWebSDR can create a good opportunity for small satellites developers to test and validate new theoretical concepts in the field.

Figure 14. An illustrative picture showing how simple the omnidirectional antenna system for SDR-based GS from the network of SatNOGS [19].

2 Theoretical background analysis

The current communication scheme between satellites and GSs is based on a point-to-point transmission, i.e., SISO communication scheme. However, in modern terrestrial communications, such as cellular networks, the diversity systems have become standard solutions to overcome the effects of the disturbances and boost the performance of such systems. Moreover, several concepts on how to exploit the benefits of cooperative communications are already applied in terrestrial and maritime IoT networks. Examples of deployed concepts are macrodiversity [20] and distributed antenna system [21]. Accordingly, these modern approaches can also fit into the application of improving communication with small satellites.

Section 2.1 of this chapter provides the analysis of the currently existing reception system of small satellites signals based on single GS. Then, **Section 2.2** emphasis the problem statements of the analyzed conventional reception structure. Possible solutions are briefly discussed in **Section 2.3**.

2.1 Conventional single ground station system analysis

In satellite communications, the radio link from the satellite, as a transmitter, to the GS, as a receiver, is referred to as downlink. One of the metrics to evaluate the link quality is the rate at which errors are detected at the receiver and that measure is known as the Bit Error Rate (BER) [22]. BER is simply the number of the falsely detected bits to the total number of transmitted bits during the observation time. Seeking for as low BER as possible, is the main objective of every digital communication link designer. However, different factors and challenges would face such designing procedure as it involves a comprehensive study about the communication channel, the surrounding environment, receiver resources, in addition to a compatible selection of a modulation scheme [23]. These considerations would consequently specify the required power at the transmitter to survive the propagation impairments and establish a reliable radio communication link with low BER [24]. This section is dedicated to carry out the simulation of the traditional single downlink communication system in addition to the analysis of its performance under the requirements of the new generations' communications. Its performance will indicate whether or not this traditional SISO link is in favour of the future communications trends. Such analysis will emphasise the motivations behind the contribution of this thesis. **Figure 15** visualizes the downlink between a satellite and a GS based on the conventional SISO structure.

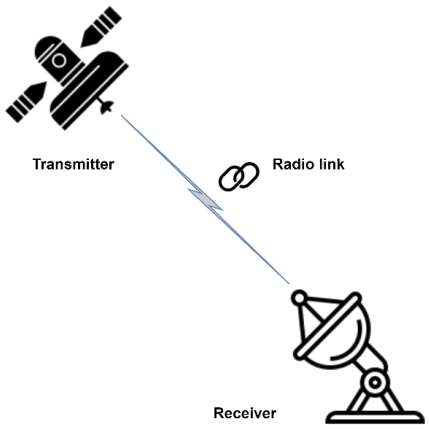

Figure 15. A downlink based on the traditional SISO configuration.

For calculating BER of the simulated downlink in this analysis, the channel is selected to be Additive White Gaussian Noise (AWGN), a commonly used channel model in satellite communications [25]. Meanwhile, the involved modulation scheme is chosen to be the Binary Frequency Shift Keying (BFSK), one of the basic modulations used by radio-amateur satellites. Such radio communication system utilizing a BFSK and considering an AWGN channel can be configured as in **Figure 16**.

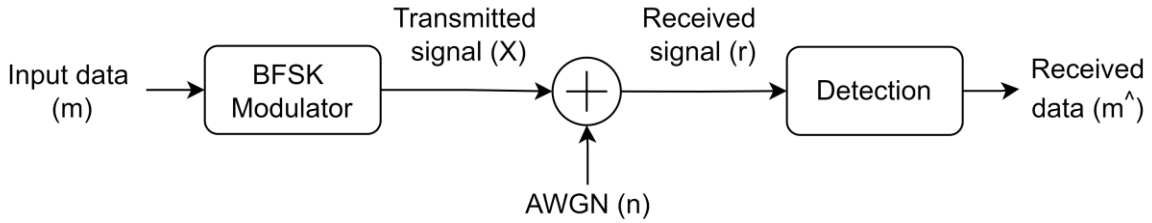

Figure 16. Satellite downlink's block diagram with traditional SISO configuration

The simulation procedure starts with streaming the input bits, i.e., the message (m), in a unipolar form of either 0 or 1. Then, because BFSK uses orthogonal signalling which maps input data into complex representations, an input 1 is mapped into 1 whereas input 0 is mapped into j. Therefore, the generated modulated signal (X) will be a complex signal with two possible representations, either (1+0j) or (0+1j), respectively representing inputs 1 and 0. These complex signals will be broadcasted from the satellite's antenna to the GS through the free space as a channel, which will be AWGN channel in this simulation. Through signal's propagation, noise will be added to the signal and because the transmitted signal is complex, the additive noise in the simulation will be complex as well. Hence, adding the complex noise (n) to the complex transmitted signal (X) will form the received signal (r) according to:

$$r = X + n \tag{2.1}$$

As mentioned earlier, the transmitted signal (X) has two representations and consequently we will have two possible states for the received signal (r) as follows:
For input 1, $X = (1 + 0\,j)$ and hence the corresponding received signal will be,

$$r = ((1 + n) + (0 + n)\,j) \tag{2.2}$$

Similarly, for input 0,

$$r = ((0 + n) + (1 + n)\,j) \tag{2.3}$$

That would create the detection hypothesis at the receiver to compare the real part to the imaginary part of the received signal and decide whether it is 1 if the real part is greater than the imaginary part, or 0 if the other way around. Thus, the detection hypothesis is:

$$\text{Real}(r) \underset{0}{\overset{1}{\gtrless}} \text{Imag}(r) \tag{2.4}$$

In orthogonal signaling like BFSK, the demodulator detects the received symbols based on the decision threshold as demonstrated in **Figure 17 (a)**. This figure gives an idea of how the false detection at the receiver, correspondingly the BER, is different from antipodal signaling schemes such as Binary Phase Shift Keying (BPSK) for the same signal quality shown in **Figure 17 (b)**, where E_b is the energy per bit.

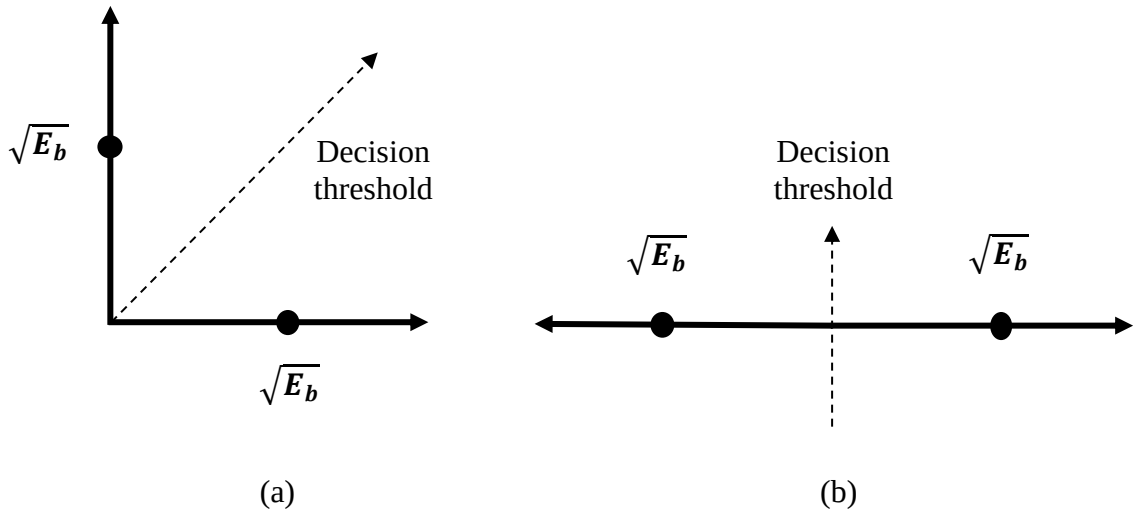

(a) (b)

Figure 17. Binary signal vectors with (a) orthogonal signaling (b) antipodal signaling.

MATLAB is used to simulate this system and evaluate the BER from the simulated model. To verify the simulation results, the theoretical BERs of the BFSK system are calculated using the Error Function (erfc) and Q function as stated in the following two formulas [26]:

$$\text{BER} = \frac{1}{2}\,\text{erfc}\left(\sqrt{\frac{E_b}{2N_o}}\right) \tag{2.5}$$

$$\text{BER} = Q\left(\sqrt{\frac{E_b}{N_o}}\right) \tag{2.6}$$

where (E_b/N_o) is the energy per bit to the noise power spectral density.

The implementation MATLAM script in **Appendix A** reflected pretty matched BER curves from simulation and theory as illustrated in **Figure 18** with the same expected behavior that the system performance is improved when increasing E_b/N_o, i.e., the BER decreases when increasing the transmission power.

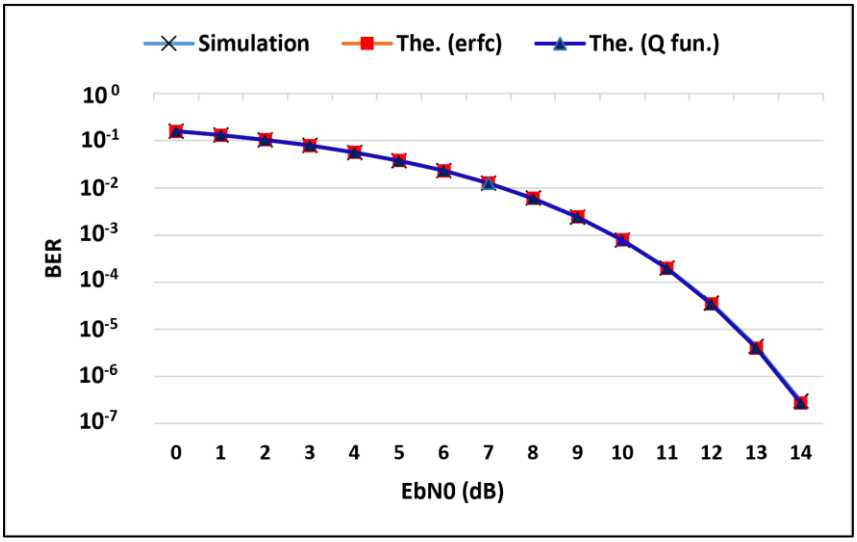

Figure 18. Simulation and theoretical (The.) BER curves for SISO-based downlink

In general, with limited transmission power, the BER is directly related to the signaling rate. The higher the bit rate, the more likely errors will occur and accordingly the higher BER due to the decrease in E_b/N_o [27].

Different signaling rates are tested in MATLAB simulation to calculate the BER of the system at each bit rate and see how the performance of the system would react to higher data bit rates. Doing so will indicate whether this traditional SISO configuration can still fulfill the high data rates requirements of the new generations of wireless communications. When observing the performance over different data rates while the signal power was fixed to achieve an E_b/N_o of 10 dB at 60 kbps, the resulting curve is presented in **Figure 19.**

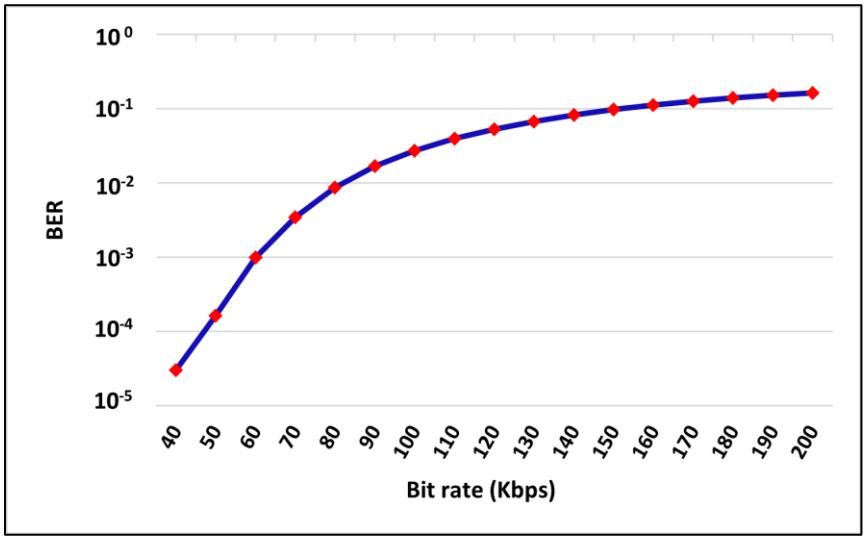

Figure 19. SISO-based downlink BER performance versus data rate

Based on **Figure 19**, the SISO system performance degrades and results into higher BER when increasing the data rate. Generally, this SISO link is designed for small satellites utilizing short packet-oriented transmissions with E_b/N_o equal to 10 dB and better, which gives an acceptable small packet error rate. Retransmission of packets is possible if needed when using Automatic Repeat Request (ARQ), Cyclic Redundancy Check (CRC), or Forward Error Correction (FEC) coding (e.g., Reed-Solomon block codes and convolutional codes).

Therefore, for the traditional single GS system configuration to function efficiently with lower BERs, we must either stream out at low signaling rates, increase the transmitted power, or deploy higher gain antennas. However, that would be totally impractical and against the requirements of new generations communications of high data rates signaling (to handle the role of space gateway for huge number of terrestrial IoT sensors) and hostile environments serving.

Moreover, small satellites have limited resources and hence increasing the transmission power is not an option for such a category of satellites. The third option to improve the BER is to deploy higher gain transmitting and receiving antennas. Doing so onboard small satellites leads to larger size satellites and higher power consumption by more complex attitude control system. On the other hand, higher gain receiving antenna at the GS requires more precise and mechanically robust steering system and yet causes the inability to track multiple satellites at a time. This is simply summarizing the fact of why SISO systems are not promising schemes to effectively fulfill the demands of the upcoming technology trends and hence alternative techniques are in need.

2.2 Addressing the research gap and problem statements

The simulation of the current reception system addresses a research gap in which the reception quality of small satellites signals must be improved. Meantime, the enormously growing number of small satellites in space also necessitates the efficient utilization of GSs, ideally with the possibility of tracking several satellites at once. This research gap can help the popular small satellites successfully integrate into the traditional terrestrial IoT networks for the future 6G ubiquitous SIoT networks. Accordingly, this dissertation contributes to a GS-based solution to improve the reception quality of small satellites' signals and yet this solution ensures simplicity, efficiency, scalability, and affordability.

In summary, the traditional scheme based on a single GS to receive small satellites signals has the following problems:

A. A conventional reception system based on a single GS is incapable of tracking multiple satellites simultaneously due to the narrow beamwidth of the steered high gain directional antenna. Consequently, the growing number of active small satellites always reflects an increased number of expensive GSs.
B. Increasing the transmission power improves the performance of such conventional reception systems. However, such a solution is deemed impractical for small satellites as they have size limitations and hence limited power resources and restricted capability of amplifier's cooling.
C. Signaling at high data rates increases the BER and degrades the system performance as shown in the system analysis. Therefore, such a conventional scheme cannot fulfill the aspirations of new generations of communications in exploiting high data rates with limited power to accommodate larger number of users.
D. A small satellite in the LEO, when becomes visible to its main GS, can establish a downlink to offload its data only once during a complete orbital period and for a short communication window [28]. Accordingly, to increase the download capacity, more than one GS around the world must be rented.
E. GSs must utilize expensive high-gain directive antennas with a complex steering mechanism to precisely orient the antenna towards the satellite when visible to establish a radio link with good signal quality and low BER.
F. Steering engines are mounted on the antenna mast outdoors, making them more prone to severe environmental conditions causing unexpected sudden mechanical failures.

G. Typical GSs for current small satellites, like CubeSats, have high probability of communication outages with unavoidable consequences when the transmitted signal experiences deep fade, strong interference from terrestrial sources, or when having sudden mechanical failures as expressed in F [29].
H. Another drawback of the traditional GSs is the fact that they, in most communications missions, use mainly the downlink and not necessarily the uplink in each of the satellite's passes because of asymmetric volume of uplink and downlink data. Though, it is still vital for these conventional GSs to build the costly infrastructure for the uplink including expensive power amplifier and power supply, cooling, RF filters, and Rx / Tx switching relays regardless of their inefficient utilization. This significantly increases the budget of assembling conventional GSs and yet inefficiently blocking the system capacity for the unbalanced downlink/uplink traffic.
I. The number of small satellites has doubled in only two years, recording more than 2000 active satellites and yet new expensive GSs must be built to avoid pass overlapping above each GS.
J. The conventional GSs have some other common sources of errors to consider such as antenna pointing, checking, rotator delay, the satellite predictor, mechanical vibrations of GS's antenna, Two-line-element (TLE) accuracy, and the reliability and lifespan of cables and connectors placed on the steerable antenna system.

2.3 Possible solutions

After addressing the research gap and emphasizing the main issues of the conventional reception scheme based on a single GS, this section navigates through some possible solutions on how to ensure adequate received signal quality, reach sufficient downlink capacity, effectively use GSs with the enormous increase in the number of small satellites, and manage the asymmetry in uplink/downlink data volume requirements.

2.3.1 Power control

In this technique, the transmitter's power is adjusted in accord with the attenuation level in the transmitted signal. Hence, the main idea of power control is to continuously change the power of the transmitted signal with respect to the degradation level that signal is suffering through its path. Therefore, the GS must send a control signal to the satellite requesting an increase in the Effective Isotropic Radiated Power (EIRP) to improve link quality [30]. Consequently, this technique can cause some capacity implications sending too many control signals between the satellite and the GSs to adjust their EIRP. However, according to the

characteristics of small satellites' amplifiers, they are designed to work in optimal operation point to keep the high energy efficiency with acceptable signal distortion and this solution causes an energy deficiency. In addition, expensive and capable GS with full Rx/Tx operation is required during the whole satellite pass to control the output power of the satellite transmitter and yet this concept does not allow an efficient use of the natural asymmetry in uplink/downlink data volume to optimize costs of GS network. Furthermore, small satellites have limited size and restricted power resources and therefore the concept of increasing the transmission power is in contrary to the operator's aspirations. For the mentioned reasons, this technique is not going to be considered in this dissertation.

2.3.2 Onboard processing

The concept of this solution is to reduce data volume or/and apply more powerful FEC coding for decreasing BER [31, 32]. This is done by Satellite Onboard Processing (OBP) where modern loss-less compression source coding methods are utilized to push the volume of data down. In addition, more advanced FEC approaches such as Low-density Parity Check (LDPC) codes [33], polar codes [34], Bose–Chaudhuri–Hocquenghem (BCH) codes [35], and concatenated codes [36] can be used to decrease the required E_b/N_o for maintaining an acceptable BER in comparison to currently used simple codes like Reed Solomon or convolutional codes. However, this technique will not be considered here because it requires processing modifications onboard the satellites, pushing up the computation power requirements available onboard small satellites with limited power and insufficient radiation protection of sensitive electronic systems. Moreover, it does not even support the possibility of simultaneous tracking of several satellites by one GS. Lastly, this approach requires a modification at the satellite side while this work is dedicated only for a solution that can be implemented at the GS.

2.3.3 Antenna beamwidth

Deploying higher gain antennas at GSs means lower BER, but also requires more precise and expensive mechanical steering system to handle the larger antenna size and weight. Furthermore, such a system with steerable antenna is unable to track multiple satellites simultaneously. On the other hand, deploying higher gain antennas onboard small satellites also improves the link quality and reduces BER. Nevertheless, it requires complex attitude control system with more power resources, demanding more energy consumption from the power-limited small satellites. Moreover, this solution prevents the usage of multiple GSs at the same time to back up the main GS in case of outages. Inversely, utilizing lower gain

antennas relaxes the requirements on satellites and on the GSs, enables the use of more GSs at the same time to back up the main one, or even enables the use of one GS for more satellites at the same time. However, these advantages will be on the price of increasing the BER. Phased antenna array with beamforming at GSs is also an option to improve the reception quality with the capability of tracking multiple satellites at once through multiple independent beams [37]. However, such antennas are extremely complex and expensive, making them applicable only for capable GSs at higher frequency bands (S, X, Ku, Ka).

2.3.4 Spatial diversity

Spatial diversity is a critical strategy to combat the consequences of signal's degradation issues by processing multiple copies of the same signal propagated through multiple independent channels [38]. This diversity can be achieved at the transmitter, receiver, or at both sides. A system with no diversity, i.e., single transmit antenna and single receive antenna is often referred to as SISO. A transmit diversity system would have multiple transmit antennas and one receive antenna and that is referred to as Multiple-input Single-output (MISO). On the other hand, the receive diversity system has single transmit antenna and multiple receive antennas, which is also known in the literature as Single-input Multiple-output (SIMO). Moreover, it is possible that one system can achieve transmit and receive diversities and that is called (MIMO), referring to Multiple-input Multiple-output antennas [26]. Since this work intends to find a solution that can be implemented at the GS side to improve the reception of small satellites' signals, the receive diversity is the right diversity technique to utilize. The receive diversity involves the transmission of the signal by one antenna (Tx antenna) and collecting multiple versions of the transmitted signal by multiple receiving antennas (Rx antennas) through multiple independent (uncorrelated) channels as illustrated in **Figure 20.**

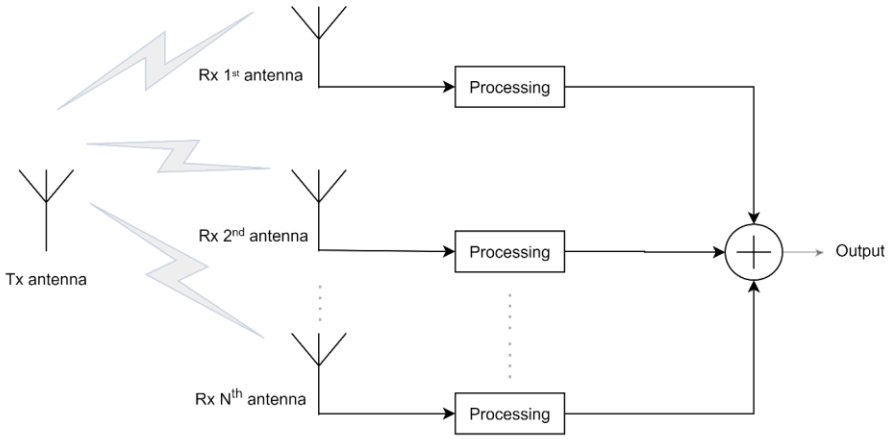

Figure 20. Receive diversity system configuration.

Receive diversity is an effective solution to improve the reception quality of small satellites' signals and yet neither power control nor any additional OBP is required from the small satellite. Employing a diversity-based reception system creates a diversity gain that can compensate for the missing gain in the link budget if the receiving current high-gain directive antenna with its complex steering resources is replaced by much affordable omnidirectional or sector antennas. These simple and cheap omnidirectional antennas enable the system to track multiple satellites and use natural asymmetry traffic of uplink/downlink through cheap Rx-only stations for the signal reception and reserve expensive full Rx/Tx-stations usage only when the uplink is required. Furthermore, the diversity-based system is scalable to involve more GSs if necessary to increase the diversity gain on demand. Excellent immunity to small satellite-to-GS communication outages is another advantage of the diversity approach if compared to the conventional single GS reception system.
Motivated by the analysis of the current reception system based on single GS, this dissertation aims to answer the question whether a cooperative reception scheme of multiple GSs with diversity combining can improve the reception of small satellites downlink signals or not and whether such a network of cooperative GSs can be used for simultaneous tracking of multiple small satellites at a time in addition to the other advantages mentioned earlier.

To achieve the aimed purpose, the rest of this thesis is structured as follows: **Chapter 3** addresses the objectives of this work; **Chapter 4** depicts the simulation of the proposed cooperative reception methodology, develops the combining algorithm of two options, pre-detection or post-detection combining point, and lastly provides the setups of the four deployment experiments to combine real small satellite signals; **Chapter 5** presents and discusses the simulation and the deployment results of the suggested scheme versus the conventional single GS; And finally, **Chapter 6** draws the conclusions, summarizes the benefits of this work, and discusses some possible future progress.

3 Dissertation Objectives

Inspired by the desired 6G ubiquitous SIoT future coverage, the main objective of this thesis is to contribute to a successful integration of the popular but restricted resources (electric energy, inner volume and mass allocation for instruments, efficiency of ionizing radiation shielding, heat transfer limitations) small satellites into SIoT networks. To overcome the problematic scenarios, emphasises in **Chapter 2**, of such integration, this dissertation proposes a cooperative reception scheme in which multiple GSs are networked to share their received streams for improving the reception quality of small satellites' signals. The presented reception scheme in this dissertation provides a solution which ensures: A GS-based solution that can be applied at the currently existing GSs and has nothing to modify at the transmitter (i.e., the small satellite) side, an improved reception quality with reduced BER and minimized probability of satellite-to-GS communication outages, a reception structure that enables the tracking of multiple satellites at once, and a simple yet efficient developed combining method that can perform well with noncoherent and non-perfectly synchronized SDR receivers. Such benefits of a diversity-based reception scheme can improve the performance of small satellites' radio receivers, involve many radio enthusiasts with their simple GSs, and help such popular satellites successfully integrate into the future 6G SIoT networks by testing this new concept as a GS-based solution.

In summary, the presented dissertation has the following objectives:

I. To structure the conventional SISO downlink communication system between a satellite and a GS, analyze its performance, address its problematic scenarios, and accordingly identifies the research gap.
II. To propose and simulate a cooperative reception scheme based on a SIMO configuration for satellite communications and analyze its performance.
III. To build the proposed combining algorithm and apply it on the system in II.
IV. To suggest a couple of improvement techniques to enhance the system in III.
V. To validate the proposed cooperative reception scheme along with the developed combining approach in a real deployment to combine real satellite signals.
VI. To analyze, compare, and visualize the improvements and results of the proposed scheme in all earlier steps.
VII. To conclude the study findings which should sufficiently answer the question whether the reception diversity is promising enough to assure a successful

embracement of such restricted satellites into the future inclusive IoT networks and whether the achieved diversity gain is good enough to trigger the idea of replacing the expensive high gain directive antennas and their complex steering resources with much affordable omnidirectional antennas.

To meet these objectives, **Chapter 2** was dedicated for the traditional system analysis stated in objective I, while **Chapter 4** fulfils the objectives II, III, IV, and V by presenting a simulation model based on a SIMO configuration, developing a simple yet efficient combining method, suggesting a couple of further improvement techniques, and validating the proposed diversity-based scheme through four real deployment experiments where multiple versions of the small satellite VZLUSAT-2's signal were recorded by multiple GSs over the United States and Canada and combined into one version. The objective VI is met in **Chapter 5** where the findings are visualized, discussed, and commented on. Lastly, **Chapter 6** concludes the thesis findings and sufficiently answers the questions raised in objective VII.

4 Dissertation Methodology

In **Chapter 2**, it was mentioned that out of the possible solutions to improve the reception quality of small satellites signals, this dissertation utilizes spatial diversity as an affordable but effective solution that can be applied at current GSs. Therefore, moving towards the main theme of this chapter, the topic of spatial diversity is going to be deeply addressed.

Diversity refers in general to any technique which takes advantage of processing multiple copies of the signal broadcasted through multiple frequency slots, time slots, polarizations, or antenna configurations. Antenna diversity (also known as spatial diversity) can be achieved by different antenna arrangements to transmit and receive different versions of the same signal after propagating through space via different communication channels. This technique is widely used in radio communications relying on the fact that different channels are uncorrelated and hence they would have different levels of impairments, e.g., fading, interference and attenuation [39].

To answer the question of where antenna diversity can be configured, it should be categorized into three main schemes: transmitter diversity (MISO), receiver diversity (SIMO), or at both (MIMO) [40]. In this thesis, since the goal is to propose a GS-based solution to improve the detection quality and overcome the previously addressed problems of the current system with no modification at the transmitter side, the receive diversity scheme will be considered.

The rest of this chapter is organised as follows: **Section 4.1** reviews the reported receive diversity employments in the literature while **Section 4.2** models the proposed cooperative reception scheme. **Section 4.3** develops the combining method followed by **Section 4.4** which carries out the simulation process of the proposed reception scheme. Lastly, the real deployment of the cooperative reception system in combining real small satellites signals is accomplished in **Section 4.5** through four real combining experiments.

4.1 Reported employments of receive diversity

Receiver-based diversity combining is a well-known technique which has been deeply studied, maturely developed, and widely applied in different mobile communication systems. For example, it was shown in [41] that applying receive diversity combining at the Analog Feedback Communication System (AFCS) reduced the detected errors. The same study suggested that such communication system with receive diversity could reach the

required error threshold with less iterations compared to the single receiver system. Furthermore, in 5G wireless systems for modern smart cities applications, multiple Orthogonal Frequency Division Multiplexing (OFDM) versions of modulated images from monitored smart homes and industries were received and combined with Maximal Ratio Combining (MRC) to improve the BER at the receiver [42]. In the area of energy harvesting, the receive diversity combining was suggested to increase the harvested RF energy by using three concentric dipoles at the receiver [43]. Another receive diversity scheme was presented in [44] to increase the harvested RF energy using different combining techniques such as Selection Combining (SC) and MRC to harvest enough power for the wireless nodes enabling self-powering of these nodes. The simultaneous reception of two ionospheric-reflected signals in the range of (3–30) MHz generated a Signal to Noise Ratio (SNR) gain and hence improved the detection quality of the Near Vertical Incidence Skywave (NVIS) system as long as these two signals were uncorrelated with a correlation coefficient of less than 0.7 [45].

For reducing the probability of outages in mobile networks, a receive diversity system was highly recommended rather than increasing the transmission power according to [46]. The study conducted in [47] revealed that utilizing a SIMO scheme for underwater sonar system enabled the distributed receivers to precisely locate the target despite the hostile underwater environment. A multi-reception technique also reflected remarkable system performance of the Underwater Optical Communication (UWOC) system in [48] and the Free Space Optical (FSO) communication in [49]. Based on the findings presented in [50], applying receive diversity with MRC on Underwater Acoustic (UWA) communication system mitigated the sever underwater multipath effects and reflected higher output SNR and lesser BER.

To enhance the Signal to Interference Ratio (SIR) of the wireless networks with large-scale coverage area, the authors of [51] considered multiple antennas at the receiver side. Moreover, a SIMO system configuration was adopted in [52] to boost up the power of the received signal, mitigate the interference level at the receiver, and gain a network scaling. Moreover, the configurations of SISO, (1×8) SIMO with MRC, and (1×8) Multiuser-MIMO (MU-MIMO) were applied and examined on a wireless sensors network for their effectiveness in reducing sensors off probability in [53]. Out of these tested schemes, the (1×8) SIMO with MRC surpassed others in sustaining received Signal-to-interference Plus Noise Ratio (SINR) values of more than the threshold and therefore obtaining the least off probability. The Quality of Service (QoS) at mobile devices when receiving signals from satellites was investigated and tested for the service continuity in [54] under two scenarios,

with and without multi connectivity to 5G cellular networks. The multi-connectivity to a satellite and to cellular networks has ensured a reliable and continuous service at the mobile receiver, the investigation revealed.

Furthermore, a site-based diversity was overviewed in [55] as an effective scheme to mitigate rain attenuation effects on satellites signals at tropical climates. In addition, a cluster diversity combining was suggested to accelerate the delivery of indoor autonomous vehicles' emergency alerts with less required rebroadcasts according to [56]. Another employment of SIMO structure was reported in [57] to combine two downlinks from two receiving nodes by MRC as a part of this study to improve the performance of a Non-orthogonal Multiple Access (NOMA) network. The deep fading consequences inside tunnels were suppressed by utilizing multiple properly spaced receiving antennas in a diversity scheme as confirmed in [58]. MRC was deployed to enhance the performance by combining faded signals received by spatially distributed cellular base stations as depicted in [59]. Moreover, the study conducted in [60] concluded that increasing transmit and receive antennas improved the performance in high-mobility communication systems even when rapidly switching channels.

According to the surveyed literature, receive diversity has proven its effectiveness and reliability in improving the system performance in a wide range of applications. Nevertheless, receive diversity has not been previously investigated in satellite communications except in combining large and capable satellites' signals for improving the location accuracy as depicted in [61] and [62].

To the best of our knowledge, noncoherent diversity combining methods have not yet been applied to the signals of small CubeSat satellites, captured using cheap, noncoherent and imprecisely time synchronized public SDR receivers, aiming for a system capable of tracking many of these satellites at once.

4.2 Cooperative reception system modelling

Motivated by the improvements reported in the reviewed literature, the receive diversity scheme is proposed and structured in this dissertation to improve the reception quality of small satellites' signals. Since the receive diversity system involves the collection of multiple copies of the same transmitted signal by multiple receive antennas through multiple independent channels, **Figure 21** visualizes the employment of this scheme in satellite communications. As **Figure 21** demonstrates, the same message signal can be transmitted by the transmitter's antenna and received by N receive antennas to collect N versions of the

received signals (r_1, r_2, …, and r_N) after propagating through multiple independent channels (h_1, h_2, …, and h_N). These N different propagation paths would reflect different and independent impairment impacts on the same transmitted signal. Therefore, processing multiple received copies of the same transmitted signal will help in case that one or more of these paths severely degrade the signal strength by extracting the message signal from the other good quality copies received by such system. Accordingly, receiving and processing multiple versions of the signal at the receiver and then combining the demodulated streams is promising in improving the radio link quality and decreasing the probability of outages.

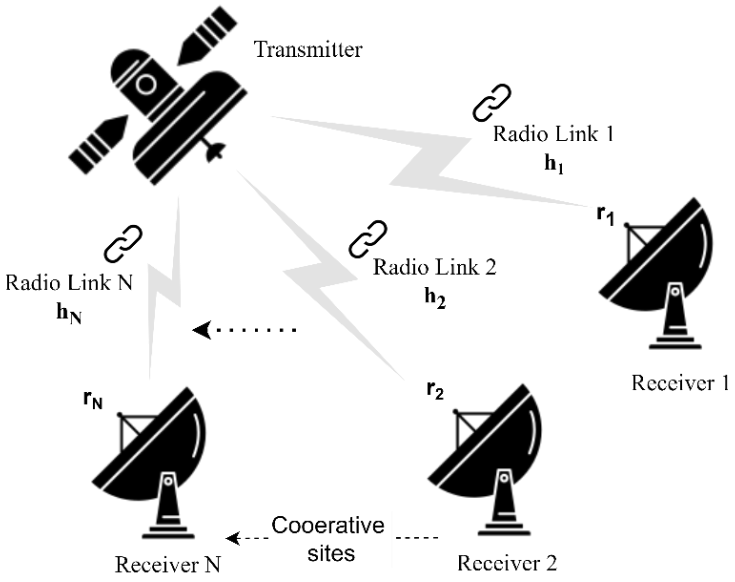

Figure 21. A cooperative reception scheme in satellite communications

In terms of system outages as a statistical quantity, we suppose that N GSs are operating individually in a single mode. Then, they would correspondingly have attenuations of ($A_1(t)$, $A_2(t)$, …, and $A_N(t)$), where $A_n(t)$ is the attenuation at the n^{th} GS. However, for these GSs to cooperatively work in a diversity mode, the cooperative receiving system would have a joint attenuation of:

$$A_s(t) = \min\{A_1(t), A_2(t), \ldots, \text{and } A_N(t)\} \quad (4.1)$$

where $A_s(t)$ is the diversity system attenuation when N GSs are involved. Therefore, the attenuation of the system in a receiving diversity mode will be the minimum one among all the cooperative GSs. Consequently, if one or two stations experience an outage due to high attenuation or steering engine failure, the receive diversity scheme will still be able to receive good quality signal from other sites and share it with those attenuated stations [63, 64]. To provide an analytical formulation of this reduction in system outages according to the

proposed collaborative scheme, the initial number of involved GSs is assumed to be two. Then, the general diversity formulation for greater number of receiving sites can be implied. The outage probability of the diversity mode versus single mode can be framed as follows:

Assuming the probability of an outage in a single receiving site is (P_{out}), the probability of successful reception is therefore, (1- P_{out}). Suppose we engage only two GSs in the receive diversity system, then the system reception probability can be [65]:

- Success probability of $(1- P_{out})^2$, when both GSs are receiving good quality signal.
- Success probability of (1- P_{out}). (P_{out}), when only one GS is receiving good signal.
- Outage probability of (P_{out}. P_{out}) = $P_{out}^{\ 2}$ when both GSs fail to receive a good signal.

So far, when only two GSs are engaged, the system outage probability is decreased from P_{out} to P_{out}^2. Accordingly, when N GSs are engaged in the receive diversity system, the outage probability becomes $P_{out}^{\ N}$. Keeping in mind that the probability value is always less than one, a power of N will significantly reduce the probability of outages if compared to the traditional SISO systems.

After these motivational probabilistic formulations on how much the collaborative receiving system is rewarding, it is vital then to develop a general foundation for the suggested platform at which the necessary processing and combining will take place. This is aimed to be done in a Virtual Ground Station (VGS) where all signal's versions are taken from individual receivers, processed, combined, and redirected. Therefore, the following part is dedicated to getting an overview of the VGS.

The VGS is a computerized radio receiver where all the received streams from the cooperative GSs are going to be stored and processed. Thus, no further modifications are required at each of the GSs but to be connected to the network for sharing the received data streams. Once these multiple versions of the same transmitted data are received and demodulated separately by the corresponding GSs and then shared to the VGS, this virtual receiver starts synchronizing them and forming the combining-ready matrix. After that, the virtual receiver triggers the diversity combining algorithm which takes advantage of each received version reflecting more efficient and reliable detection of the originally sent data. That would be the scenario if the combining is performed at the already detected streams (i.e., post-detection combining). However, if the combining is intended to be a pre-detection one, the virtual receiver synchronizes and standardizes the received raw symbols to form the combing-ready matrix and then applies the combining algorithm. At last, the detection will

be done on the combined stream to retrieve the original data. Detailed steps of the pre- and post-detection combining will be provided when presenting the algorithms in the next sections of this chapter. **Figure 22** illustrates the proposed cooperative reception model and the virtualization of the radio receiver at which the processing and the combining takes place.

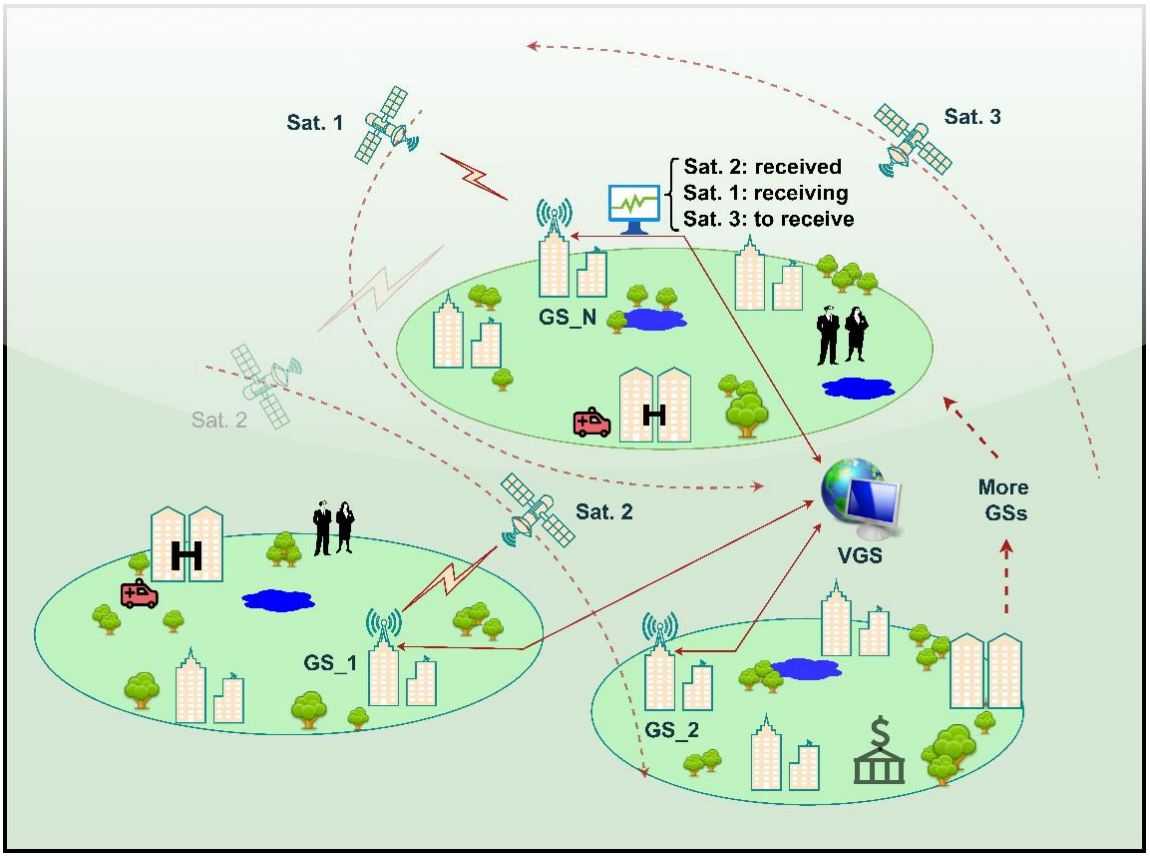

Figure 22. System model: Cooperative omnidirectional GSs (GS_1, GS_2, …, GS_N) along with the VGS are networked to receive data from multiple satellites simultaneously.

Figure 22 depicts a network of omnidirectional GSs spatially distributed across a large area, along with several satellites at varying distances from these GSs. Then, a VGS can receive the digitized bandwidth from each omnidirectional GS. Depending on their relative positions with respect to the GSs, individual satellites can be received by one or more GSs, with the VGS able to implement signal diversity combining for individual satellites at suitable times. Based on this concept, the proposed VGS doesn't only improve the system performance but also makes it potential to track more than one satellite at a time through the cooperative GSs. When discussing the system resources in a post-detection combining, the cooperating GSs should have omnidirectional antennas, Low Noise Amplifiers (LNAs), SDRs with soft / hard demodulation tools, and a PC for streaming, while the VGS should have a processor to perform the combining of multiple demodulated streams. On the other hand, in a pre-detection combining, the cooperating sites should utilize affordable hardware part of

SDRs for basic RF procedures (frequency down-converting, filtering, digitization), while the VGS should also have software part of SDRs with soft/hard decision demodulation tools to demodulate the combined stream. Having the necessary combining platform overviewed, it is the time now to develop the combining algorithm.

4.3 Developed combining method

To get the diversity payoff of an implemented diversity configuration, multiple versions of the same signal must be combined using suitable combining methods. Already existing combining algorithms are varying in their complexity and efficiency. Before going into the developed approach in this thesis, it is worth a brief investigation into the existing combiners and then present the proposed combining method with detailed simulation steps.

4.3.1 Existing combiners

SC is the simplest known combiner where the SNR is estimated for all received copies and then the system selects the copy with the highest SNR value [66]. However, this selection will limit the benefits of having other non-selected copies which may have valuable information the selected copy may not have. In this case, the selected copy will probably improve the performance but not significantly. Another combining algorithm is the Equal Gain Combining (EGC) where all received copies are equally weighted, regardless of their SNR values, and then added up together [67]. Thus, this method does not require any SNR information but involves equal weighting of all versions. The third combining scheme is the MRC, unlike EGC, utilizes adaptable weights to strengthen the streams [68]. These weights values are proportional to the SNR value of each stream. The signal copy with the highest SNR value is multiplied with the highest weight value to maximize that signal strength even more. Doing so, MRC method is the optimal one in terms of improving the system performance but at the price of system complexity as it implies weights adaptation with respect to the measured SNR values for all received versions.

In summary, SC requires SNR calculations of all sites but selects the highest one only, while EGC does not require SNR calculation but involves equal weighting of all signals. MRC is the most efficient combining method; however, it is the most complex algorithm as it requires SNR calculations as well as adaptable weighting of all signals. In this context, one of the contributions of this thesis is to develop a new combining algorithm to meet the requirements of simplicity and efficiency at once.

4.3.2 Mathematical modeling of the developed combiner

In this dissertation, a simple yet efficient receive diversity combining algorithm that can be deployed in satellite communications is proposed. The algorithm suggests combining multiple received copies of the same transmitted signal after being received by different GSs. The combining procedure takes place at the VGS where all necessary steps are performed with no further complications or modifications required at the receiving sites. This algorithm intends to take advantage of every received copy to finally result in a reliable combined stream. It aims to combine the N detected streams from N GSs and therefore it is considered a post-detection combining algorithm. The following part will carry a step-by-step mathematical analysis of the proposed processing model.

Once the VGS receives the N demodulated downlink replicas, $r_1, r_2, \dots, r_N$, with equal data length L, the combining matrix **C** is generated to eventually have the dimensions of N-by-L. Subsequently, the VGS triggers the combining algorithm to combine these multiple streams in a way so that the resulting combined stream, r_c, would have lesser BER than all BERs from the received versions. If we structure the combining matrix as:

$$\mathbf{C} = \begin{bmatrix} \mathbf{r_1(1)} & \cdots & \mathbf{r_1(L)} \\ \vdots & \ddots & \vdots \\ \mathbf{r_N(1)} & \cdots & \mathbf{r_N(L)} \end{bmatrix}$$

Then, instead of just selecting the stream $r_{n^{th}}$ out of the received versions based on SC method with respect to the criterion:

$$\min_{n \in (1:N)} \text{BER}\,(r_{n^{th}}) \tag{4.2}$$

The aimed combined stream r_c should achieve even lesser BER and it should be none of the received versions, i.e.,

$$\min_{c \notin (1:N)} \text{BER}\,(r_c) \tag{4.3}$$

By interpreting the criterion in **Equation (4.3)** from the likelihood perspective, the combined stream's likelihood, L_c, can be represented as:

$$L_c\,(r_c | r_1, r_2, \dots, r_N) \tag{4.4}$$

Since the received versions, $r_1, r_2, \dots, r_N$, are independent, the likelihood is therefore equivalent to the joint Probability Mass Function (PMF) of these N versions and can be alternatively expressed as:

$$\prod_{i=1}^{N} L_c\,(r_c|r_i) \tag{4.5}$$

Equation (4.5) represents the likelihood quantity the VGS should maximize in the combining process to provide as good estimate of the transmitted stream as possible.

To this context, one concept to reach this goal is to combine these streams with respect to the maximization of the likelihood function through the selection of the more likely occurring bit of each column in **C** to generate r_c according to:

$$r_c(k) = \text{mode}\,\{r_1(k), r_2(k), \dots, r_N(k)\}, \tag{4.6}$$

where (mode) is the function that picks the most frequently occurring entry at each column in **C**, and k =1, 2, …, L. If we assume that the original transmitted stream is r_0, the probability of detection errors can be expressed as [26],

$$P_e(k) = P\,(r_c(k) \neq r_0(k)) \tag{4.7}$$

In general, the minimization of the error probability P_e corresponds to the maximization of the probability to provide a good estimate P to the originally transmitted data. Therefore, in the proposed combining, the VGS must generate a combined stream r_c whose probability is:

$$P\,(r_0 = r_c|r_{1:N}, H) \tag{4.8}$$

where H denotes the channels impulse response matrix. The probability in **Equation (4.8)** can be further expressed using the conditional probabilities [26] as follows:

$$P\,(r_0 = r_c|r_{1:N}, H) = \frac{P\,(r_0=r_c) f_{r_{1:N}|r_0,H}(r_{1:N}|r_0=r_c,H)}{f_{r_{1:N}|H}(r_{1:N}|H)} \tag{4.9}$$

where $f_{r_{1:N}|H}$ is the conditional Probability Density Function (PDF) of $r_{1:N}$ given H, while $f_{r_{1:N}|r_0,H}$ is the conditional PDF of $r_{1:N}$ given r_0 and H. Since the two terms $P\,(r_0 = r_c)$ and $f_{r_{1:N}|H}(r_{1:N}|H)$ are independents of the aimed r_c, the maximization of the probability to generate good-estimated combined stream is therefore reduced to maximizing only the dependent PDF term:

$$f_{r_{1:N}|r_0,H}(r_{1:N}|r_0 = r_c, H) \tag{4.10}$$

Thus, we can set a Maximum Likelihood (ML) goal in generating the combined stream as:

$$r_{c_{ML}} = \underset{r_c \notin r_{1:N}}{\operatorname{argmax}} f_{r_{1:N|r_0,H}}(r_{1:N}|r_0 = r_c, H) \quad (4.11)$$

If the conditional PDF term in **Equation (4.11)** is reformed using the general communication model of estimating the received signal in a MIMO system: $\{r_{1:N} = H\, r_0 + n_{1:N}\}$ [26], we obtain:

$$f_{r_{1:N|r_0,H}}(r_{1:N}|r_0 = r_c, H) = f_{n_{1:N}}(r_{1:N} - Hr_c) \quad (4.12)$$

where f_n is the PDF of the white Gaussian noise (n) which can be expressed as:

$$f_n(n) = \frac{1}{(\pi\sigma^2)^n} e^{-\frac{1}{\sigma^2}\|n\|^2} \quad (4.13)$$

Then, the left side of **Equation (4.11)** can be maximized by reducing $\|n\|^2$ for the aimed combined stream and hence the ML can be achieved if $(r_{1:N} - Hr_c)$ is minimized based on:

$$r_{c_{ML}} = \underset{r_c \notin r_{1:N}}{\operatorname{argmin}} ||r_{1:N} - Hr_c||^2 \quad (4.14)$$

To meet the criterion of distance reduction, i.e., the term $||r_{1:N} - Hr_c||^2$ in **Equation (4.14)**, the likelihood modal hypothesis is applied on each column in the matrix **C** to generate the combined stream r_c which follows the tendency of the data towards the original data distribution. Hence, the combined stream should achieve lesser distance to the original stream than the distance from each received version to the original data. Therefore, the combined stream can be derived from the received versions on a bit-by-bit inspection of the data tendency in all the received streams. This is promising to bring data into the combined stream that can better fit the original data distribution. The Euclidean Distance (ED) results of the r_0-to-r_c and r_0-to-$r_{1:N}$ can verify how much reduction in that distance between the combined version and the original data the proposed algorithm can provide.

4.4 Simulated cooperative reception model

This section presents the simulation process of the proposed cooperative reception model. **Subsection 4.4.1** simulates the proposed scheme, applies the combining algorithm on the already detected streams as a post-detection combining algorithm, and emphasizes the algorithm's drawback. **Subsection 4.4.2** presents three optional further improvement techniques to overcome the addressed drawback. Then, the combining algorithm is developed and tested in **Subsection 4.4.3** to have the capability of combining undetected received complex symbols as a pre-detection combining algorithm.

4.4.1 Cooperative reception with raw post-detection combining

The MATLAB simulation of the cooperative reception system starts with generating random unipolar input data and then mapping these input bits into complex BFSK symbols. In the next step, N different complex AWGN streams will be generated and added to form N multiple uncorrelated versions of the received signal to feed the detector. The detector passes the detected bit stream from each received version to the VGS to establish the combining square matrix **C** where the n^{th} row corresponds to the detected bits from the n^{th} GS.

The VGS then starts applying the ML hypothesis on that square matrix based on a vertical bit disagreement rule. This ML detection is performed at the combining matrix in an ascending tempo starting from the 1^{st} row to the N^{th} one representing the possibilities of combining multiple streams gradually. Therefore, the first trial represents conventional single-site detection as it involves the first row only while the following step is for two-site combining since it engages the 1^{st} and 2^{nd} rows and so on until the last trial is for combining the N sites all together. This helps visualize the system's BER improvement when gradually increasing the number of cooperative sites. The simulation is performed on a million-bit data stream with up to 14 cooperative receiving sites whose SNRs of 0 dB to 13 dB.

This likelihood combining is promising to provide a bit detection with more certainty and reliability since it takes into consideration how frequent each bit is in all the detected streams from all sites. The algorithm relies on the most frequently happening bit to be the right one and therefore it should be the only value in all entrees. For instance, in the third bit combining trial, if we have 6 entrees, out of 14, detected 0s while the remaining 8 sites have detected 1s, the combining algorithm will consider this position in the combining matrix to be all 1s. Therefore, the algorithm finds the most frequent bit and replaces the other entrees with that most frequent value. The implementation MATLAB script of the cooperative reception scheme along with the developed raw combining algorithm is provided in **Appendix B**.

Nevertheless, this algorithm will have possible errors applying this hypothesis when the number of the cooperative sites is even and consequently the number of entrees is so. This possible error specifically occurs only when having equal entrees of detected 0s and 1s (e.g., 7 entrees of 1 and 7 entrees of 0 in a 14-site cooperative system). Therefore, further improvement techniques are optionally provided to compensate for these few possible errors.

4.4.2 Further improvement techniques

To enhance the performance of the algorithm even more and to overcome the earlier mentioned drawback, a couple of Signal Processing (SP) techniques are proposed and

examined in even and odd combining trials. For the whole combination of streams, the best and the worst ones are identified based on evaluating the performance metrics such as BER. In the MATLAB simulation of the proposed system, the BER of the N detected streams can be directly calculated and consequently the highest BER stream is specified. However, in a real system implementation, this can be done by relying on the calculation of the BER of the satellite's identifiers (i.e., the default content such as Preamble, Sync-Word, Callsign, and some of the fixed data parts) within the signal received by each receiving site. The worst stream can be identified to be the one with the highest BER while the best stream is the one with the lowest BER. Then, the best and worst streams are used at each combining trial to improve the performance by applying one of the following SP techniques.

4.4.2.1 Exclusion of the worst stream

Before combining the streams, the highest BER stream is excluded, as demonstrated in **Figure 23**, to consequently reflect better performance and compensate for the errors caused by combining an even number of sites.

4.4.2.2 The best stream replacing the worst one

The highest BER stream is replaced with the lowest BER stream before performing the combining process as illustrated in **Figure 24**. Therefore, the number of detected errors at the VGS is expected to decrease as we are injecting the best quality stream in replacement of the excluded highest error stream.

4.4.2.3 The best stream is repeatedly injected

In this technique, the best stream is repeatedly tailed into the combining matrix at each trial to impose more weight for this best stream as shown in **Figure 25**. The more sites are involved, the more weight is imposed for the best stream according to this technique. This assumption is promising because the best stream will always reflect the least detection errors and accordingly improve the system performance.

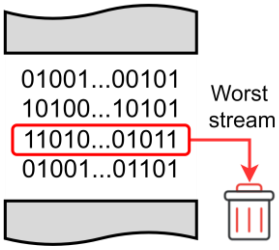

Figure 23. Excluding the worst stream.

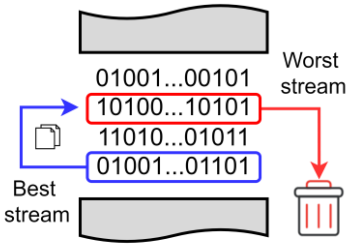

Figure 24. Replacing the worst stream by the best one.

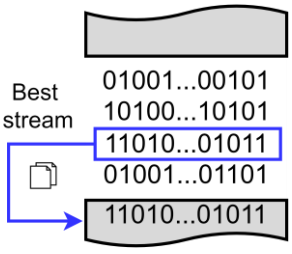

Figure 25. Tailing the best steam.

The improvement techniques can be modeled the same as the raw combining except the required pre-combining procedures of each technique. For instance, in the first technique,

the worst stream should be excluded out of the combining matrix and then the same modeling applies for combining the new (N-1)-by-L combining matrix C as demonstrated earlier to get the following ML criteria:

$$r_{c_{ML}} = \underset{r_c \notin r_{1:N-1}}{\operatorname{argmin}} ||r_{1:N-1} - Hr_c||^2 \quad (4.15)$$

The MATLAB implementation of all improvement techniques is provided in **Appendix C**.

4.4.3 Cooperative reception with pre-detection combining

Up to this point, the proposed algorithm is presented as a post-detection combining, where detected streams are combined to achieve less BER. However, for the algorithm to be powerful, it must have a reconfigurable combining point to execute pre- as well as post-detection combining. Towards that, the proposed algorithm is modified to be a pre-detection combining and that means it combines the received BFSK complex symbols.

Once the N omnidirectional GSs receive their N versions, these streams are sent to the VGS. The VGS then applies a simple symbol standardization hypothesis to finally convert the real and imaginary parts of each symbol into standard values of 1s and Js. This standardization hypothesis is based on the comparison of the real to the imaginary parts of the received symbols. In one complex symbol, if the real part is greater than the imaginary part, that symbol is standardized to (1+0j). Otherwise, the symbol is standardized to (0+1j). After getting all symbols referenced to the standard BFSK constellation, the VGS assembles the combining-ready matrix whose dimensions are (N-by-L), where N and L are the number of the engaged GSs and the length of the received streams, respectively. Then, the VGS gradually combines the versions starting from only the first stream and ending at all N streams, representing single to N-stream combining trials.

The combining mechanism at each trial relies on the ML of each certain symbol location after considering the symbols at the same location in other versions. The algorithm replaces all symbols, at that location in all combined streams, with the value which holds the ML. Hence, the most frequent symbol becomes the dominant one and replaces all the corresponding entrees. The flowchart depicted in **Figure 26** provides detailed simulation steps of the proposed cooperative reception scheme along with the pre-detection combining algorithm. For more convenience in the system visualization, the flowchart omits the transmitter side since there is no modifications to the SISO system presented and analyzed in **Chapter 2**.

The symbols m, X, r_n, n, N, $r_n^{\wedge}$, r^c, and $m_n^{\wedge}$ stand for the message, transmitted signal, the n^{th} version of the received signal, the AWGN noise, the number of GSs in the cooperative system, the n^{th} standardized version of the received signal, the combined received signal, and the retrieved message, respectively. L is the length of the data, while i = 1, 2, …, L.

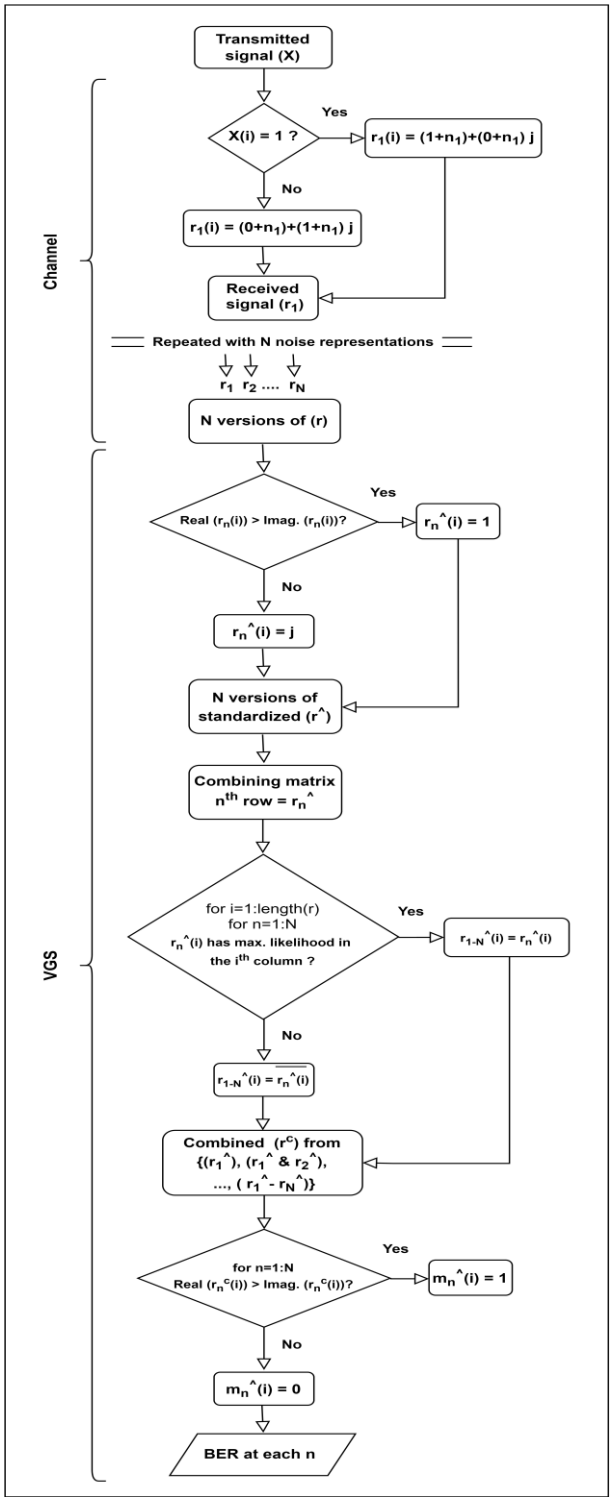

Figure 26. Pre-detection combining algorithm's flow chart.

In MATLAB simulation provided in **Appendix D**, 12 receiving sites are gradually engaged in the combining trials where the SNR values range from 0 dB to 11 dB. The setting of this pre-detection combining is designed in a way to present the proposed system's soundness in overcoming severe transmission and reception scenarios . For that purpose, the combining algorithm is tested under five scenarios: Uncorrelated when the sites receive signals with SNRs of (0-11) dB for the 12 sites in order; Below average when all sites receive signals with SNRs of (2-3) dB; Above average when the sites receive signals with SNRs of (8-9) dB; Correlated when all the sites receive signals of 7 dB SNR; Severe when all sites receive signals of 0 dB SNR except one site with SNR of 8 dB.

When it comes to system resources, the proposed pre-detection algorithm significantly reduces the infrastructure requirements at each of the involved GSs. An omnidirectional antenna with LNA and affordable SDR units (e.g., AirSpy R2, FUNcube Dongle, LimeSDR, Ettus Research, … etc.) would be sufficient for each receiving site along with a PC for data sharing. These affordable SDRs handle the basic hardware RF procedures such as frequency down conversion, analogue to digital conversion up to 10 MHz of bandwidth for these affordable SDRs, decimation, and filtration. On the other hand, the VGS will carry out the standardization, combining, and detection requiring an open-source software with soft/hard demodulation tools such as GNU Radio to perform the reduced software functionalities at each receiving site. Besides the reduction in resources and BER, the proposed SIMO scheme with its VGS enables the operators to track more than a satellite at once as many satellites become more available to a network of stations than to an individual GSs and hence the communication window is also increased.

After providing a sufficient analysis to the conventional researched system in **Chapter 2,** addressing its problem statements and introducing the research objectives accordingly in **Chapter 3**, the previous sections of this chapter exhibited a preliminary theoretical framework to solve the problematic scenarios and offer many features for a practical, affordable, scalable, and yet efficient cooperative reception scheme. By which, the popular but resources-restricted small satellites can be successfully integrated into the future ubiquitous 6G IoT networks. The following section is dedicated to validating the claimed theoretical concept by processing and combining real small satellites signals. The proposed cooperative reception scheme along with the developed combining approach are going to be deployed and validated in engaging multiple GSs in a diversity mode. The performance of the deployed diversity-based system is observed and validated versus each individual GS.

4.5 Deployed cooperative reception model

Inspired by the model depicted in **Section 4.2** and simulated in **Section 4.4**, this section carries out the validation of the cooperative reception concept in combining multiple versions of the default content in a real small satellite's beacon signal. To execute the objectives of this part of the dissertation, the rest of **Section 4.5** is organized as follows: **Subsection 4.5.1** reveals the selected small satellite as a signal source, its orbital characteristics, and its transmission format. **Subsection 4.5.2** presents the utilized open-source online platform of networked-GSs, at which the uncorrelated versions of the small satellite beacon were recorded. **Subsection 4.5.3** exhibits the procedures to perform at the suggested VGS starting from the preprocessing and signals visualization, searching for the satellite's identifiers, aligning the received records, and ending at the combining process. Lastly, **Subsection 4.5.4** depicts four real combining experiments conducted to validate the concept of diversity-based reception in improving the reception of small satellites' signals.

4.5.1 Signal source

The small satellite, VZLUSAT-2, is selected as a signal source since its main GS is hosted by the University of West Bohemia in Pilsen, Czech Republic. VZLUSAT-2 is a Czech nanosatellite, also categorized as 3U CubeSat, whose main mission is in-orbit demonstration and Earth observation. **Table 1** lists some of the features of VZLUSAT-2.

TABLE 1
MAIN FEATURES OF VZLUSAT-2

Aspect	Quantity
North American Aerospace Defense Command (NORAD) ID	51085
Initial altitude (km)	535
Downlink frequency (MHz)	437.325
Baud rate (beacon mode)	4800
EIRP (dBm)	~30
Date deployed	Jan. 26th 2022
Status	Active
Modulation format	FSK/MSK
Satellite documentation	[69]
Dashboard	[70]
Orbital observation	[71]

The VZLUSAT-2's orbital speed is relatively high, indeed all small satellites are, so that one complete rotation around the Earth takes approximately 95 minutes. The high orbital speed results in a high Doppler effect and short communication window for the relevant GS. For such GSs, this adds another challenging factor to the limited output power and low gain a transmitting antennas of these small satellites.

To offload the collected data from onboard sensors, VZLUSAT-2 utilizes the transmission mode 5 of GomSpace AX100 transceiver (FSK/MSK modulation, Preamble, 4-byte attached sync marker, 3-byte Golay coded length field) during the communication session to the main GS in Pilsen. According to the default setting of the transmission format, VZLUSAT-2 switches to the beacon mode 10-15 minutes after terminating the communication session with the main GS. When the beacon mode is active, VZLUSAT-2 sends its beacon signal every 10 seconds to indicate the healthy status of the satellite to the operator and radio-amateur observers.

In addition to healthy status, the beacon signal includes several fixed identifiers and synchronization signals such as periodic Preamble for bit synchronization, Sync-Word for synchronization of packet beginning, Header to indicate the type and length of useful data, and Callsign of satellite. Therefore, recording multiple versions of VZLUSAT-2's beacon provides a great opportunity for achieving the goals of this research in calculating the BER of the retrieved fixed parts from the individually received beacons and compare them with the BER of the combined version.

The live orbital observation tool, available at [71], was used to identify the locations at which the GSs must be selected for recording the aimed multiple versions of the VZLUSAT-2's beacon. Accordingly, VZLUSAT-2 was tracked after passing over its main GS in Pilsen, aiming at an area over which VZLUSAT-2 switches to the beacon mode. During the time of recording the data in this research, VZLUSAT-2 was heading north towards the United States and Canada after terminating the session with the main GS in Europe. Thus, possible VZLUSAT-2 visibilities to available GSs in these areas were further explored and scheduled.

4.5.2 Signal recordings

As a reflection of the current popularity of amateur small satellites, many global platforms for networked SDR GSs have been recently developed. A great example is SatNOGS, a global project to connect all GSs together in an open-source network where a remote access for registered GSs' operators to calculate future passes of small satellites and schedule their observations is provided.

In this work, SatNOGS was utilized to access the global network of GSs across Europe and United States with parts of Canada, as shown respectively in **Figures 27** and **28**, and search for the visibilities of the VZLUSAT-2 after the time at which the communication to the main GS in Pilsen is terminated.

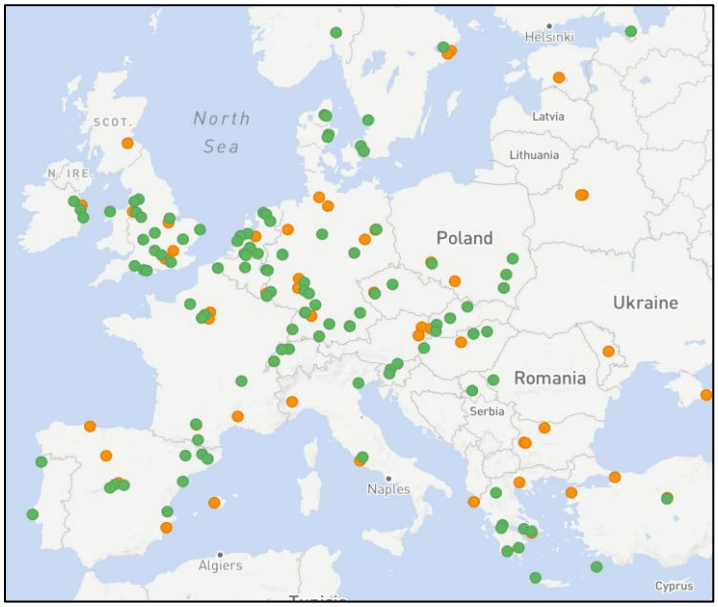

Figure 27. Registered SatNOGS GSs across Europe [19].

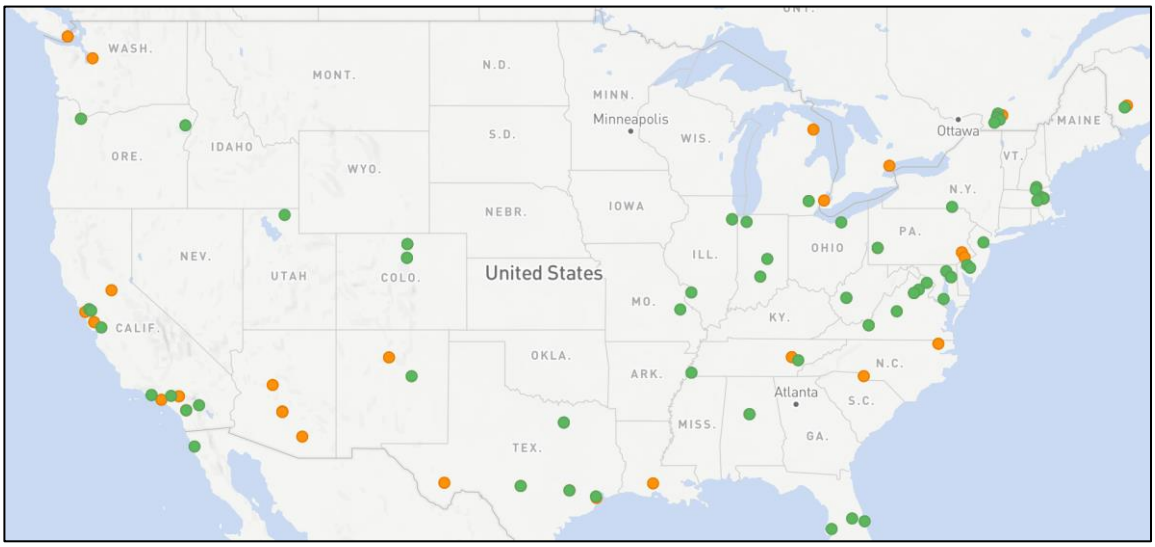

Figure 28. Registered SatNOGS GSs across the United States and Canada [19].

For each recorded observation, SatNOGS provides a waterfall diagram as an initial visualization of each received signal spectrum along the time (an example of a waterfall with clear successive beacons is shown in **Figure 29**), an audio file of the whole observation for further processing and analysis purposes, and decoded payload data (useful telemetry with fixed part of packet removed) in hexadecimal format only if the quality of the received signal is good enough for the built-in decoding tools. In small satellites' GSs, many received beacon packets stay uncoded by built-in decoding tools due to the low quality of received signal reflecting too high BER caused by low antenna gain and weak transmitted signal.

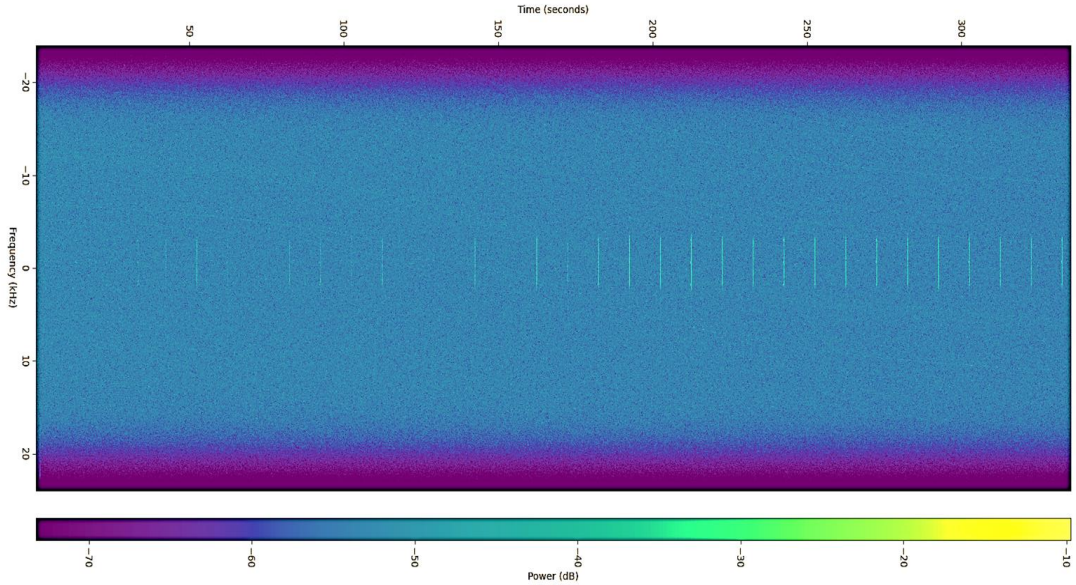

Figure 29. Example of a waterfall with clear successive beacons.

According to the cooperative reception model, demonstrated previously in **Figure 22**, the received audio signals must then be shared with the VGS to perform some experimental procedures of evaluating the combining methods on the fixed part of the packets. As for processing the records in this work, the time-discrete audio files are downloaded and used as described next.

4.5.3 Signal processing and combining

Once the recordings become downloadable to the dashboard of the observer, they must be offloaded into a PC in one directory for further processing and combining. The processing steps were performed in MATLAB using the VGS's PC whose features are listed in **Table 2**.

TABLE 2
MAIN FEATURES OF UTILIZED PC

Aspect	Quantity
Operating system	Windows 10 Pro
Processor	Intel(R) Core(TM) i7-1065G7 CPU
Frequency	1.5 GHz
RAM	16 GB
System type	64-bit O.S., x64-based processor

The upcoming four parts of this subsection are dedicated to clarifying the developed algorithm's processing steps starting from visualizing the collected audio records according to their start times, end times and overlapped parts of observations, searching for the default content of the satellite's identifiers in the received records, aligning the records in time due to not perfectly synchronized recordings of SatNOGS stations, and ending at combining the detected VZLUSAT-2's identifiers packets.

4.5.3.1 Preprocessing: Initial visualization

Before going into the analysis of the collected records, it is worth exploring when roughly each record starts and ends at, which records are the earliest and the latest, at what time the first overlapping occurs among the collected records' times, and accordingly when the combining becomes possible and when it is not. To explore such aspects, the algorithm loads the audio records into MATLAB and retrieves date, time, and length (in samples) of each record as a preprocessing step. The date of the recording and the start time are included by default in the name of the audio files provided by SatNOGS and can be read by MATLAB. Moreover, more details about the dates, the starting and ending times of each record can be retrieved from the information of the audio files using some MATLAB built-in functions such as **audioinfo**. Then, the algorithm sorts the times and identifies when the earliest and the latest visibilities of VZLUSAT-2 were, and to which GSs.

To explore the overlapping of the records' times, the records must be initially visualized in a figure where the horizontal axis represents the observation start and end times, and the vertical axis represents a shift for better visualization and has nothing to do with the power or the amplitude of the records. The outcomes of the applied algorithm in this part are the number, names, and lengths of records, the start and end times of each record, the earliest and the latest visibilities, graphical visualization of the records in a time manner, and when the combining becomes possible and when it is not.

4.5.3.2 Searching for identifiers packets

Communication systems always follow certain transmission packet formats with parts of known content that can help the receiver synchronize and identify the received data packets. According to the VZLUSAT-2's documentation available at [69], the transmission mode switches to the beacon mode 10-15 minutes after the uplink/downlink session with the main GS terminates. When the beacon mode is active, VZLUSAT-2 regularly transmits at least 64-bit long Preamble with periodic sequence (of 0,1,0,1…) for bit synchronization followed by a 32-bit (4 bytes) Sync-Word to indicate the start of the packet, 24-bit (3 bytes) Header and the 80-bit (10 bytes) fixed part of the data stream. The order, lengths, and the contents of these patterns (i.e., satellite identifiers) are fixed by default in the beacon mode as shown in **Figure 30**. Therefore, searching for these patterns in the received signals and calculating their individual BERs fulfills the aim of this dissertation in validating the diversity combining concept by comparing the individual BERs to the BER of the combined version.

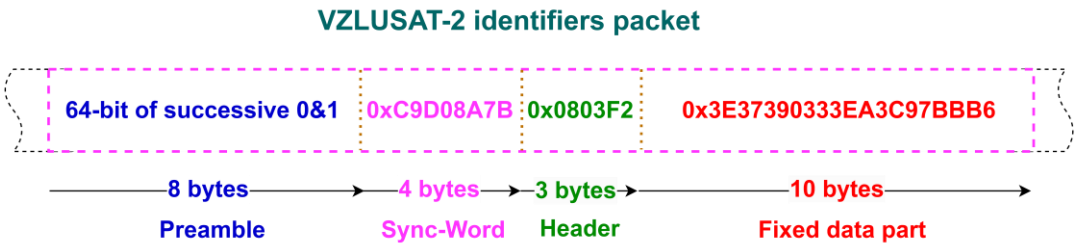

Figure 30. VZLUSAT-2's identifiers packet format in a beacon mode.

The identifiers' contents, shown in **Figure 30** in hexadecimal format, are first converted into binary to result a 200-bit packet in its symbol-based format which is introduced in MATLAB to represent the default contents in their short format. Searching for the identifiers packet within the received audio records requires the conversion of the symbol-based packet into the long format where each symbol is represented by several samples according to the sampling frequency of the audio records and transmitted baud rates. The default sampling rate of the records from SatNOGS network is 48000 samples per second while the baud rate of VZLUSAT-2 is 4800 symbols per second which means every symbol is represented by 10 samples. Accordingly, the identifiers packet in its long format becomes 2000-sample long including the 640-sample Preamble, 320-sample Sync-Word, 240-sample Header, and 800-sample for the fixed data part. Meantime, the received time-discrete audio records must also be converted to digital. The algorithm then triggers the search process which tends to find a match for the 2000-sample packet or similar patterns in the received records considering a given error tolerance.

After setting a tolerance of 400 errors for the 2000-bit identifiers packet, the algorithm searches for the best match of the identifiers packet in the received records within a search window of four seconds to handle the slight asynchronized timeline of the recordings from the SatNOGS network caused by latencies in the SDRs and computers used. The algorithm returns the start and end indices of the detected patterns and calculates the Number of Errors (NOEs) present individually at each detected packet in its short format. Therefore, MATLAB searches for the identifiers packet in its long format (i.e., 2000-sample) in the received audio samples from each observation. Then the detected pattern is converted to its short 200-bit format and compared to the default packet to calculate the NOEs. The outcomes of the algorithm in this part are the number of detected packets in each record, start and end indices of each detected packet, and NOEs for each 200-bit detected fixed part of packet.

4.5.3.3 Aligning the records

Since the combining is intended to be in a time manner, the records must be aligned while maintaining their visibility order. To do so, the start of each record is stretched backward and zero padded to match the start of the earliest record. The same zero padding applies at the end of each record, so they match the end of the latest record. Accordingly, the previously saved start and end indices of each record's packets are shifted by the same number of the inserted zeros in the front padding process of that record. The algorithm double checks if the padding process, front and rear, went well after simple calculations based on the original lengths, the required front and rear zeros, and the resulting lengths of the padded records.

4.5.3.4 Combining the records

After aligning the records, the next is to trigger the combining process. The combining algorithm checks in all records for the availability of the identifiers packets whose start and end indices lie within the combining window of 5 seconds. Only if the algorithm finds multiple versions within a time window, they will be combined into one version. The combining window is shifted by 3 seconds at each trial regardless of whether the combining takes place or not until the window reaches the time of the latest record. At each performed combining trial, a counter is increased by one and the improvement of the system performance is observed by comparing the NOE of the combined version with the NOEs of all individual records the combined version is generated from. When it comes to the combining method, the simple yet efficient method developed in (**Section 4.3**) is going to be projected in combining the received records in this section. Suppose at a combining trial, we have N versions (entrees) of the detected identifiers packets (pack_1, pack_2, ... pack_N) to combine. The algorithm concatenates them on top of each other to form a pre-combining matrix **C**:

$$\mathbf{C} = \begin{bmatrix} \mathbf{pack_1(1)} & \cdots & \mathbf{pack_1(end)} \\ \vdots & \ddots & \vdots \\ \mathbf{pack_N(1)} & \cdots & \mathbf{pack_N(end)} \end{bmatrix}$$

Instead of limiting the improvement of the diversity system to only reach the performance of the best version according to SC method [72, 73] , and to avoid making the system more complicated with more evaluation and adaptive weightings of the N entrees according to MRC [74], the developed combiner seeks for a combined packet (Pack_c) which is none of the received N packets. Therefore, the goal of the developed combining can be stated as in:

$$\min_{c \notin (1:N)} \text{BER}\,(\text{pack}_c) \tag{4.16}$$

Minimizing the combined packet's errors also corresponds to maximizing the likelihood of that combined packet to well approach the default content. Therefore, if given that all N packets are received, the likelihood of the combined packet (L_c) to maximize is:

$$L_c\,(\text{pack}_c|\text{pack}_1, \text{pack}_2, \dots, \text{pack}_N) \tag{4.17}$$

Because the involved receiving sites are sufficiently apart, the received packets are independent and hence the likelihood in **Equation (4.17)** becomes equivalent to PMF of the N packets and hence,

$$\prod_{i=1}^{N} L_c\,(\text{pack}_c|\text{pack}_i) \tag{4.18}$$

Equation (4.18) expresses the likelihood quantity to maximize in the combining process for getting a combined stream that matches the default packet content the most. This likelihood maximization goal must be applied on the matrix C for combining N packets, i.e., N rows. To do so, the combiner relies on the most likely occurring bit of each column in C based on:

$$\text{pack}_c(k) = \text{mode}\,\{\,\text{pack}_1(k), \text{pack}_2(k), \dots, \text{pack}_N(k)\} \tag{4.19}$$

where, k=1, 2, …, length (pack_c) and **mode{x}** is a function that picks the most likely occurring value in the vector x.

Assuming the default packet is Pack_0, then we can express the probability of error (P_e) in the combined packet to be the probability (P_r) that the k^{th} bit in the combined packet does not match the value of the corresponding position in Pack_0, or:

$$P_e(k) = P_r\big(\text{pack}_c(k) \neq \text{pack}_0(k)\big) \tag{4.20}$$

Minimizing the probability of errors (P_e) in the combined version corresponds to maximizing the probability (P) for getting a combined version Pack_c that can better match the original packet Pack_0. Thus:

$$P\,(\,\text{pack}_0 = \text{pack}_c|\text{pack}_{1:N}, H) \tag{4.21}$$

where H represents the matrix of the channels' impulse response.

The probability in **Equation (4.21)** can be also represented using conditional probabilities according to [26]:

$$P\left(\text{pack}_0 = \text{pack}_c \,|\text{pack}_{1:N}, H\right) = \frac{P\left(\text{pack}_0 = \text{pack}_c\right) f_{\text{pack}_{1:N}|\text{pack}_0,H}(\text{pack}_{1:N}|\text{pack}_0 = \text{pack}_c, H)}{f_{\text{pack}_{1:N}|H}(\text{pack}_{1:N}|H)} \quad (4.22)$$

where the conditional probability terms at the denominator and numerator respectively represent the PDFs of $\text{Pack}_{1:N}$ given H and $\text{Pack}_{1:N}$ given Pack_0 and H.

Because the term $P\left(\text{pack}_0 = \text{pack}_c\right)$ and the denominator PDF term are both independent of pack_c, getting the probability (P) in the left side of **Equation (4.22)** maximized corresponds to maximizing the only dependent PDF term:

$$f_{\text{pack}_{1:N}|\text{pack}_0,H}(\text{pack}_{1:N}|\text{pack}_0 = \text{pack}_c, H)$$

Therefore, the ML goal when combining $\text{pack}_{1:N}$ to generate pack_c can be expressed as:

$$\text{ML}(\text{pack}_c) = \underset{\text{pack}_c \notin \text{pack}_{1:N}}{\text{argmax}} f_{\text{pack}_{1:N}|\text{pack},H}(\text{pack}_{1:N}|\text{pack}_0 = \text{pack}_c, H) \quad (4.23)$$

When reforming the PDF quantity in **Equation (4.23)** using the standard model in MIMO communication systems [26]: $\text{pack}_{1:N} = H\ \text{pack}_0 + n_{1:N}$, we obtain:

$$f_{\text{pack}_{1:N}|\text{pack}_0,H}(\text{pack}_{1:N}|\text{pack}_0 = \text{pack}_c, H) = f_{n_{1:N}}(\text{pack}_{1:N} - H\ \text{pack}_c) \quad (4.24)$$

where f_n represents the PDF of white Gaussian noise (n) according to [26]:

$$f_n(n) = \frac{1}{(\pi\sigma^2)^n} e^{-\frac{1}{\sigma^2}\|n\|^2} \quad (4.25)$$

Therefore, maximizing the left side of **Equation (4.25)** is directly related to getting $\|n\|^2$ of pack_c reduced. Indeed, the ML of the combined stream can be met by minimizing the distance quantity $(\text{pack}_{1:N} - H\ \text{pack}_c)$, or i.e.,

$$\text{ML}(\text{pack}_c) = \underset{\text{pack}_c \notin \text{pack}_{1:N}}{\text{argmin}} ||\text{pack}_{1:N} - H\ \text{pack}_c||^2 \quad (4.26)$$

To reduce the indicated distance term, the developed combining follows the tendency of data at each column in **C**. The combining algorithm relies on the most likely occurring bit in each column to be the selected value at the corresponding position in the combined packet. This tendency-based combining should generate a combined packet whose less ED to the original identifiers packet than any other individually received packet.

4.5.4 Proof of concept experiments

Four experiments to combine parts/all the identifiers, in real VZLUSAT-2's beacon signal, were conducted to prove the concept of the diversity-based reception scheme. These experiments reflect the continual step-by-step development of the combining algorithm starting from limited number of recordings and overlapped packets as a simple case to start with to test the performance and then by combining a greater number of packets from different times up to large scale combining in real time manner with time synchronized packets from individual streams. **Experiment A** was performed to observe the NOE's improvement in combining the best match of the satellite's identifiers detected by multiple GSs. **Experiment B** focused on combining all detected Sync-Words from multiple GSs in a time manner and observing the NOE of the combined Sync-Word and comparing it with NOEs of all individual Sync-Words within the same combining window. **Experiment C** intended to combine the whole identifiers packet detected by six GSs in a time manner and evaluate the system performance. **Experiment D** performed the same task in the former experiment but with nine GSs to test the system scalability when engaging more sites in the cooperative reception scheme.

4.5.4.1 Experiment A

In this experiment, the main goal was to receive multiple VZLUSAT-2's beacons and retrieve the best match of each of the satellite's identifiers from every received beacon. Then, the detected best match of each identifier from all GSs were combined and evaluated versus each GS's best detected match. In this context, five GSs from the United States and Canada were involved to receive the VZLUSAT-2's beacon signal on the 30th of September 2022. The names, locations, and coordinates of the GSs at which the VZLUSAT-2's beacons were recorded are provided in **Table 3**.

TABLE 3
DETAILS OF 5 GROUND STATIONS TO RECORD THE SIGNALS IN EXPERIMENT A

No.	SatNOGS observation ID	GS name	GSs location	Coordinates
1st	6548664	280 Grove UHF-02	MA, USA	42.314°, -71.448°
2nd	6548729	1461 VE2DSK VHF UHF	QC, Canada	45.651°, -73.564°
3rd	6548804	526 W2GRK UHF	NY, USA	40.641°, -74.339°
4th	6548857	805 RPi3	PA, USA	40.676°, -75.608°
5th	6548763	1452 VE2DTL UHF VHF	MTL, Canada	45.315°, -73.750°

After the VGS received the five recordings, the audio files were loaded into MATLAB to start the preprocessing process to retrieve the recordings' numbers, dates, time frames, and

the lengths in samples. Then, MATLAB started the processing and combining process that can be summarized as:

- The received time-discrete baseband audio samples are converted into digital stream of 1 and 0.
- The algorithm finds only the best match for each identifier's default content in its long format and returns the detected pattern's start and end indices as well as the ED as a measure of how well the extracted version approaches the default content.
- The algorithm extracts the five replicas of each identifier from the involved five GSs and forms a square pre-combining matrix where the n^{th} row corresponds to the n^{th} version of that identifier received by the n^{th} GS.
- The algorithm combines each column in the pre-combining matrix relying on the ML of the entrees at that column. The most likely occurring bit in that column is selected as the right one.
- The error of each individually received identifier is calculated and compared to the combined version's error.

The MATLAB script for **Experiment A** is provided in **Appendix E**.

4.5.4.2 Experiment B

In this experiment, the main goal was to focus on only combining multiple versions of VZLUSAT-2's Sync-Word but in a time manner. The NOEs of the Sync-Word versions to combine at each combining trial must be evaluated versus the NOE of the combined Sync-Word. In this experiment, five GSs from the United States and Canada were involved in this experiment to receive the VZLUSAT-2's beacon signal on the 11^{th} of March 2023. The names, locations, and coordinates of the GSs at which the VZLUSAT-2's beacons were recorded are provided in **Table 4**.

TABLE 4
DETAILS OF 5 GROUND STATIONS TO RECORD THE SIGNALS IN EXPERIMENT B

No.	SatNOGS observation ID	GS name	GSs location	Coordinates
1^{st}	7260639	526-W2GRK-UHF	NJ, USA	40.641°, -74.339°
2^{nd}	7260640	1461 VE2DSK VHF UHF	QC, Canada	45.651°, -73.564°
3^{rd}	7260641	2302-AB3ZW	MD, USA	39.462°, -76.332°
4^{th}	7260644	2834-kc0iyt	MA, USA	40.676°, -75.608°
5^{th}	7260633	901-VE2WI- UHF	MTL, Canada	45.315°, -73.750°

The whole process performed in this experiment is summarized in the following steps:

- Loading the observations audio files into MATLAB.

- Converting them from time-discrete baseband samples into digital stream of 1 and 0.
- Finding the up-sampled Sync-Words (320-sample length) in each observation when the errors are less than the defined error tolerance (i.e., threshold), counting them, identifying the start and end indices of each found version.
- Calculating errors in the detected Sync-Words in their short format (32-bit) .
- Retrieving the date, observation start time, and the observation duration from the original audio files. The standard audio file naming format should include the date and the start time of the recording while the duration can be retrieved by using the **audioinfo** function in MATLAB which returns a structure containing all the required information.
- Then, the time at which each observation ends can be calculated by adding the start time to the duration of that observation.
- By sorting the start and end times of all observations, we can identify the earliest and the latest ones.
- Calculating the total satellite's visibility duration by subtracting the earliest from the latest.
- Creating a time reference vector which should start at the time of the earliest observation and end at the time of the latest one.
- Multiplying the total visibility duration, in seconds, by the sampling rate, yields the number of samples in the reference vector which should accommodate all the observations if stacked in a time manner.
- All observations are zero padded, before their start and after their end, to match the length of the reference vector. The earliest observation, for example, gets no zeros at the beginning since its start time matches the start time of the reference vector. On the other hand, no zeros are added after the end of the latest observation because its end matches the end time of the reference vector.
- In a time manner, starting from the time of the earliest record to the time of the latest record and within a search window of 5 seconds, all observations are checked for the presence of Sync-Words within each search window.
- If there are, the algorithm combines them and shifts the search window forward. The counter for the combining is increased by one and errors are calculated for the individual Sync-Words before the combining and for the combined version. If there

aren't any Sync-Words within a search window, the window is shifted forward. In either case, the search window shift is 3 seconds.

- At each combining trial, the NOE in the combined Sync-Word is compared to NOEs in the individual Sync-Words within the same combining window.

The MATLAB script for **Experiment B** is provided in **Appendix F**.

4.5.4.3 Experiment C

To validate the proposed concept and the developed likelihood combining method, this experiment aimed to combine all the identifiers (Preamble followed by Sync-Word, Header, and fixed data part as shown previously in **Figure 30**) detected from six GSs in a time manner. In this experiment, SatNOGS was utilized to access the global network of GSs across the United States and Canada and search for the visibilities of the VZLUSAT-2 after the time at which the communication to the main GS in Pilsen is terminated. The visibility search revealed six possible observations at the GSs listed in **Table 5** according to the corresponding times and locations indicated in the table.

TABLE 5
DETAILS OF SIX GROUND STATIONS TO RECORD THE SIGNALS IN EXPERIMENT C

No.	SatNOGS observation ID	GS name	Location	Time frame (HH:MM:SS)
1st	7260546	526-W2GRK	NJ, USA	02:22:51 - 02:27:52
2nd	7260550	2617-K2PI	VA, USA	02:23:05 - 02:27:03
3rd	7260625	385-52 HancockSt	MA, USA	02:24:06 - 02:27:21
4th	7260626	432-kc1fha	NH, USA	02:23:50 - 02:27:50
5th	7260638	1461-VE2DSK	QC, CA	02:22:07 - 02:31:11
6th	7260643	2834-kc0iyt	MA, USA	02:23:17 - 02:28:09

The processing steps in **Experiment C** can be summarized as follows:

- The six recorded audio files are offloaded into the VGS's PC and stored in one directory. Then, the audio files are loaded into MATLAB for processing.
- Before going into the analysis of the collected records, it is worth exploring the timeline of observations and their overlapping as described earlier in **Subsection 4.5.3.1**. The MATLAB script for visualizing of the records is provided in **Appendix G**.
- By sorting the start and end times of all observations, we can identify the earliest and the latest ones.
- Calculating the total satellite's visibility duration to the six GSs by subtracting the earliest from the latest.

- Creating a time reference vector which should start at the time of the earliest observation and end at the time of the latest one. Also, multiplying the total visibility duration, in seconds, by the sampling rate of VZLUSAT-2, yields the number of samples in the reference vector which should accommodate all the observations if stacked in a time manner.
- Converting the audio records from time-discrete into digital.
- Searching for the up-sampled identifiers packet (2000-sample length) in each observation when the errors are less than the defined error tolerance (i.e., threshold), counting them, identifying the start and end indices of each found version.
- All observations are zero padded, before their start and after their end, to match the length of the reference vector. The earliest observation, for example, gets no zeros at the beginning since its start time matches the start time of the reference vector. On the other hand, no zeros are added after the end of the latest observation because its end matches the end time of the reference vector.
- In a time manner, the combining algorithm navigates through the six records within a combining window of five seconds and checks for the possibility that more than two identifiers' packets are present. If it happens that a combining window includes more than two packets, the pre-combining matrix **C** is generated by concatenating the detected packets on top of each other.
- Then, the likelihood combining is performed on each column in the matrix **C** to generate the combined version.
- The counter for the combining is increased by one and the algorithm shifts the search window forward. If there aren't any packets within a search window, the window is also shifted forward. In either case, the search window shift is 3 seconds.
- The next step is to convert the detected packets from the long sample-based format into the short symbol-based representation according to the ratio (sampling rate of SatNOGS /baud rate of VZLUSAT-2) which yields 10 samples per symbol as mentioned in **Section 4.5.3.2**.
- Calculating errors of the detected identifiers' packets in the short format of 200-bit.
- At each combining trial, the error of the combined version is compared to the individual errors of the packets from which the combined version is generated.

- The results are visualized in a way so that each GS can compare the NOE of any individually received `packet in that GS to the NOE of the combined version generated in the same time window in which its individual packet is received.

The MATLAB script for **Experiment C** is provided in **Appendix H**.

4.5.4.4 Experiment D

Experiment D aims to test the system scalability in combining the VZLUSAT-2's identifiers packet in a time manner exactly as performed in **Experiment C** but with extended number of cooperative sites to include three more GSs. Thus, no more settings or procedures to clarify here in this experiment more than what was previously expressed in **Experiment C**. The details of nine GSs involved in **Experiment D** are given in **Table 6**.

TABLE 6
DETAILS OF NINE GROUND STATIONS TO RECORD THE SIGNALS IN EXPERIMENT D

No.	SatNOGS observation ID	Time frame (HH:MM:SS)
1st	7260546	02:22:51 - 02:27:52
2nd	7260550	02:23:05 - 02:27:03
3rd	7260625	02:24:06 - 02:27:21
4th	7260626	02:23:50 - 02:27:50
5th	7260638	02:22:07 - 02:31:11
6th	7260640	02:23:30 - 02:32:24
7th	7260641	02:22:40 - 02:29:58
8th	7260643	02:23:17 - 02:28:09
9th	7260644	02:23:01 - 02:27:22

The MATLAB scripts provided in **Appendix G** and **Appendix H** also apply to the implementation of **Experiment D** after saving the nine records in the defined file directory.

5 Main Results Achieved

The results are presented in two main sections in this chapter in accordance with the implementation steps. **Section 5.1** depicts the results of the simulated cooperative model from initial phases of research including the raw post-detection combining, the further improvement techniques, and the pre-detection combining. The findings of post-detection combining, the suggested improvement techniques, and the concept of VGS are published in [75, 76], while the results of the pre-detection combining are published in [77]. The main achieved experimental results of the deployed model of diversity combining are presented in **Section 5.2** confirming the whole concept of cooperative reception with diversity combining of real satellite signals captured by six and nine GSs. The outcome of combining the best detected match for VZLUSAT-2's identifiers are accepted for publication in [78], while the findings of combining all detected Sync-Words in a time manner are published in [79]. Lastly, the results of combining all VZLUSAT-2's identifiers in a time manner along with the performance evaluation versus the current system are published in [80].

5.1 The results of the simulated cooperative model

5.1.1 The results of the raw post detection combining

The BER results of the raw combining algorithm at each combining trial are presented in linear and logarithmic scales respectively in **Figures 31** and **32**. It is clear to see that the BER gets improved as we engage more receiving sites in the cooperative system. Interesting behaviour in the combining trials is that the BER of the system is slightly improved when observing two successive trials, from an odd number of sites to an even number. On the other hand, significant BER reduction between two successive trials is achieved when the first one is for even number of sites and the following one is odd.

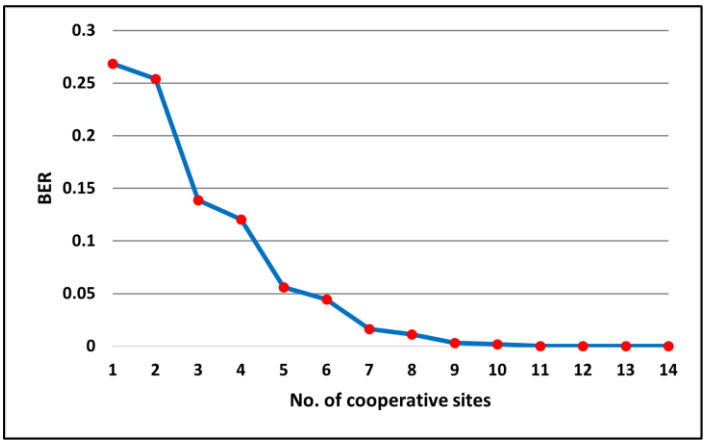

Figure 31. Linear BERs for combining 14 cooperative sites with SNRs of (0–13) dB

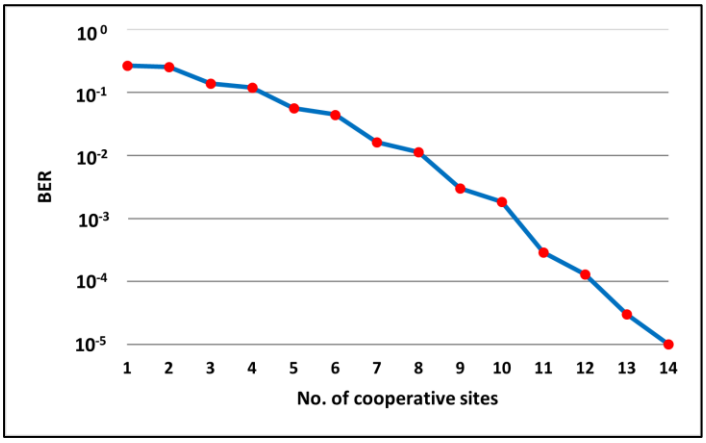

Figure 32. Logarithmic BERs for combining 14 cooperative sites with SNRs of (0–13) dB.

This behaviour is attributed to the fact that the detection hypothesis is based on bit disagreement rule which has more errors likely to occur when the number of entrees is even, as explained earlier in **Section 4.4.1**.

The ED can be measured to indicate how close the received versions and the combined one are from the original message stream through:

$$\mathrm{ED}_{a,b} = \mathrm{sqrt}\big((a-b) * (a-b)'\big),$$

where a and b can be any signal vectors of the same length.

In a million-bit length of data streams, the least calculated ED between the original message and the received versions, $r_{1:N}$, is 18.0831, whereas it is only 3.1623 between the original message signal and the combined stream r_c. This can reflect how alike the combined stream and the original message are and how well the combined stream approached the original data distribution.

5.1.2 The results of further improvement techniques

To overcome the downside of combining even number of sites, three improvement techniques are suggested in **Section 4.4.2** to modify the raw combining algorithm. **Table 7** lists the achieved BER of each suggested technique versus the raw combining BER values. Excluding the worst stream out of the combined streams has reflected slight improvement compared to the raw combining BER values. Replacing that worst stream with the best one has improved the performance even better. The best achieved BER values are when always injecting the best stream into the combining matrix reaching zero error at early stages of combining trials.

TABLE 7
BER RESULTS FROM RAW DIVERSITY COMBINING AND PROPOSED IMPROVEMENTS

No. of sites	Raw	Worst excluded	Worst replaced	Best tailed
1	0.26862	0.26862	0.26862	0.26862
2	0.25414	0.21686	0.11775	0.05261
3	0.13884	0.10295	0.0468	0.00645
4	0.12037	0.08797	0.05483	0.00044
5	0.05619	0.03321	0.01966	2e-5
6	0.04439	0.025	0.01785	0
7	0.01624	0.00694	0.00501	0
8	0.01131	0.00445	0.00362	0
9	0.00301	0.00087	0.00069	0
10	0.00183	0.00041	0.0004	0
11	0.00029	5e-5	6e-5	0
12	0.00013	2e-5	4e-5	0
13	3e-5	0	0	0
14	1e-5	0	0	0

Figures 33 and **34** present the simulation BER results of the original combining algorithm as well as the three proposed ones for further improvement respectively in linear and logarithmic scales. The infinitive logarithmic quantities resulting from zero BERs explain why the linear scale results are also provided here as they are more informative. Obviously, the three SP algorithms improved the system performance in achieving less detected errors compared to the raw combining. Rejecting the worst quality stream slightly enhanced the system performance with more than 50% errors reduction in the combining trials of more than 7 sites. Replacing that worst stream with the best one led to an even better performance. In the last proposed technique, the best stream was repeatedly tailed to the combining matrix imposing more detection weight for the least corrupted received signal version. Doing so, the system achieved zero errors detection process as early as only 6 sites were engaged in the given simulation settings.

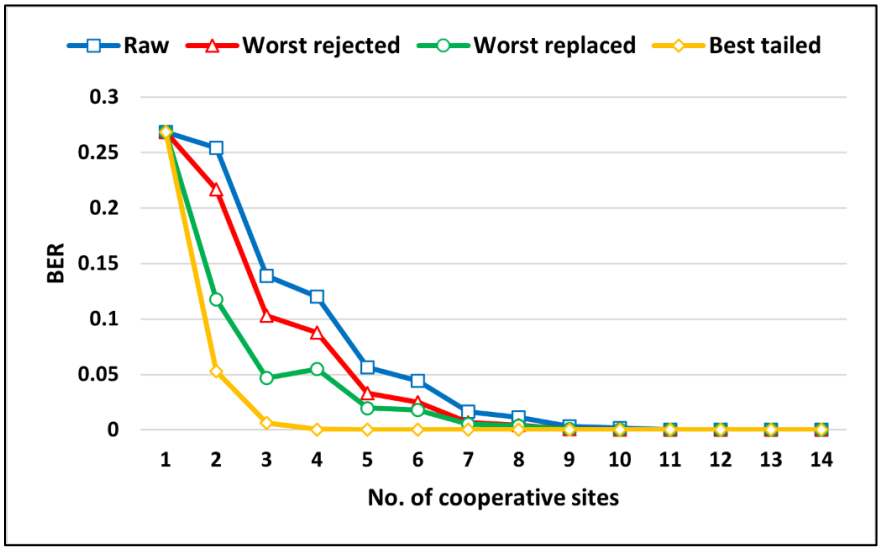

Figure 33. Linear BER curves from raw and the proposed improvement techniques.

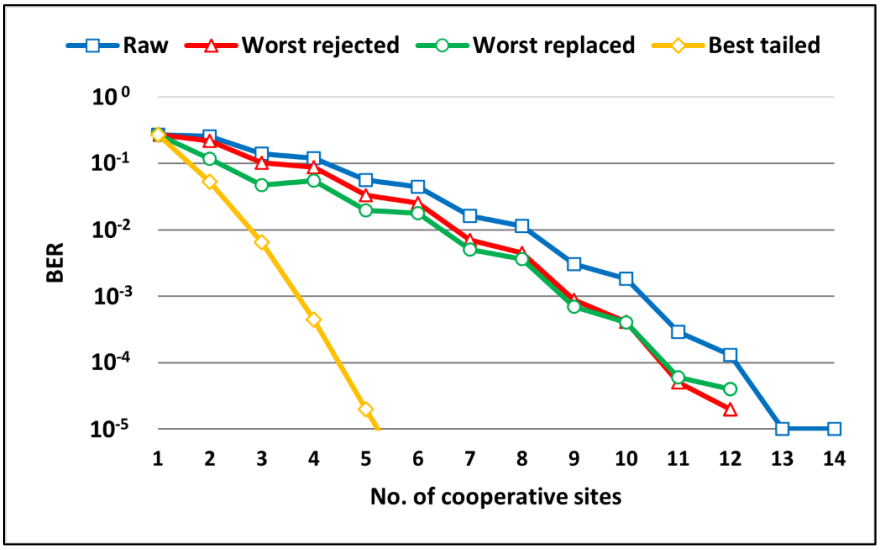

Figure 34. Logarithmic BER curves from raw and the proposed improvement techniques.

The proposed improvement algorithms have been tested for consistency to different data sample lengths and shown great scalability by reflecting the same system behavior. **Table 8** summarizes the elapsed execution times for the 1-milion data set, used in this investigation, in addition to other tested data lengths.

TABLE 8
ELAPSED TIMES IN (SECONDS) TAKEN BY THE ALGORITHMS TO COMBINE 14 STREAMS

Data length	Worst excluded	Worst replaced	Best tailed
10e5[1]	9.439559	10.967350	19.539677
10e4	0.948979	1.131833	2.061516
10e3	0.108183	0.130703	0.256498
10e2	0.043260	0.050263	0.056976
2×10e5	18.795995	21.877629	38.563990

[1] Denotes the used data length in this work.

5.1.3 The results of the pre-detection combining

To present the results of the proposed system when utilizing the pre-detection combining, the following five scenarios are applied for combining twelve receiving sites as elaborated in **Section 4.4.3**:

1. **Uncorrelated**: 12 sites with SNRs of (0-11) dB.
2. **Below average**: 12 sites with SNRs of (2-3) dB.
3. **Above average**: 12 sites with SNRs of (8-9) dB.
4. **Correlated**: 12 sites with SNRs of 7 dB.
5. **Severe**: 12 sites with SNRs of 0 dB but one of 8 dB.

For the five testing scenarios, the individual (single), the combining, the average (Avg.), and the minimum (Min.) BERs are presented in **Figures 35, 36, 37, 38,** and **39** in the linear scale due to the infinite logarithmic quantities resulting from zero BER as emphasized earlier in this chapter.

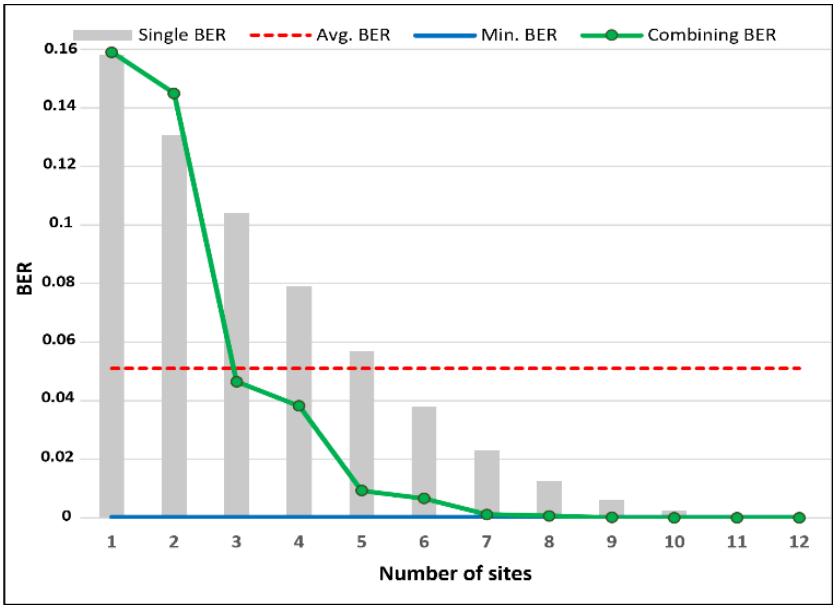

Figure 35. BERs from the uncorrelated scenario of 12 sites with SNRs of (0-11) dB.

In **Figure 35**, the cooperative network under the first scenario achieved a combining BER that was lower than the average BER of the twelve sites when only three sites were involved. It was also shown that the combining BER outperformed the minimum BER among the twelve sites when combining nine sites.

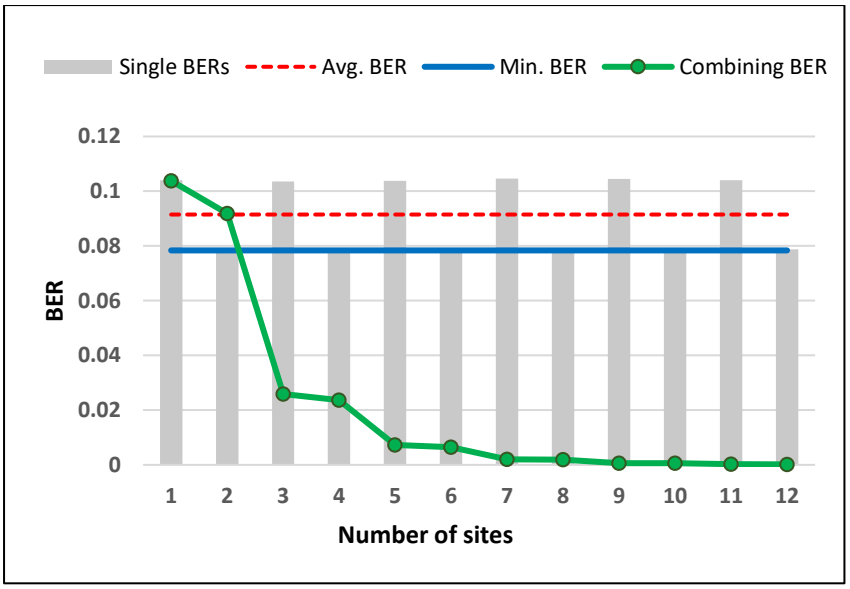

Figure 36. BERs from the below average scenario of twelve sites with SNRs of (2-3) dB.

In **Figure 36**, the combining BER maturely surpassed the average as well as the minimum BERs when only three sites were combined.

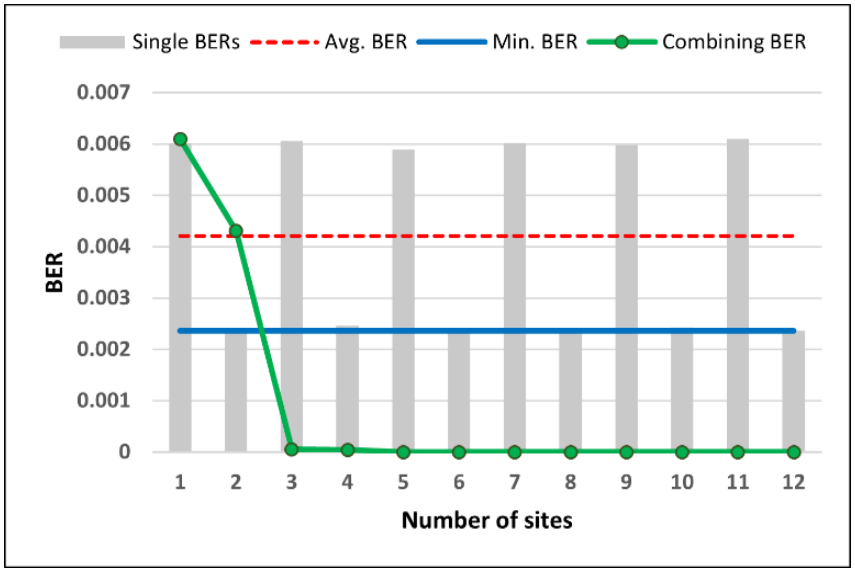

Figure 37. BERs from the above average scenario of 12 sites with SNRs of (8-9) dB.

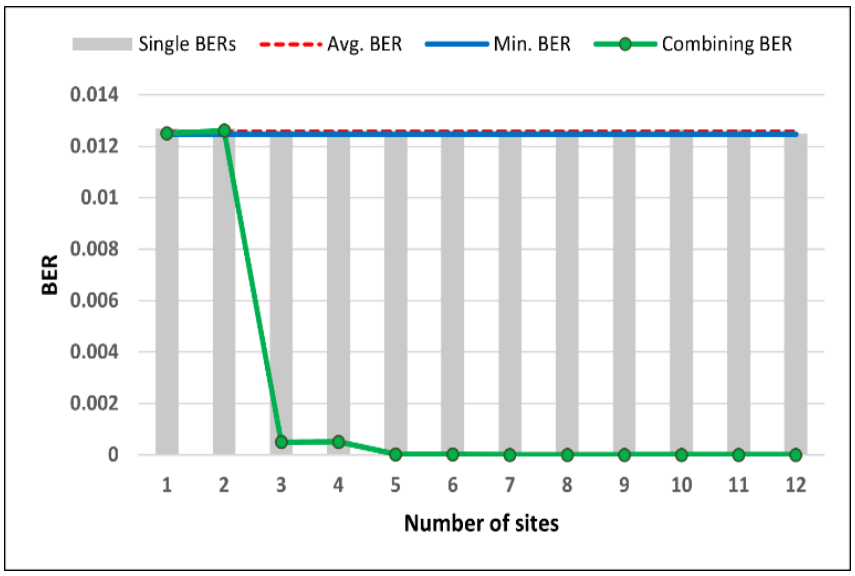

Figure 38. BERs from the correlated scenario of 12 sites with SNRs of 7 dB.

In **Figures 37** and **38**, the resulting BERs for combining 12 sites under above average and correlated scenarios, respectively, performed as good as in the previous scenario in overpassing the average and minimum BERs when only three sites were combined.

Even when only one site, out of twelve ones, received good signal, the proposed scheme achieved a combining BER of better than the average BER and the minimum BER requiring three and eleven sites respectively as shown in **Figure 39**.

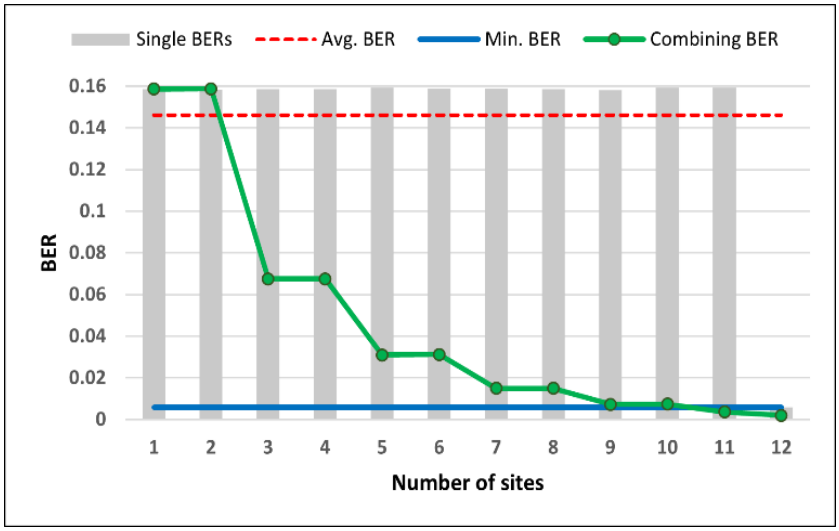

Figure 39. BERs from the severe scenario of 12 sites with SNRs of 0 dB but one of 8 dB.

Overall, the SIMO-based reception system performed remarkably well in all tested scenarios when the received versions are combined before being demodulated.

5.2 The results of the deployed cooperative model

For the purpose of validating the theoretical concept of networking multiple GSs to improve the reception quality of small satellites' signals, this section depicts the results of **Section 4.5** including **Experiment A** for combining the best detected match of the Preamble, Sync-Word, Header, and Callsign from five VZLUSAT-2's beacon signals, **Experiment B** for combining all detected Sync-Words from five VZLUSAT-2's beacon signals in a time manner, **Experiment C** for combining all detected identifiers' packets from six VZLUSAT-2's beacon signals in a time manner, and **Experiment D** for combining all identifiers in a time manner as in **Experiment C** but from nine VZLUSAT-2's beacon signals.

5.2.1 The results of Experiment A

Table 9 lists the recording numbers, the corresponding SatNOGS observation IDs, the locations of the receiving GSs, recording dates and times, the lengths of the five recordings in samples, and finally whether each GS was able to decode the received stream or not. Looking at the last column of **Table 9**, it is shown that only the 1st and 2nd recordings were good enough for the corresponding GSs to decode the received streams and retrieve the transmitted data. The 3rd GS had a waterfall with visible beacons but was not good enough to decode the data. In the 4th and the 5th recordings, no beacons were recognized in their waterfalls and accordingly the corresponding GSs could not get any decoded data. As a result, such combination of good, bad, and failed recordings is typical for this experiment

when applying receive diversity scheme. The suggested scheme can then show how much improvement is achieved if these five GSs work cooperatively to retrieve the original data.

TABLE 9
RETRIEVED DETAILS OF 5 GROUND STATIONS TO RECORD THE SIGNALS IN EXPERIMENT A

No.	SatNOGS observation ID	GSs location	Date (yyyy-mm-dd)/ Time (HH-MM-SS)	Length in samples	(waterfall with visible beacon? audio file? decoded data? if yes how many packets?)
1st	6548664	MA, USA	2022-09-30/14-39-30	16,080,960	(Yes, Yes, Yes-4)
2nd	6548729	QC, Canada	2022-09-30/14-37-17	24,084,288	(Yes, Yes, Yes-4)
3rd	6548804	NY, USA	2022-09-30/14-41-01	10,219,072	(Yes, Yes, No)
4th	6548857	PA, USA	2022-09-30/14-39-37	18,481,472	(No, Yes, No)
5th	6548763	MTL, Canada	2022-09-30/14-38-13	19,240,640	(No, Yes, No)

The following four tables present the results of combining the identifiers: Sync-Words, Headers, Preambles, and Callsigns. When combining the Sync-Words, **Table 10** shows that the detected errors at the five GSs, when they worked independently, were 1, 1, 3, 3, and 4, respectively. However, there was not even one error retrieving the default Sync-Word from the combined version.

TABLE 10
RESULTS OF COMBINING THE BEST MATCH OF SYNC-WORDS FROM 5 GSS IN EXPERIMENT A

No.	SatNOGS observation ID	Sync-Word starts @	Sync-Word ends @	NOE	BER
1st	6548664	3.1315e+05	3.13181e+05	1	0.03125
2nd	6548729	1.621385e+06	1.621416e+06	1	0.03125
3rd	6548804	4.13034e+05	4.13065e+05	3	0.09375
4th	6548857	5.56114e+05	5.56145e+05	3	0.09375
5th	6548763	24119	24150	4	0.125
Combined Sync-Word		**1**	**32**	**0**	**0**

The same improvement applies when retrieving the Headers from the combined streams. In all combining trials, the combined version recorded an error less than the minimum error among the five GSs as listed in **Table 11**. This improvement reflects how reliable the reconstruction of the original data in such a system configuration was for the five stations, even those that failed to receive the satellite signal. Based on **Table 12**, the recordings from the 4th and 5th GSs were severely degraded since they resulted in 154 errors in identifying the Preamble with such high BER. These two GSs can still be involved in such a cooperative reception system because even with high BER, the identifiers packets were well detected in the combined stream. **Table 13** shows that the combined Callsign has less errors compared to all other individual ones. This cooperation in receiving weak small satellites' signals can significantly reduce the probability of outages at any GS in the presented model.

TABLE 11
RESULTS OF COMBINING THE BEST MATCH OF HEADER FROM 5 GSS IN EXPERIMENT A

No.	SatNOGS observation ID	Header starts @	Header ends @	NOE	BER
1st	6548664	1.6003e+05	1.60061e+05	3	0.09375
2nd	6548729	2.23144e+05	2.23175e+05	3	0.09375
3rd	6548804	1.09915e+05	1.09946e+05	3	0.09375
4th	6548857	9.91337e+05	9.91368e+05	3	0.09375
5th	6548763	8965	8996	2	0.0625
Combined Header		**1**	**32**	**0**	**0**

TABLE 12
RESULTS OF COMBINING THE BEST MATCH OF PREAMBLE FROM 5 GSS IN EXPERIMENT A

No.	SatNOGS observation ID	Preamble starts @	Preamble ends @	NOE	BER
1st	6548664	9.6961e+05	9.70009e+05	0	0
2nd	6548729	9.4112e+05	9.41519e+05	0	0
3rd	6548804	5.7151e+05	5.71909e+05	0	0
4th	6548857	5.3613e+05	5.36529e+05	154	0.385
5th	6548763	1.6459e+05	1.64989e+05	154	0.385
Combined Preamble		**1**	**400**	**0**	**0**

TABLE 13
RESULTS OF COMBINING THE BEST MATCH OF CALLSIGN FROM 5 GSS IN EXPERIMENT A

No.	SatNOGS observation ID	Callsign starts @	Callsign ends @	NOE	BER
1st	6548664	9650	9721	15	0.20833
2nd	6548729	2.156205e+05	21.56276e+05	15	0.20833
3rd	6548804	5.35142e+05	5.35213e+05	17	0.23611
4th	6548857	2.63946e+05	2.64017e+05	16	0.22222
5th	6548763	8.42379e+05	8.42450e+05	17	0.23611
Combined Callsign		**1**	**72**	**7**	**0.09722**

5.2.2 The results of Experiment B

Experiment B's observations order, IDs, time frames, lengths, and whether the GSs were able to receive the waterfalls, audio files, and decoded data are listed in **Table 14**.

TABLE 14
RETRIEVED DETAILS OF 5 GROUND STATIONS TO RECORD THE SIGNALS IN EXPERIMENT B

No.	SatNOGS observation ID	GSs location	Date (yyyy-mm-dd)/ Time (HH-MM-SS)	Length in samples	(waterfall with visible beacon? audio file? decoded data? (if yes how many packets?))
1st	7260639	NJ, USA	2023-03-11/15:29:16	14916032	(Yes, Yes, No)
2nd	7260640	QC, Canada	2023-03-11/15:25:53	25653184	(Yes, Yes, Yes (27))
3rd	7260641	MD, USA	2023-03-11/15:28:19	21029440	(Yes, Yes, No)
4th	7260644	MA, USA	2023-03-11/15:28:51	12573120	(Yes, Yes, Yes (2))
5th	7260633	MTL, Canada	2023-03-11/15:27:32	16577728	(No, Yes, No)

The results of the search for 320-sample (i.e., long format) Sync-Word replicas within each recording for a threshold of 55 errors were as listed in **Table 15**. There were 9, 41, 2, 12, and 0 Sync-Words found in the 1st to the 5th observation, respectively. The earliest recording was found to be the 2nd while the latest recording was the 3rd one. Accordingly, when calculating the total visibility duration of the VZLUSAT-2 over these five GSs, the result was (00:09:44) according to the time format (HH:MM:SS), or equivalently 584.1133 sec. after considering the fractions of seconds.

TABLE 15
RESULTS OF SYNC-WORD SEARCH IN THE OBSERVATIONS IN EXPERIMENT B

No.	SatNOGS observation ID	Number of Sync-Words	Max. error	Min. error
1st	7260639	9	50	17
2nd	7260640	41	54	1
3rd	7260641	2	54	36
4th	7260644	12	54	8
5th	7260633	0	-	-

The next step was to extend the data vector of each recording through zero padding to match the length of the reference vector starting from the earliest record and ending at the latest one as explained earlier in **Subsection 4.5.3.3**. The generated same length five extended vectors are stacked horizontally into one square combining matrix. The resulting matrix whose rows and columns are respectively the same as the number of recordings and the number of elements in the reference vector, is going to be the matrix at which the combining is performed. When running the combining algorithm, the results are listed in **Table 16**.

TABLE 16
RESULTS OF COMBINING SYNC-WORDS IN EXPERIMENT B

Combining counter	Sync-Words from	Errors before	Combining error	Combining counter	Sync-Words from	Errors before	Combining error
1	2nd + 4th	0+2	**0**	18	2nd + 4th	0+0	**0**
2	2nd + 4th	0+2	**0**	19	2nd + 3rd+4th	0+2+0	**0**
3	2nd + 4th	0+3	**0**	20	2nd + 4th	0+0	**0**
4	2nd + 4th	0+3	**0**	21	2nd + 4th	0+0	**0**
5	2nd + 4th	0+3	**0**	22	1st +2nd	0+0	**0**
6	2nd + 4th	0+4	**0**	23	1st +2nd	4+0	**0**
7	2nd + 4th	0+4	**0**	24	1st +2nd	4+0	**0**
8	2nd + 4th	0+2	**0**	25	1st +2nd	1+0	**0**
9	2nd + 4th	0+2	**0**	26	1st +2nd	1+0	**0**
10	2nd + 3rd+4th	0+5+0	**0**	27	1st +2nd	0+0	**0**
11	2nd + 4th	0+0	**0**	28	1st +2nd	1+0	**0**
12	2nd + 4th	0+0	**0**	29	1st +2nd	1+0	**0**
13	2nd + 4th	0+0	**0**	30	1st +2nd	1+0	**0**
14	2nd + 4th	0+0	**0**	31	1st +2nd	1+0	**0**
15	2nd + 4th	0+0	**0**	32	1st +2nd	1+0	**0**
16	2nd + 4th	0+0	**0**	33	1st +2nd	0+1	**0**
17	2nd + 4th	0+0	**0**	34	1st +2nd	0+1	**0**

In the first 32 combining trials, the combining algorithm performed well in getting zero detection errors which were as good as the errors of the 2nd version. However, even when such strong candidate of the 2nd version had detection errors at the 33rd and the 34th combining trials, the combined version maintained zero detection errors. Indeed, this makes the combined version more reliable in retrieving the Sync-Word with less errors than any other individually received version.

5.2.3 The results of Experiment C

The order of the six observations in this experiment, the IDs, the time frames, the lengths, and whether the corresponding GSs were able to receive the waterfalls, the audio files, and the decoded data are depicted in **Table 17**.

TABLE 17
DETAILS OF SIX GROUND STATIONS TO RECORD THE SIGNALS IN EXPERIMENT C

No.	SatNOGS observation ID	GSs location	Date (yyyy-mm-dd)/ Time (HH-MM-SS)	Length in samples	(waterfall with visible beacon?, audio file?, decoded data? (if yes how many packets?))
1st	7260546	NJ, USA	02:22:51 - 02:27:52	14490048	(Yes, Yes, Yes (1))
2nd	7260550	VA, USA	02:23:05 - 02:27:03	11425600	(Yes, Yes, No)
3rd	7260625	MA, USA	02:24:06 - 02:27:21	9407680	(Yes, Yes, No)
4th	7260626	NH, USA	02:23:50 - 02:27:50	11543104	(No, Yes, No)
5th	7260638	QC, CA	02:22:07 - 02:31:11	26155072	(Yes, Yes, Yes (11))
6th	7260643	MA, USA	02:23:17 - 02:28:09	14050624	(Yes, Yes, Yes (1))

Then, the algorithm sorts the times and identifies when the earliest and the latest visibilities of VZLUSAT-2 were, and to which GSs. To explore the overlapping of the records' times, they were visualized in a time manner in **Figure 40**, where the horizontal axis represents the observation time, and the vertical axis represents a shift for better visualization and has nothing to do with the power or the amplitude of the records.

According to the satellite's visibilities, the earliest observation was at (02:22:07) to the 5th GS while the latest one was at (02:31:11) to 5th GS as well. The first overlapping in the observations' times was at (02:22:51) between the 5th and 1st observations whereas the last time overlapping was at (02:28:09), the end of the 6th observation. In between the first and the last time overlapping, signals combining was possible. The total visibility time for the six GSs was (00:09:04), which corresponds to 544 seconds.

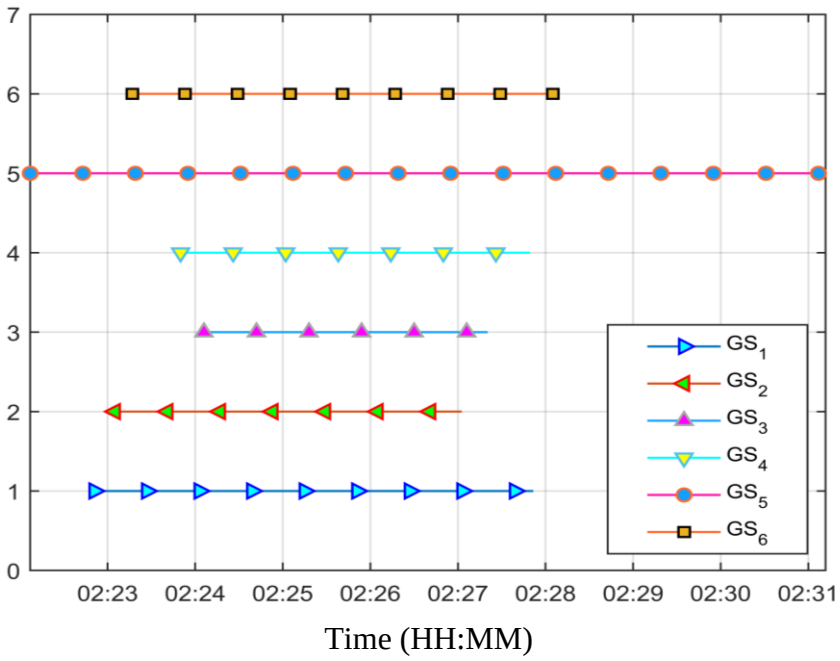

Figure 40. VZLUSAT-2's visibility times to the six GSs in Experiment C.

For the six records in **Experiment C**, there were 14, 20, 9, 0, 38, and 10 detected 2000-sample packets within the given threshold of 400 errors. Then, the algorithm checks for any redundant packets if spaced by less than the default spacing of 10 seconds and deletes them. Accordingly, the algorithm modifies the number of detected packets and the corresponding information. The updated numbers of the detected packets in the collected six records are depicted in **Table 18**.

TABLE 18
DETAILS OF RECORDS AND DETECTED PACKETS IN EXPERIMENT C

No.	SatNOGS observation ID	Lengths	Packets	Updated packets
1st	7260546	14490048	14	12
2nd	7260550	11425600	20	14
3rd	7260625	9407680	9	7
4th	7260626	11543104	0	0
5th	7260638	26155072	38	28
6th	7260643	14050624	10	7

Table 18 shows that the 4th GS had communication outage and did not receive any detectable signal within the defined error tolerance of 400 errors. Therefore, the search for the identifiers' packets in the 4th observation revealed no detected packets. The next step is to align the records in a way so that the combining can be performed in a time manner with respect to the visibility of the satellite to the six GSs. This is done through front and rear zero paddings for each record, so they match the start of the earliest and the end of the latest records. The zero paddings of the six records are summarized in **Table 19**.

TABLE 19
THE REQUIRED FRONT AND REAR ZEROS FOR ALIGNING THE RECORDS IN EXPERIMENT C

No.	SatNOGS observation ID	Original lengths	Front zeros	Rear zeros
1st	7260546	14490048	2112000	9553024
2nd	7260550	11425600	2784000	11945472
3rd	7260625	9407680	5712000	11035392
4th	7260626	11543104	4944000	9667968
5th	7260638	26155072	0	0
6th	7260643	14050624	3360000	8744448

As shown in the previous table, the 5th record neither did require zeros in the front nor in the rear paddings as it is the earliest and the latest observation. After the zero-padding process is complete, the start and end of the six records become aligned and have the same length of (26155072) samples.

For combining the six records received by six GSs in this experiment, from the time of the earliest observation to the time of the latest one, there were 11 combining trials and accordingly 11 combined packets were generated. Because 11 trials of combining multiple 2000-sample versions of the identifiers packet are huge to visualize, only 4 trials of combining multiple 200-sample parts of the Sync-Word were selected and visualized. The 2nd, 3rd, 4th, and 5th combining trials are presented respectively in **Figures 41**, **42**, **43**, and **44**. This collection of trials was carefully selected to provide sufficient insight into the combining method. Errors present in the individual versions are marked inside red ellipses. In the combined version, the corrected errors are marked inside blue ellipses while uncorrected ones are kept inside red ones.

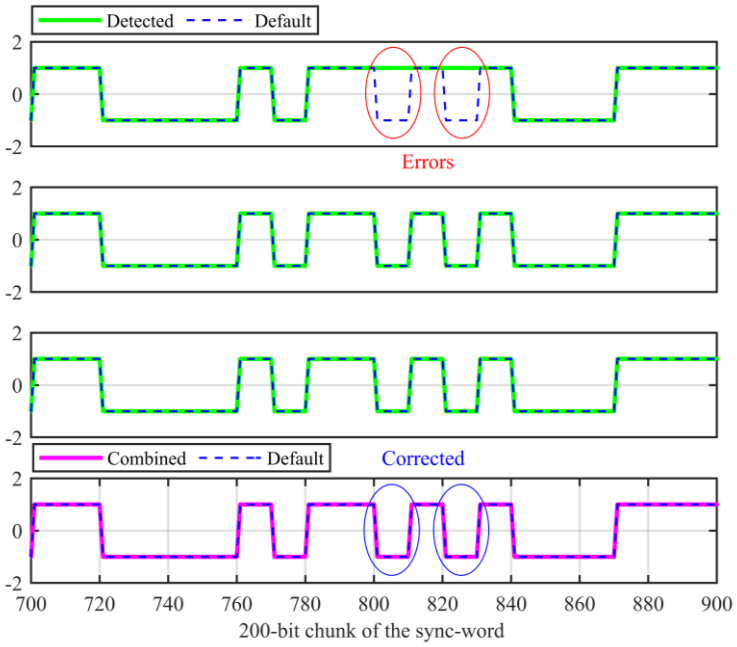

Figure 41. Combining 3 versions (200-bit long) of Sync-Word in the 2nd combining trial.

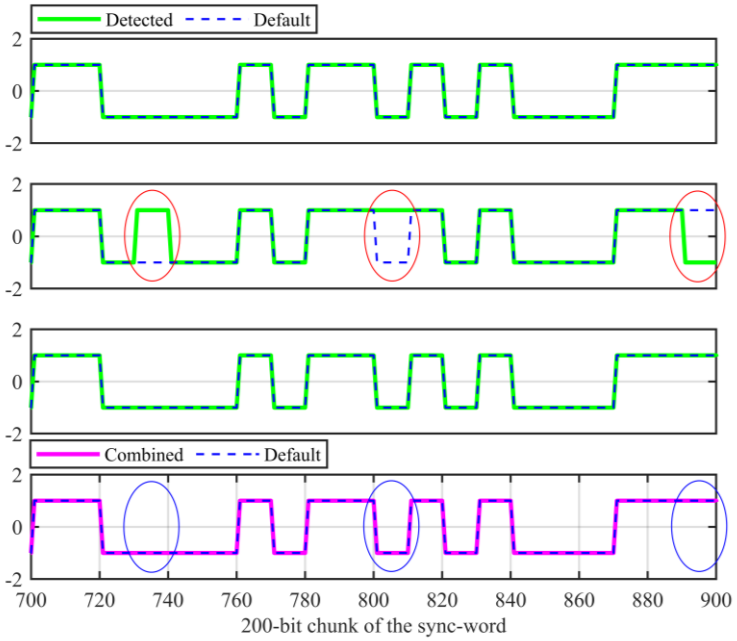

Figure 42. Combining 3 versions (200-bit long) of Sync-Word in the 3rd combining trial.

Figures 41 and **42** show that errors present respectively in the first and second versions were corrected in the corresponding combined versions.

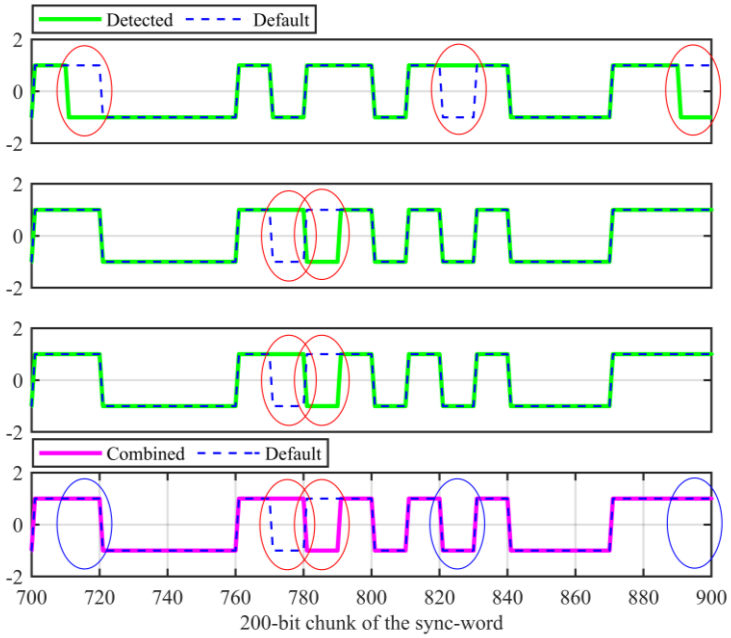

Figure 43. Combining 3 versions (200-bit long) of Sync-Word in 4th combining trial.

In **Figure 43**, the combined version corrected errors only from the first version and uncorrected the ones from other versions because more than half of the entrees at these positions were errors.

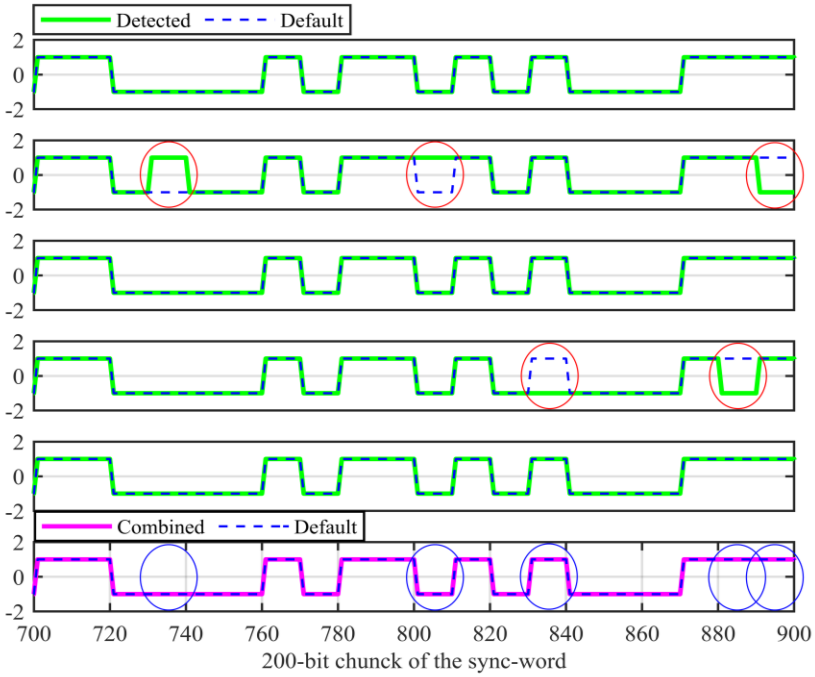

Figure 44. Combining 5 versions (200-bit long) of Sync-Word in the 5th combining trial.

In the 5th combining trial, visualized in **Figure 44**, all errors from the second and fourth versions were corrected in the combined version.

In each presented trial, the combining of multiple versions corrected some errors and provided a better-quality version than some individual ones. However, that achieved quality was as good as some other individual versions. The question then becomes, does the proposed cooperative reception provide an improved performance to only some of the involved GSs? To find the answer, a more generalized assessment of the combined version is required. The quality of the combined identifiers' packets must be compared to the quality of each individually received packet by the corresponding GS in a time manner.

In the assessment process, a referencing counter is set to zero and a time window of five seconds is generated to navigate through the generated combined packets with respect to the visibility time. Within each time window, the algorithm compares the NOE in the combined packet with the NOE of the packet available in each record individually. For instance, when validating the combined packets versus the packets in the first record, the referencing counter increases by one every time a combined packet is present along with a packet in the first record within the same window. Such a validation method provides a fair comparison for each GS and shows how beneficial or not to join the diversity-based reception scheme.

Since the 4th GS experienced an outage and its record revealed no packets, the assessment process was performed versus the 1st, 2nd, 3rd, 5th, and 6th records and the results are shown in **Figures 45**, **46**, **47**, **48**, and **49**, respectively. For more detailed validation results of NOEs for the 200-bit packets (short format) depicted in numbers, **Tables 20**, **21**, **22**, **23**, and **24** are also provided accompanied with comments.

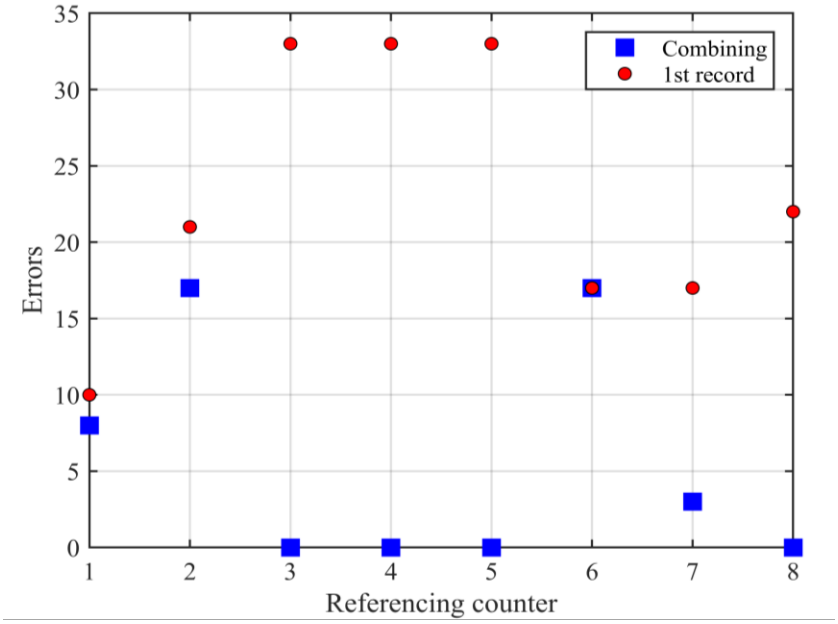

Figure 45. Validating the quality of the combined version versus the 1st record.

TABLE 20
COMPARING NOES OF THE COMBINED VERSION AND THE 1ST RECORD

Referencing Counter	NOE @ 1st	NOE @ Combined	Improvement (%)
1	10	8	20
2	21	17	19
3	33	0	100
4	33	0	100
5	33	0	100
6	17	17	0
7	17	3	82
8	22	0	100

At all comparison points, the combining provided a better-quality packet than the corresponding packets in the 1st version. The accumulative NOE at the 1st records was 186 errors in 8 packets (corresponds to a BER of 0.11625), while the combined version brought it down to only 45 errors (corresponds to a BER of 0.028125) providing an improvement in the BER of 76%.

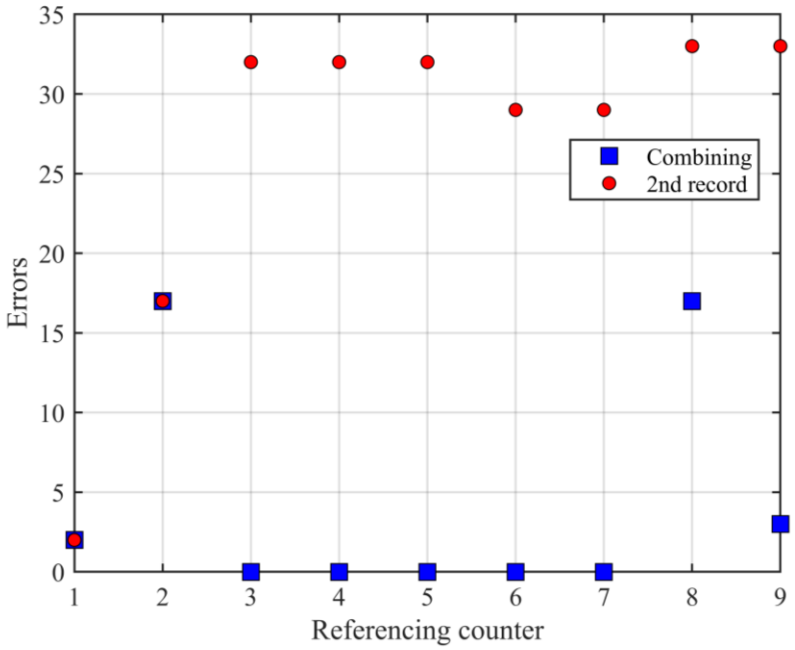

Figure 46. Validating the quality of the combined version versus the 2nd record.

TABLE 21
COMPARING NOES OF THE COMBINED VERSION AND THE 2ND RECORD

Referencing Counter	NOE @ 2nd	NOE @ Combined	Improvement (%)
1	2	2	0
2	17	17	0
3	32	0	100
4	32	0	100
5	32	0	100
6	29	0	100
7	29	0	100
8	33	17	48
9	33	3	91

For the 9 packets in the 2nd record, the accumulative NOE was 239 errors, i.e., a BER of 0.1327, while the NOE in the combined version was 39 errors, i.e., a BER of 0.0216, achieving a BER improvement of 84% over the individually received data in the 2nd GS.

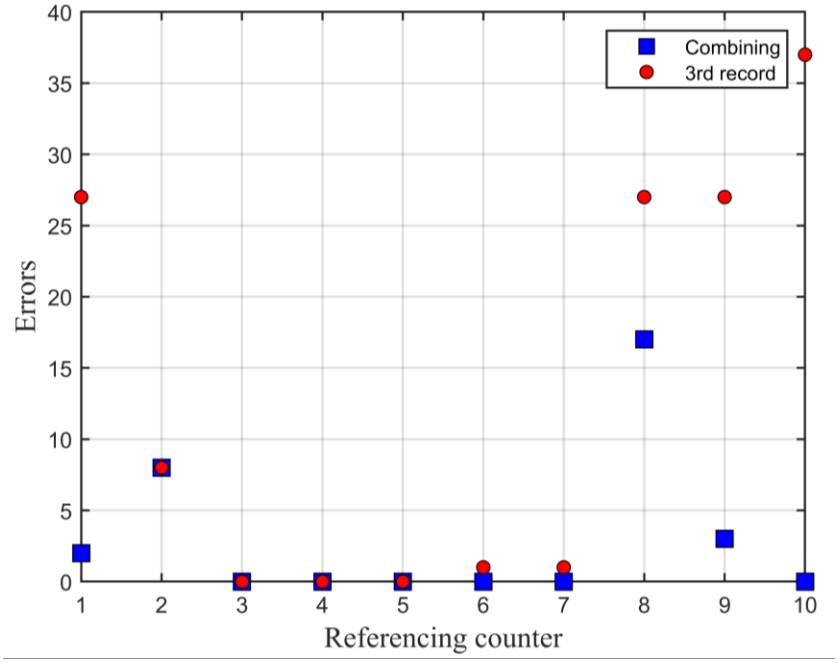

Figure 47. Validating the quality of the combined version versus the 3rd record.

TABLE 22
COMPARING NOES OF THE COMBINED VERSION AND THE 3RD RECORD

Referencing Counter	NOE @ 3rd	NOE @ Combined	Improvement (%)
1	27	2	93
2	8	8	0
3	0	0	0
4	0	0	0
5	0	0	0
6	1	0	100
7	1	0	100
8	27	17	37
9	27	3	89
10	37	0	100

The accumulative NOE at the 3rd record was 127 errors in 10 packets which corresponds to a BER of 0.064. However, the combined version had only 30 errors which corresponds to a BER of 0.015 reflecting a 77% improvement in the BER to the data received by the 3rd GS.

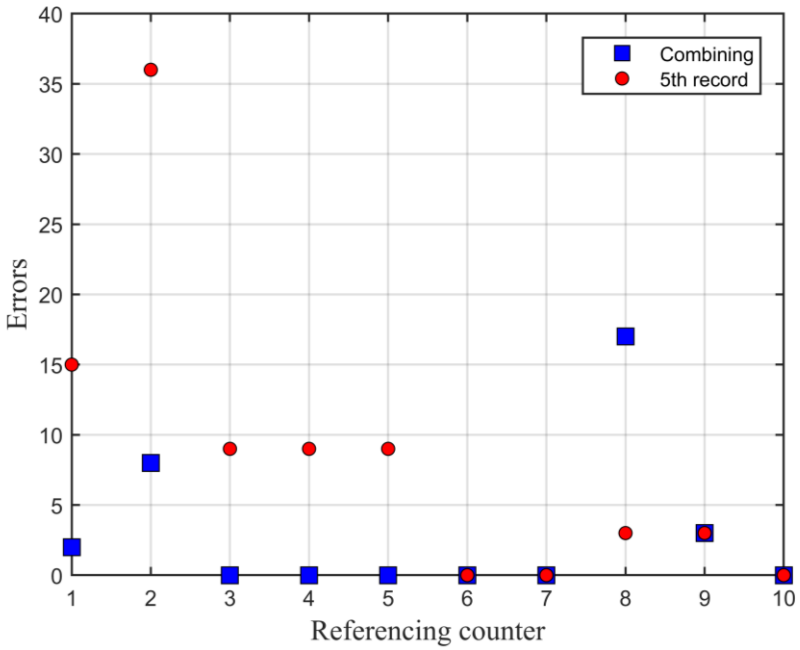

Figure 48. Validating the quality of the combined version versus the 5th record.

TABLE 23
COMPARING NOES OF THE COMBINED VERSION AND THE 5TH RECORD

Referencing Counter	NOE @ 5th	NOE @ Combined	Improvement (%)
1	15	2	87
2	36	8	78
3	9	0	100
4	9	0	100
5	9	0	100
6	0	0	0
7	0	0	0
8	3	17	-466
9	3	3	0
10	0	0	0

The accumulative NOE at the 5th records was 84 errors in 10 packets reflecting a BER of 0.042, while the NOE in the combined version was only 30 errors corresponding to a BER of 0.015. As a result, the combined version provided an improvement in the BER of 64% compared to the packets received by the 5th GS.

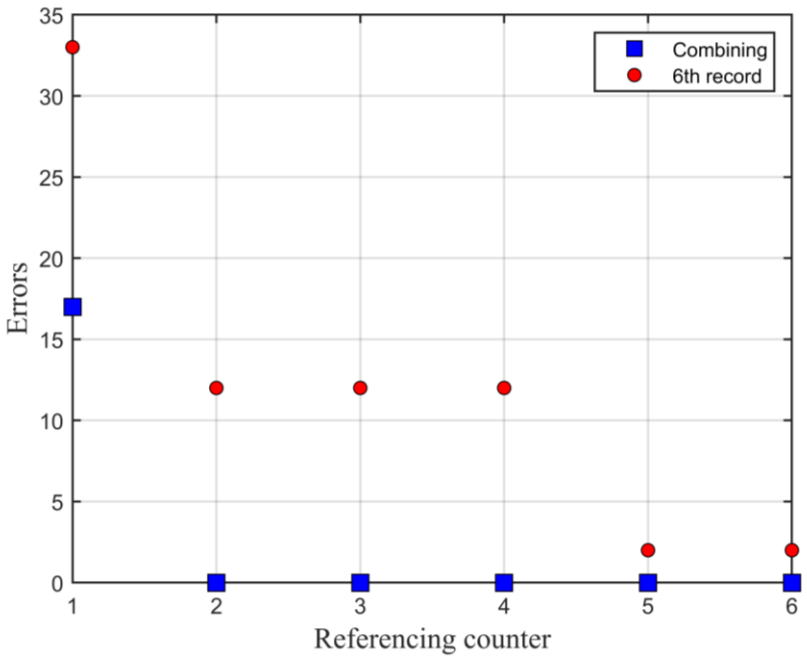

Figure 49. Validating the quality of the combined version versus the 6th record.

TABLE 24
COMPARING THE COMBINED VERSION TO THE 6TH RECORD

Referencing Counter	NOE @ 6th	NOE @ Combined	Improvement (%)
1	33	17	48
2	12	0	100
3	12	0	100
4	12	0	100
5	2	0	100
6	2	0	100

The accumulative NOE at the 6th record was 73 errors in 6 packets which corresponds to a BER of 0.0608. On the other hand, the combined version minimized it to only 17 errors which corresponds to a BER of 0.0141. Thus, the combined version provided a BER improvement of 77% compared to the 6th version if received individually.

Overall, combining the default content in VZLUSAT-2' beacon signal from six individually received beacons by six GSs generated an improved combined version if compared to all other versions. Next step is to validate this improvement by combining individual streams from extended observations of nine GSs in the diversity reception mode.

5.2.4 The results of Experiment D

In this validation experiment, the aim is to test the system scalability for engaging more GSs. Accordingly, the number of the cooperative sites is extended to three more GSs in addition to the six GSs from the previous experiment. The names and the locations of the utilized GSs to record the VZLUSAT-2's beacon in addition to the ID of each record as given by the network of SatNOGS are listed in **Table 25**.

TABLE 25
DETAILS OF NINE GROUND STATIONS TO RECORD THE SIGNALS IN EXPERIMENT D

No.	SatNOGS observation ID	GSs location	Date (yyyy-mm-dd)/ Time (HH-MM-SS)	Length in samples	(waterfall with visible beacon?, audio file?, decoded data? (if yes how many packets?)))
1st	7260546	NJ, USA	02:22:51 - 02:27:52	14490048	(Yes, Yes, Yes (1))
2nd	7260550	VA, USA	02:23:05 - 02:27:03	11425600	(Yes, Yes, No)
3rd	7260625	MA, USA	02:24:06 - 02:27:21	9407680	(Yes, Yes, No)
4th	7260626	NH, USA	02:23:50 - 02:27:50	11543104	(No, Yes, No)
5th	7260638	QC, CA	02:22:07 - 02:31:11	26155072	(Yes, Yes, Yes (11))
6th	7260640	MTL, CA	02:23:30 - 02:32:24	25653184	(Yes, Yes, Yes (27))
7th	7260641	MD, USA	02:22:40 - 02:29:58	21029440	(No, Yes, No)
8th	7260643	QC, CA	02:23:17 - 02:28:09	14050624	(Yes, Yes, Yes (1))
9th	7260644	MA, USA	02:23:01 - 02:27:22	12573120	(Yes, Yes, Yes (2))

When visualizing the nine records in a time manner according to the time frames, the resulting time order is shown in **Figure 50**.

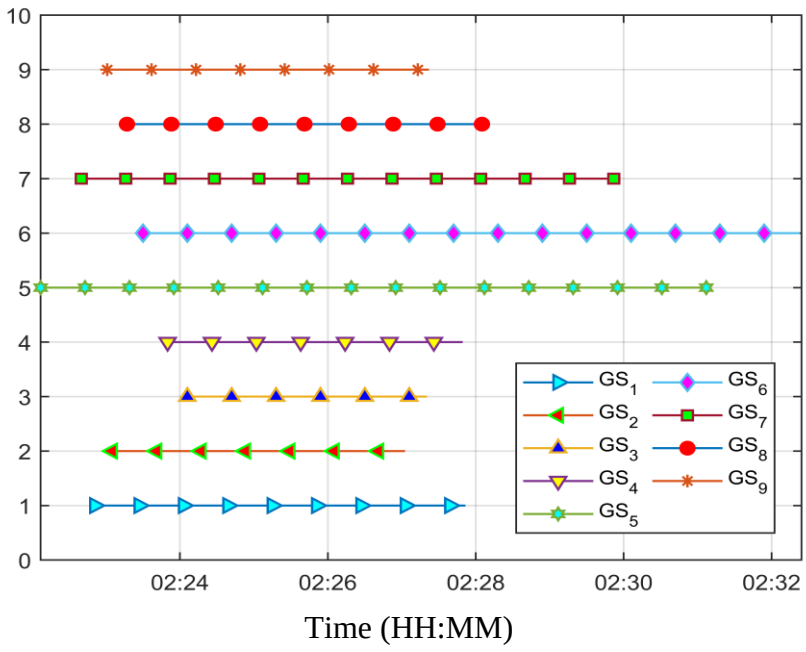

Figure 50. Visualization of VZLUSAT-2 visibility times to the nine GSs.

According to the satellite's visibilities, the earliest observation was at (02:22:07) to the 5th GS while the latest one was at (02:32:24) to the 6th GS. The first overlapping in observations times was at (02:22:40) between the 5th and 7th GSs, whereas the last overlapping was at (02:31:11), the end of the 5th observation. In between the first and the last overlapping, signals combining was possible. The total duration of the VZLUSAT-2's visibility to the nine GSs was (00:10:07), or 617.4413 seconds when considering the fractions of seconds.

When running the algorithm to search for the VZLUSAT-2's identifiers packets in the received nine records, the results were as listed in **Table 26.** For the nine records in **Experiment D**, there were 14, 20, 9, 0, 38, 58, 1, 10, and 11 detected packets within the given threshold of 400 errors. Then, the algorithm checks for any redundant packets if spaced by less than the default spacing of 10 seconds, deletes them, and modifies the number of detected packets. The updated numbers of the detected packets in the collected nine records are depicted in **Table 26**. Then, for aligning the nine records through zero padding process, the required front and rear zeros were as shown in **Table 27**.

TABLE 26
DETAILS OF RECORDS AND DETECTED PACKETS IN EXPERIMENT D

No.	SatNOGS observation ID	Lengths	Packets	Updated packets
1st	7260546	14490048	14	12
2nd	7260550	11425600	20	14
3rd	7260625	9407680	9	7
4th	7260626	11543104	0	0
5th	7260638	26155072	38	28
6th	7260640	25653184	58	43
7th	7260641	21029440	1	1
8th	7260643	14050624	10	7
9th	7260644	12573120	11	8

TABLE 27
THE REQUIRED FRONT AND REAR ZEROS FOR ALIGNING THE NINE RECORDS IN EXPERIMENT D

No.	SatNOGS observation ID	Original lengths	Front zeros	Rear zeros
1st	7260546	14490048	2112000	13035136
2nd	7260550	11425600	2784000	15427584
3rd	7260625	9407680	5712000	14517504
4th	7260626	11543104	4944000	13150080
5th	7260638	26155072	0	3482112
6th	7260640	25653184	3984000	0
7th	7260641	21029440	1584000	7023744
8th	7260643	14050624	3360000	12226560
9th	7260644	12573120	2592000	14472064

Once the nine records are zero padded and hence become aligned, next is to trigger the combining algorithm to perform the combining in a time manner. An identical combining window of five seconds is utilized again in this experiment to match the conditions of the

previous experiment. Within each combining window of five seconds, the algorithm searches for any detected packet of the VZLUSAT-2's identifiers in all the nine records to be combined into one version. Then, the quality of the combined version is observed and compared with the individual packets the combined version was generated from at each combining trial. Utilizing the same assessment method expressed earlier in the results of the previous experiment, the results of validating the quality of the combined packet versus packets from seven GSs, since the 4th and the 7th GSs experienced an outage and hence the search for packets did not reveal any detected patterns, were as depicted in **Figures 51**, **52**, **53**, **54**, **55**, **56**, and **57**. Detailed errors comparisons are presented in numbers in **Tables 28**, **29**, **30**, **31**, **32**, **33**, and **34**.

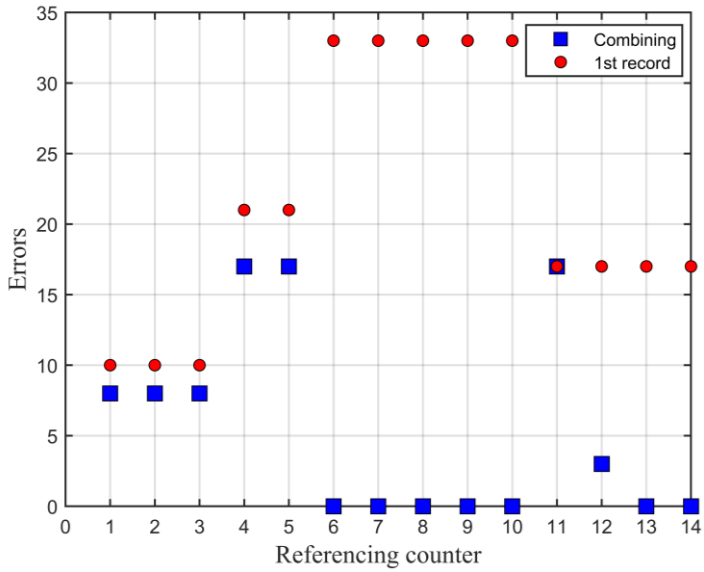

Figure 51. Validating the quality of the combined version versus the 1st record.

TABLE 28
COMPARING THE COMBINED VERSION TO THE 1ST RECORD

Referencing Counter	NOE @ 1st	NOE @ Combined	Improvement (%)
1	10	8	20
2	10	8	20
3	10	8	20
4	21	17	19
5	21	17	19
6	33	0	100
7	33	0	100
8	33	0	100
9	33	0	100
10	33	0	100
11	17	17	0
12	17	3	82
13	17	0	100
14	17	0	100

At all comparison points, the combining provided a better-quality packet than the corresponding packets in the 1st version. The accumulative NOE at the 1st records was 305 errors in 14 packets, i.e., a BER of 0.1089, while the combined version had 78 errors only, i.e., a BER of 0.02786, providing an improvement of 74.42 % in the BER.

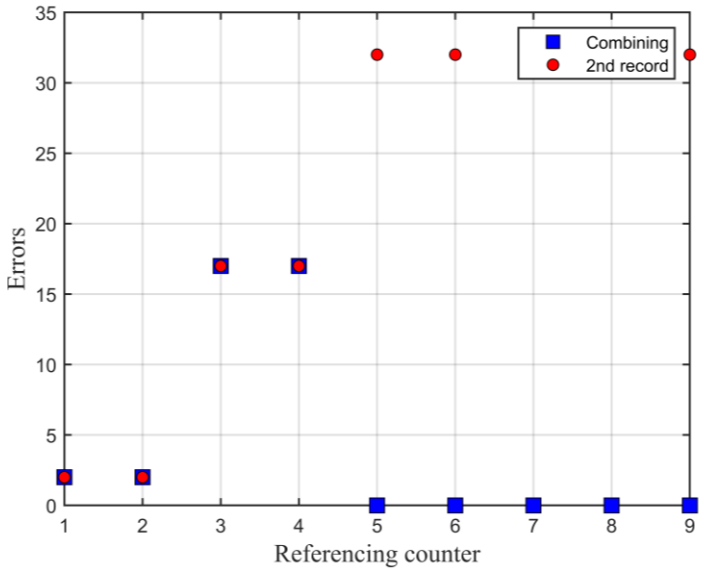

Figure 52. Validating the quality of the combined version versus the 2nd record.

TABLE 29
COMPARING THE COMBINED VERSION TO THE 2ND RECORD

Referencing Counter	NOE @ 2nd	NOE @ Combined	Improvement (%)
1	2	2	0
2	2	2	0
3	17	17	0
4	17	17	0
5	32	0	100
6	32	0	100
7	32	0	100
8	32	0	100
9	32	0	100

For the 9 packets in the 2nd record, the accumulative NOE was 198 errors, corresponding to a BER of 0.11, while the NOE in the combined version was 38 errors corresponding to a BER of 0.021. Thus, the combining achieved an improvement of 80.8% in the BER over the individually received data in the 2nd GS.

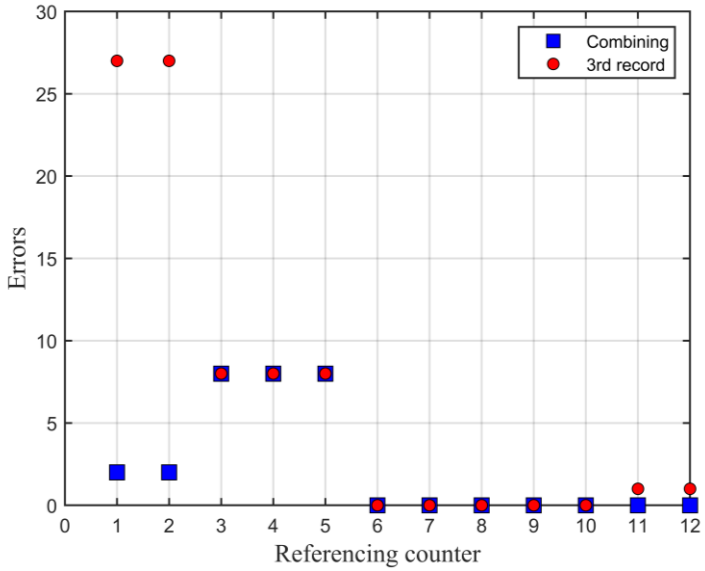

Figure 53. Validating the quality of the combined version versus the 3rd record.

TABLE 30
COMPARING THE COMBINED VERSION TO THE 3RD RECORD

Referencing Counter	NOE @ 3rd	NOE @ Combined	Improvement (%)
1	27	2	92.59
2	27	2	92.59
3	8	8	0
4	8	8	0
5	8	8	0
6	0	0	0
7	0	0	0
8	0	0	0
9	0	0	0
10	0	0	0
11	1	0	100
12	1	0	100

The accumulative NOE at the 3rd records was 80 errors in 12 packets (corresponds to a BER of 0.033), while the combined version had only 28 errors (corresponds to a BER of 0.0116) achieving an improvement in the BER of 65% over the data received by the 3rd GS.

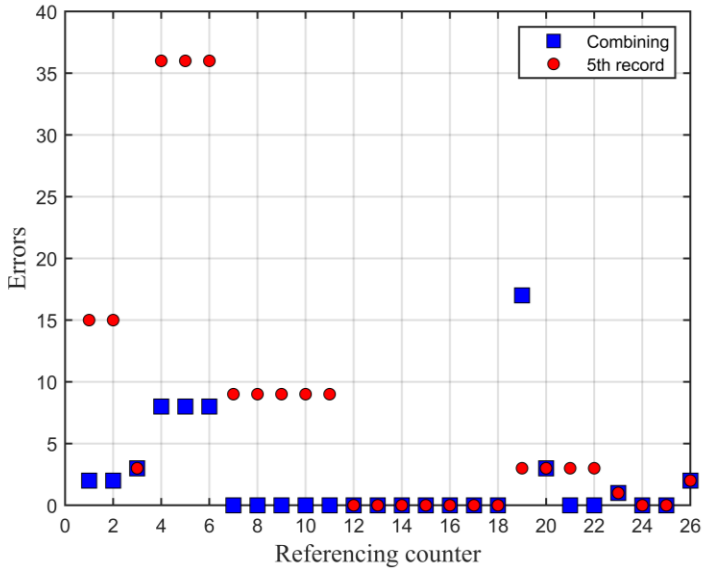

Figure 54. Validating the quality of the combined version versus the 5th record.

TABLE 31
COMPARING THE COMBINED VERSION TO THE 5TH RECORD

Referencing Counter	NOE @ 5th	NOE @ Combined	Improvement (%)
1	15	2	86.6
2	15	2	86.6
3	3	3	0
4	36	8	77.7
5	36	8	77.7
6	36	8	77.7
7	9	0	100
8	9	0	100
9	9	0	100
10	9	0	100
11	9	0	100
12	0	0	0
13	0	0	0
14	0	0	0
15	0	0	0
16	0	0	0
17	0	0	0
18	0	0	0
19	3	17	-466
20	3	3	0
21	3	0	100
22	3	0	100
23	1	1	0
24	0	0	0
25	0	0	0
26	2	2	0

The accumulative NOE at the 5th records was 215 errors in 26 packets (corresponds to a BER of 0.0413), while the NOE in the combined version was only 40 errors (corresponds to a

BER of 0.0076). As a result, the combined version provided an improvement in the BER of 81.39% compared to the packets received by the 5th GS.

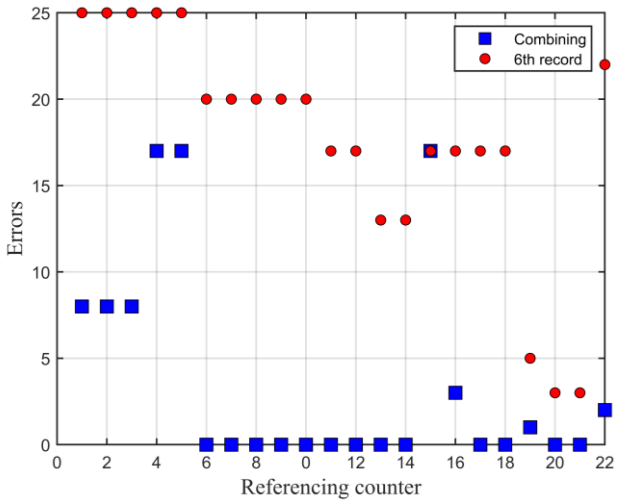

Figure 55. Validating the quality of the combined version versus the 6th record.

TABLE 32
COMPARING THE COMBINED VERSION TO THE 6TH RECORD

Referencing Counter	NOE @ 6th	NOE @ Combined	Improvement (%)
1	25	8	68
2	25	8	68
3	25	8	68
4	25	17	32
5	25	17	32
6	20	0	100
7	20	0	100
8	20	0	100
9	20	0	100
10	20	0	100
11	17	0	100
12	17	0	100
13	13	0	100
14	13	0	100
15	17	17	0
16	17	3	82.35
17	17	0	100
18	17	0	100
19	5	1	80
20	3	0	100
21	3	0	100
22	22	2	90.9

The accumulative NOE at the 6th record was 386 errors in 22 packets which corresponds to a BER of 0.0877, while the combined version minimized it to only 81 errors which corresponds to a BER of 0.0184. Thus, the combined version provided a BER improvement of 79% compared to the 6th version if received individually.

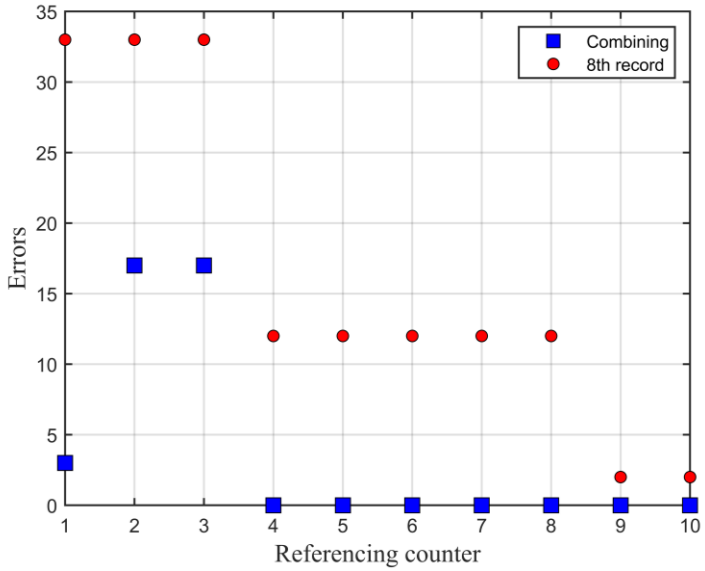

Figure 56. Validating the quality of the combined version versus the 8th record.

TABLE 33
COMPARING THE COMBINED VERSION TO THE 8TH RECORD

Referencing Counter	NOE @ 1st	NOE @ Combined	Improvement (%)
1	33	3	90.9
2	33	17	48.48
3	33	17	48.48
4	5	0	100
5	5	0	100
6	5	0	100
7	5	0	100
8	5	0	100
9	5	0	100
10	2	0	100

The accumulative NOE at the 8th record was 128 errors in 10 packets which corresponds to a BER of 0.064, while the combined version minimized it to only 37 errors which corresponds to a BER of 0.0185. Thus, the combined version provided a BER improvement of 71.1% compared to the 8th version if received individually.

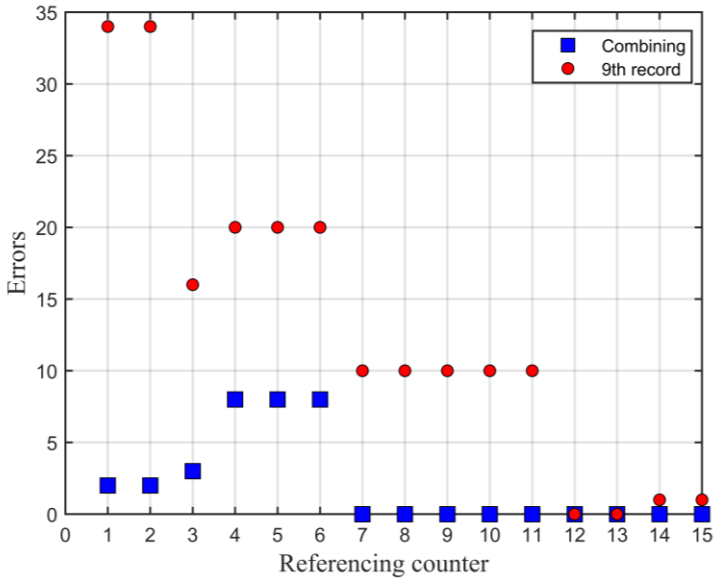

Figure 57. Validating the quality of the combined version versus the 9th record.

TABLE 34
COMPARING THE COMBINED VERSION TO THE 9TH RECORD

Referencing Counter	NOE @ 9th	NOE @ Combined	Improvement (%)
1	34	2	94.11
2	34	2	94.11
3	16	3	81.25
4	20	8	60
5	20	8	60
6	20	8	60
7	10	0	100
8	10	0	100
9	10	0	100
10	10	0	100
11	10	0	100
12	0	0	0
13	0	0	0
14	1	0	100
15	1	0	100

The accumulative NOE at the 9th record was 196 errors in 15 packets, corresponds to a BER of 0.065, while the combined version minimized it to only 31 errors, i.e., a BER of 0.0103, providing a BER improvement of 84.18% over the packets of the 9th version.

Lastly, looking at the observations' times in this experiment visualized in **Figure 50**, the combining is very likely between (02:24:00) and (02:27:24) where all observations are overlapped in time. Therefore, it is worth exploring the combining outcome during this range of time.

Within the time window of (02:24:19-02:27:24), the combining of streams from nine GSs involved in **Experiment D** (after excluding the 4th and 7th GSs since they had no detectable packets) is performed. **Table 35** summarizes the results of combining the VZULSAT-2 identifiers packets in this experiment where the combined packet achieved an average BER of 0.01269 outperforming all other individual packets from seven GSs with average BERs of 0.10125, 0.085, 0.045, 0.02875, 0.08125, 0.1, and 0.0675, respectively.

Even to the best quality stream from the 5th GS, equipped with steerable high gain antenna, the combining provided a BER improvement of more than 55%. To the 1st, 2nd, 3rd, 6th, 8th, and 9th GSs, the improvement in the average BER were 87.4%, 85%, 71.8%, 84%, 87%, and 81%, respectively. The cooperative reception did not only achieve an improvement in the BER, but also provided the GSs with more frequent packets than each GS had detected in the given time window. For instance, the 1st, 2nd, 3rd, and 8th GSs had a maximum of four packets within the whole referred time window whereas the cooperative reception system could provide 14 high quality packets within the same period. The 4th and 7th GSs in **Experiment D** had bad reception circumstances and accordingly had no packets to be involved in the combining process. However, for these two involved GSs, the cooperative scheme compensated these missed packets with shared high-quality versions resulting from the combining process.

TABLE 35
Comparing the combined version to the seven records involved in the combining

Time window (HH:MM:SS)	**02:24:19 02:24:24**	**02:24:31 02:24:36**	**02:24:39 02:24:44**	**02:24:59 02:25:04**	**02:25:19 02:25:24**	**02:25:31 02:25:36**	**02:25:39 02:25:44**	**02:25:59 02:26:04**	**02:26:11 02:26:16**	**02:26:19 02:26:24**	**02:26:39 02:26:44**	**02:26:59 02:27:04**	**02:27:19 02:27:24**	**Average BER**
Packet / GSs	Index, NOE	Index, NOE	Index, NOE	Index, NOE	Index, NOE	Index, NOE	Index, NOE	Index, NOE	Index, NOE	Index, NOE	Index, NOE	Index, NOE	Index, NOE	
1st	-	-	3rd , 10	6th, 21	9th , 33	-	-	-	-	12th, 17	-	-	-	0.10125
2nd	7th , 2	-	-	11th , 17	13th , 32	-	-	-	-	-	-	-	-	0.085
3rd	1st , 27	-	2nd , 8	-	6th , 0	7th , 1	-	-	-	-	-	-	-	0.045
5th	7th , 15	9th , 3	10th , 36	-	11th , 9	13th , 0	4th, 0	17th, 0	18th, 0	19th, 3	22nd, 1	25th , 0	27th , 2	0.02875
6th	-	-	6th, 25	9th , 25	10th ,20	-	12th , 17	15th , 13	-	-	20th , 5	22nd , 3	25th, 22	0.08125
8th	-	1st , 33	-	4th , 33	6th , 12	7th , 2	-	-	-	-	-	-	-	0.1
9th	1st , 34	3rd , 16	4th , 20	-	5th , 10	-	7th, 0	8th, 1	-	-	-	-	-	0.0675
$NOE_{comb.}$	2	3	8	17	0	0	0	0	0	0	1	0	2	0.01269

6 Conclusions

Small satellites have become very popular nowadays and already attracted attention for the future integration in the Sixth Generation (6G) inclusive Internet of Things (IoT) networks. This study contributes to successful integration of such popular but limited resources satellites into the aimed future IoT coverage through a cooperative reception scheme. In which, multiple Ground Stations (GSs) are networked to share their individually received streams of weak small satellite signals for further processing and diversity combining. Initially, three simulation-based studies were conducted in this dissertation. These preliminary studies modeled and simulated the cooperative reception structure and developed a simple yet efficient Maximum Likelihood (ML) combiner. The system performance was tested for diversity combining under different scenarios including bad quality received signals expected from simple and cheap Software-defined Radios (SDRs) GSs with low gain antennas and functioned well in reducing the Bit Error Rate (BER). The collaborative scheme of GSs with good and bad reception scenarios resulted in a combined version with low BER at early stages of combining trials requiring few sites to combine. Even when only one GS received good quality signal while the rest of GSs received low quality signals in the cooperative scheme, the resulting combined stream achieved low BER with enough number of sites to combine. Such improvement is promising for simple omnidirectional GSs like SatNOGS's where the reception of weak signals is highly probable.

Inspired by the promising results of these preliminary studies, this work deployed the suggested reception scheme into practical experiments of combining multiple versions of a real and weak small satellite (named VZLUSAT-2) beacon collected by multiple GSs and turned out productive in four experiments, from the simplest one to the final verification experiment. **Experiment A** verified the fact that the combined VZLUSAT-2's Preamble, Sync-Word, Header, and fixed data part were better than their best detected matches from the received five observations. In **Experiment B,** the combined VZLUSAT-2's Sync-Word generated from all detected Sync-Words in five observations in a time manner was always better than any individually detected Sync-Word. When six versions of the VZLUSAT-2's beacon signal were separately recorded and then the identifiers' packet was combined in **Experiment C**, the resulting version was always better than any other individual packet version. Indeed, over the packets received individually by the six GSs in order, the improvements in the BERs achieved by diversity combining were 76%, 84%, 77%, 100%, 64%, and 77%. **Experiment D** tested the system's scalability to combine nine versions of

the VZLUSAT-2's beacon and the BER reduction of the proposed cooperative scheme is consistently confirmed by achieving 74%, 80%, 65%, 100%, 81%, 79%, 100%, 71%, and 84% for the nine GSs in order.

The validated reception scheme did not only reduce BER, but also minimized the probability that an involved GS experiences an outage. In fact, in **Experiment D,** the 4th GS had an outage and received no packets from the satellite. Nevertheless, under the cooperative scheme, this outage in one individual GS can be compensated by a combined version whose quality is better than any other individual version in the networked GSs.

The generated diversity gain is promising enough to even trigger the idea that such cooperative reception can compensate the replacement of the present expensive steerable receiving antennas and their complex steering resources by affordable omnidirectional ones for small satellites telemetry. Considering the doubled number of newly launched small satellites in only two years (2020-2022), the presented scheme precludes the need to build new expensive GSs for newly launched small satellites and proposes the utilization of current SDR-based simple GSs as a huge network of cooperative nodes for non-coherent diversity combining of received signals. The diversity gain replaces the need for directional antennas on rotators and the large frequency bandwidth of the signals digitized in SDR allows such a network to cooperatively receive simultaneous simple data transmissions from large number of small satellites.

6.1 Summarizing the benefits of the dissertation

Comprehensively viewing the cooperative reception scheme, the advantages are:

1. The proposed scheme decreases BER because such a system relies on detecting data from multiple received streams efficiently based on the developed ML combiner.
2. Resistance to singular failures as it provides multiple alternatives for each involved GS in case it experiences communication failure. Therefore, the proposed scheme reduces system outages.
3. The expensive high-gain antenna required at conventional single GSs for establishing good communication can be replaced by an affordable low-gain omnidirectional antenna where the diversity gain compensates for the lesser antenna gain.
4. Such a system enables GSs' operators to track more than one satellite at a time.
5. Engaging multiple GSs with different frequency bands, antenna gains, and transmission/reception capabilities in one VGS creates a network that can provide a variety of complex and different services in an area.

6. A GS engaged in a cooperative reception scheme no longer requires an antenna rotator and other expensive indoor and outdoor steering resources because it utilizes omnidirectional antennas.
7. Extending the communication window with a satellite since that satellite will pass over multiple GSs in the network instead of just single GS. Therefore, that certain satellite will be available more frequently to the cooperative system than it would be for a GS working in a single mode.
8. Offers an option to the owner of an involved low-cost GS not to necessarily upgrade to the high-cost GS when needed since such capable stations are already cooperating in the network and can offer shared services.
9. The proposed scheme crucially decreases the budget to build GSs through the exclusion of the expensive uplink resources when the downlink is the only intended link to establish. Therefore, the proposed scheme overcomes the drawback of inefficiently blocking the system capacity with pricy uplink and downlink infrastructure when only downlink is required.
10. The source codes for the diversity combining used in the simulation and in the validation experiments in this thesis are available in GitHub for the developers of online SDR-GSs platforms or for their users to test the concept of cooperative reception scheme on individual small satellites.
11. Availability of low-cost and open-source current networks of SDR receivers such as (SpyServer, WebSDR, OpenWebRx), that can be used to stream the captured satellite signal out over the Internet. **Figure 58** shows the coverage map of such available SDR networks for UHF receivers. Another global coverage map for remotely accessible GSs from SatNOGS platform is presented in **Figure 59**.

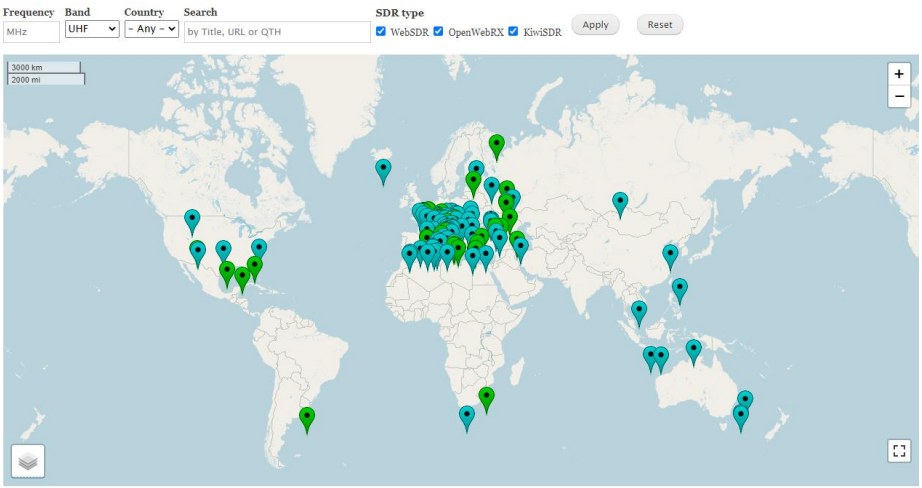

Figure 58. Coverage map of open-source SDR networks availability for UHF receivers.

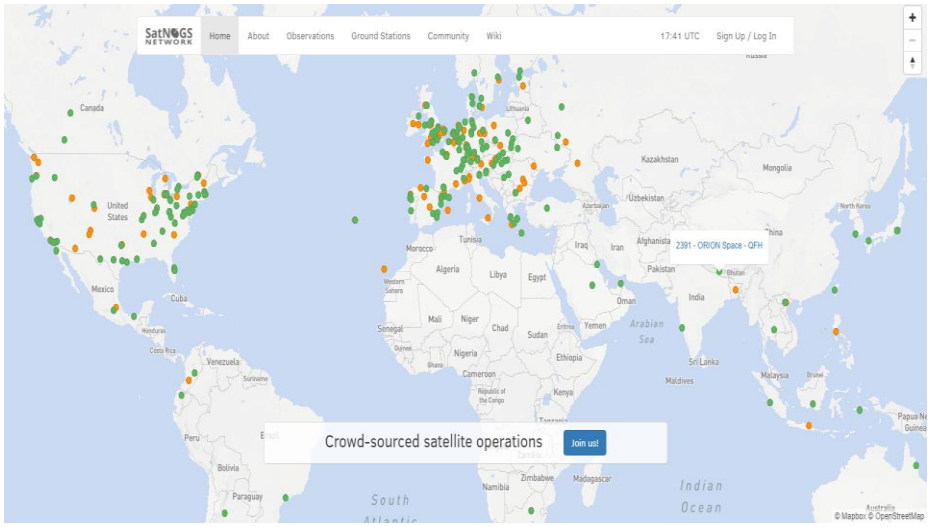

Figure 59. Coverage map of online-accessible GSs around the world from SatNOGS.

6.2 Future work Suggestions

This dissertation opens the door for several recommendations for future progress in the presented topic by testing new concepts in improving the reception of small satellites signals such as:

A. Preselection of the involved GSs based on the long-term statistics. In real implementation of such proposed system, we will be always limited in the number of streams generated by the cooperative GSs to be processed in one VGS by network connectivity of the involved GSs, their processor powerfulness, or by the number of streams that can be processed in that single VGS. Therefore, we can create and utilize long term statistics that some GSs have trouble with signal quality at a particular frequency (jammed by another terrestrial services) or from a particular direction (obstacles in sky view). Accordingly, for a given satellite and its actual position, only the optimal GSs will be selected to involve in the cooperative reception based on these accumulative statistics. Such a future progress helps not to waste limited resources to probably improper selection of the GSs in the cooperative scheme.

B. Generating an output with soft decision for improving FEC decoding. Some FEC decoding algorithms, like Viterbi, can use the probability information at the output of the demodulator to improve FEC decoding.

C. Developing and deploying methods for online detection and exclusion of little beneficial streams for diversity combining. Some methods for selecting the best combination of candidates to combine out of the received streams are vital in improving the performance of the diversity combining reception system.

References

[1] N. Cao, Y. Chen, X. Gu, and W. Feng, "Joint Bi-Static Radar and Communications Designs for Intelligent Transportation," *IEEE Transactions on Vehicular Technology*, vol. 69, no. 11, pp. 13060-13071, 2020.

[2] N. Cao, Y. Chen, X. Gu, and W. Feng, "Joint Radar-Communication Waveform Designs Using Signals From Multiplexed Users," *IEEE Transactions on Communications*, vol. 68, no. 8, pp. 5216-5227, 2020.

[3] A. Salam and S. Shah, "Internet of Things in Smart Agriculture: Enabling Technologies," presented at the 2019 IEEE 5th World Forum on Internet of Things (WF-IoT), 2019.

[4] A. H. A. Hussain *et al.*, "Urban Traffic Flow Estimation System Based on Gated Recurrent Unit Deep Learning Methodology for Internet of Vehicles," *IEEE Access*, vol. 11, pp. 58516-58531, 2023.

[5] T. Wu, F. Wu, C. Qiu, J.-M. Redoute, and M. R. Yuce, "A Rigid-Flex Wearable Health Monitoring Sensor Patch for IoT-Connected Healthcare Applications," *IEEE Internet of Things Journal*, vol. 7, no. 8, pp. 6932-6945, 2020.

[6] A. Hussain, K. Zafar, and A. R. Baig, "Fog-Centric IoT Based Framework for Healthcare Monitoring, Management and Early Warning System," *IEEE Access*, vol. 9, pp. 74168-74179, 2021.

[7] X. Fang, W. Feng, T. Wei, Y. Chen, N. Ge, and C.-X. Wang, "5G Embraces Satellites for 6G Ubiquitous IoT: Basic Models for Integrated Satellite Terrestrial Networks," *IEEE Internet of Things Journal*, vol. 8, no. 18, pp. 14399-14417, 2021.

[8] D. C. Nguyen *et al.*, "6G Internet of Things: A Comprehensive Survey," *IEEE Internet of Things Journal*, vol. 9, no. 1, pp. 359-383, 2022.

[9] J. Chu, X. Chen, C. Zhong, and Z. Zhang, "Robust Design for NOMA-Based Multibeam LEO Satellite Internet of Things," *IEEE Internet of Things Journal*, vol. 8, no. 3, pp. 1959-1970, 2021.

[10] N. Saeed, A. Elzanaty, H. Almorad, H. Dahrouj, T. Y. Al-Naffouri, and M.-S. Alouini, "CubeSat Communications: Recent Advances and Future Challenges," *IEEE Communications Surveys & Tutorials*, vol. 22, no. 3, pp. 1839-1862, 2020.

[11] N. C. L. Initiative, "Cubesat 101: basic concepts and processes for first-time CubeSat developers," NASA CubeSat Launch Initiative no. October 2017.

[12] I. Vertat, M. Pokorny, R. Linhart, and T. Kavalir, "Signal quality evaluation for picosatellite communication systems," in *2012 International Conference on Applied Electronics*, 2012, pp. 331-334: IEEE.

[13] CBL-Electronics, "Issues to be solved designing a Cubesat," 24050 Palosco (BG) ITALY July 20th 2022, Available: https://www.cblelectronics.com/en/blog/issues-be-solved-designing-cubesat, Accessed on: September 20th 2023.

[14] I. Vertat, R. LInhart, M. Pokorny, J. Masopust, P. Fiala, and J. Mraz, "Small satellite ground station in Pilsen—experiences with VZLUSAT-1 commanding and future modifications toward open reference ground station solution," in *2018 28th International Conference Radioelektronika (RADIOELEKTRONIKA)*, 2018, pp. 1-6: IEEE.

[15] S. Busch, P. Bangert, S. Dombrovski, and K. Schilling, "UWE-3, in-orbit performance and lessons learned of a modular and flexible satellite bus for future pico-satellite formations," *Acta Astronautica*, vol. 117, pp. 73-89, 2015.

[16] E-USOC. (September 20th). *Ground Station*. Available: https://www.eusoc.upm.es/ground-station/

[17] PolySat. (September 20th). *Cal Poly's New Ground Station Is Moving Along*. Available: https://www.polysat.org/newsblog/2014/11/1/cal-polys-new-ground-station-is-moving-along

[18] Aalto-University. (September 20th). *Aalto Ground Station*. Available: https://www.aalto.fi/en/spacecraft/for-radio-amateurs

[19] SatNOGS. (2023, September 20th). *Open Source global network of satellite ground-stations*. Available: https://satnogs.org

[20] W. Chen, D. Sun, C. Han, J. Yang, F. Gong, and W. Wang, "Macrodiversity Reception with Distributed Hard-Decision Receivers for Maritime Wireless Sensor Networks," *Sensors*, vol. 20, no. 14, p. 3925, 2020.

[21] X. Fan, "Facilitating the deployment of next billion IoT devices with distributed antenna systems," in *The ACM MobiSys 2019 on Rising Stars Forum*, 2019, pp. 1-6.

[22] T. Lassouaoui, F. Hutu, Y. Duroc, and G. Villemaud, "Theoretical BER Evaluation of Passive RFID Tag-To-Tag Communications," presented at the 2020 IEEE Radio and Wireless Symposium (RWS), 2020.

[23] B. Sklar, *Digital communications*, Third ed. New Jersey: Prentice hall Upper Saddle River, NJ, USA:, 2001.

[24] A. Bensky, *Short-range wireless communication*. Newnes, 2019.
[25] X. Pan, Y. Zhan, P. Wan, and J. Lu, "Review of channel models for deep space communications," *Science China Information Sciences,* vol. 61, no. 4, 2018.
[26] J. G. Proakis, *Digital communications*, Fifth ed. New York: McGraw-Hill, Higher Education, 2008.
[27] K. Prabu, "Analysis of FSO Systems with SISO and MIMO Techniques," *Wireless Personal Communications,* vol. 105, no. 3, pp. 1133-1141, 2019.
[28] P. I. Theoharis, R. Raad, F. Tubbal, M. U. Ali Khan, and S. Liu, "Software-Defined Radios for CubeSat Applications: A Brief Review and Methodology," *IEEE Journal on Miniaturization for Air and Space Systems,* vol. 2, no. 1, pp. 10-16, 2021.
[29] N. A. Salam Bauomy and E. A. Elbeh, "Design of SDR Simulation for Wireless Communication between Ground Station and CubeSat Implemented by LabVIEW," presented at the 2020 8th International Japan-Africa Conference on Electronics, Communications, and Computations (JAC-ECC), 2020.
[30] H. Fukuchi, A. Yoshii, and Y. Suzuki, "Quantitative evaluation of adaptive satellite power control using Japanese rain radar data," in *2012 International Symposium on Antennas and Propagation (ISAP)*, 2012, pp. 1469-1472: IEEE.
[31] D.-H. Jung and D.-G. Oh, "Outage Performance of Shared-Band On-Board Processing Satellite Communication System," presented at the 2018 IEEE 88th Vehicular Technology Conference (VTC-Fall), 2018.
[32] V. Joroughi, M. A. Vazquez, A. I. Perez-Neira, and B. Devillers, "Onboard Beam Generation for Multibeam Satellite Systems," *IEEE Transactions on Wireless Communications,* vol. 16, no. 6, pp. 3714-3726, 2017.
[33] S. Ning, "Improving resistive RAM hard and soft decision correctable Bers by using improved-LLR and reset-check-reverse-flag concatenating LDPC code," *IEEE Transactions on Circuits Systems II: Express Briefs,* vol. 67, no. 10, pp. 2164-2168, 2019.
[34] L. Xiang, Y. Liu, C. Xu, R. G. Maunder, L.-L. Yang, and L. Hanzo, "Iterative receiver design for polar-coded SCMA systems," *IEEE Transactions on Communications,* vol. 69, no. 7, pp. 4235-4246, 2021.
[35] B. Gong, C. Ding, and C. Li, "The dual codes of several classes of BCH codes," *IEEE Transactions on Information Theory,* vol. 68, no. 2, pp. 953-964, 2021.
[36] D. N. Bailon, M. Bossert, J.-P. Thiers, and J. Freudenberger, "Concatenated codes based on the plotkin construction and their soft-input decoding," *IEEE Transactions on Communications,* vol. 70, no. 5, pp. 2939-2950, 2022.
[37] G. He, X. Gao, L. Sun, and R. Zhang, "A review of multibeam phased array antennas as LEO satellite constellation ground station," *IEEE Access,* vol. 9, pp. 147142-147154, 2021.
[38] M. Kim and D. Park, "Learnable MIMO Detection Networks Based on Inexact ADMM," *IEEE Transactions on Wireless Communications,* vol. 20, no. 1, pp. 565-576, 2021.
[39] L. Sanguinetti, A. Kammoun, and M. Debbah, "Theoretical Performance Limits of Massive MIMO With Uncorrelated Rician Fading Channels," *IEEE Transactions on Communications,* vol. 67, no. 3, pp. 1939-1955, 2019.
[40] A. K. Sarangi and A. Datta, "Capacity Comparison of SISO, SIMO, MISO & MIMO Systems," presented at the 2018 Second International Conference on Computing Methodologies and Communication (ICCMC), 2018.
[41] R. Tengshe and N. Kumar, "Receive Diversity in Analog Feedback Communication," presented at the 2019 PhD Colloquium on Ethically Driven Innovation and Technology for Society (PhD EDITS), 2019.
[42] L. Kansal, G. S. Gaba, N. Chilamkurti, and B. G. Kim, "Efficient and Robust Image Communication Techniques for 5G Applications in Smart Cities," (in English), *Energies,* vol. 14, no. 13, Jul 2021.
[43] N. Rezazadeh and L. Shafai, "A Pattern Diversity Antenna for Ambient RF Energy Harvesting in Multipath Environments," presented at the 2018 18th International Symposium on Antenna Technology and Applied Electromagnetics (ANTEM), 2018.
[44] D. Altinel and G. K. Kurt, "Diversity Combining for RF Energy Harvesting," presented at the 2017 IEEE 85th Vehicular Technology Conference (VTC Spring), 2017.
[45] J. Male, J. Porte, T. Gonzalez, J. M. Maso, J. L. Pijoan, and D. Badia, "Analysis of the Ordinary and Extraordinary Ionospheric Modes for NVIS Digital Communications Channels," (in English), *Sensors,* vol. 21, no. 6, Mar 2021.
[46] M. Das and B. Sahu, "Effect of MRC Diversity on Outage Probability in Mobile Networks," presented at the 2019 Global Conference for Advancement in Technology (GCAT), 2019.
[47] C. F. He, Y. Y. Wang, W. B. Yu, and L. Song, "Underwater Target Localization and Synchronization for a Distributed SIMO Sonar with an Isogradient SSP and Uncertainties in Receiver Locations," (in English), *Sensors,* vol. 19, no. 9, May 1 2019.

[48] N. Nath and S. Anees, "Performance Analysis of SIMO-UWOC System," presented at the 2020 IEEE International Conference on Advanced Networks and Telecommunications Systems (ANTS), 2020.
[49] A. R. Zheng, Y. Huang, and S. M. Gao, "Modeling and Spatial Diversity-Based Receiving Improvement of In-Flight UAV FSO Communication Links," (in English), *Applied Sciences-Basel*, vol. 11, no. 14, Jul 2021.
[50] A. B. Zhao, C. G. Zeng, J. Hui, K. R. Wang, and K. Y. Tang, "Study on Time Reversal Maximum Ratio Combining in Underwater Acoustic Communications," (in English), *Applied Sciences-Basel*, vol. 11, no. 4, Feb 2021.
[51] D. Jiang and Y. Cui, "Enhancing Performance of Random Caching in Large-Scale Wireless Networks With Multiple Receive Antennas," *IEEE Transactions on Wireless Communications*, vol. 18, no. 4, pp. 2051-2065, 2019.
[52] N. Lee, F. Baccelli, and R. W. Heath, "Spectral Efficiency Scaling Laws in Dense Random Wireless Networks With Multiple Receive Antennas," *IEEE Transactions on Information Theory*, vol. 62, no. 3, pp. 1344-1359, 2016.
[53] Y. Yu, L. Mroueh, P. Martins, G. Vivier, and M. Terre, "Radio Resource Dimensioning for Low Delay Access in Licensed OFDMA IoT Networks," (in English), *Sensors*, vol. 20, no. 24, Dec 2020.
[54] H. Chung, J. Kim, G. Noh, S. H. Won, T. Choi, and I. Kim, "Demonstration of Service Continuity Based on Multi-Connectivity with Cellular and Satellite Access Networks," presented at the 2021 International Conference on Information and Communication Technology Convergence (ICTC), 2021.
[55] F. Samat, M. J. Singh, A. Sali, and N. Zainal, "A Comprehensive Review of the Site Diversity Technique in Tropical Region: Evaluation of Prediction Models Using Site Diversity Gain of Greece and India," *IEEE Access*, vol. 9, pp. 105060-105071, 2021.
[56] S. Chang, "An Emergence Alert Broadcast Based on Cluster Diversity for Autonomous Vehicles in Indoor Environments," *IEEE Access*, vol. 8, pp. 84385-84395, 2020.
[57] D.-T. Do, T.-L. Nguyen, S. Ekin, Z. Kaleem, and M. Voznak, "Joint User Grouping and Decoding Order in Uplink/Downlink MISO/SIMO-NOMA," *IEEE Access*, vol. 8, pp. 143632-143643, 2020.
[58] Z. Zhao, J. Wang, W. Hou, Y. Li, and B. Ai, "Optimized Scheme of Antenna Diversity for Radio Wave Coverage in Tunnel Environment," *IEEE Access*, vol. 8, pp. 127226-127233, 2020.
[59] A. Al-Rimawi, J. Siam, A. Abdo, and D. Dardari, "Performance Analysis of Dynamic Downlink PPP Cellular Networks Over Generalized Fading Channels With MRC Diversity," *IEEE Access*, vol. 9, pp. 39019-39027, 2021.
[60] X. Hou, J. Ling, and D. Wang, "Performance of High-Mobility MIMO Communications With Doppler Diversity," *IEEE Access*, vol. 8, pp. 31574-31585, 2020.
[61] Z. Zhu, C. Jiang, and Y. Bo, "Performance Enhancement of GNSS/MEMS-IMU Tightly Integration Navigation System Using Multiple Receivers," *IEEE Access*, vol. 8, pp. 52941-52949, 2020.
[62] E. Panholzer and S. Lindenmeier, "A New GNSS Micro-Diversity System," presented at the 2022 52nd European Microwave Conference (EuMC), 2022.
[63] S. Matthie, S. Senega, and S. Lindenmeier, "An Antenna Diversity and Combining System for Improved Mobile GNSS Reception," presented at the 2019 49th European Microwave Conference (EuMC), 2019.
[64] G. Aruna and M. P. Barman, "Performance Analysis of Advanced Diversity Receivers in the Presence of Multiple Interferers," presented at the 2018 International Conference on Wireless Communications, Signal Processing and Networking (WiSPNET), 2018.
[65] T. Pratt and J. E. Allnutt, *Satellite communications*, Third ed. New Jersey: John Wiley & Sons, 2019.
[66] P. Yadav, S. Kumar, and R. Kumar, "A Review of Transmission Rate over Wireless Fading Channels: Classifications, Applications, and Challenges," *Wireless Personal Communications*, vol. 122, no. 2, pp. 1709-1765, 2021.
[67] G. Yang, Y.-C. Liang, R. Zhang, and Y. Pei, "Modulation in the Air: Backscatter Communication Over Ambient OFDM Carrier," *IEEE Transactions on Communications*, vol. 66, no. 3, pp. 1219-1233, 2018.
[68] V. K. Upaddhyay, P. S. Chauhan, and S. K. Soni, "Effective capacity analysis of SIMO system with MRC and SC over Inverse-Gamma shadowing," *International Journal of Electronics*, vol. 109, no. 2, pp. 181-199, 2021.
[69] VZLU. (2022, February 27th). *The Main Systems of the VZLUSAT-2 Nanosatellite Put into Operation*. Available: https://www.vzlu.cz/the-main-systems-of-the-vzlusat-2-nanosatellite-put-into-operation/?lang=en
[70] SatNOGS. (2023, February 27th). *VZLUSAT-2 Dashboard*. Available: https://dashboard.satnogs.org/d/L8ywE9oMz/vzlusat-2?orgId=1&refresh=5s
[71] Cesium. (2023, February 27th). *VZLUSAT-2 live orbital observation*. Available: https://pilsencube.zcu.cz/vzlusat2/over8.php

[72] M. K. Simon and M.-S. Alouini, "Digital communications over fading channels (mk simon and ms alouini; 2005)[book review]," *IEEE Transactions on Information Theory*, vol. 54, no. 7, pp. 3369-3370, 2008.
[73] H. Al-Hmood and H. Al-Raweshidy, "Selection combining scheme over non-identically distributed Fisher-Snedecor F fading channels," *IEEE Wireless Communications Letters*, vol. 10, no. 4, pp. 840-843, 2020.
[74] D. H. Tashman, W. Hamouda, and Networking, "Physical-layer security on maximal ratio combining for SIMO cognitive radio networks over cascaded κ-μ fading channels," *IEEE Transactions on Cognitive Communications*, vol. 7, no. 4, pp. 1244-1252, 2021.
[75] H. N. Al-Anbagi and I. Vertat, "Cooperative reception of multiple satellite downlinks," *Sensors*, vol. 22, no. 8, p. 2856, 2022.
[76] H. N. Al-Anbagi and I. Vertat, "Collaborative Network of Ground Stations with a Virtual Platform to Perform Diversity Combining," in *2022 International Conference on Applied Electronics (AE)*, 2022, pp. 1-6: IEEE.
[77] H. N. Al-Anbagi and I. Vertat, "Pre-detection Combining of Small Satellite Downlink's Replicas," in *2022 International Conference on Electrical, Computer and Energy Technologies (ICECET)*, 2022, pp. 1-6: IEEE.
[78] H. N. Al-Anbagi and I. Vertat, "Noncoherent Combining of Small Satellites Signals - Proof of Concept," in *2023 3rd International Scientific Conference of Engineering Sciences (ISCES)*, Diyala, Iraq, 2023: IEEE, forthcoming 2023.
[79] H. N. Al-Anbagi and I. Vertat, "Towards Successful Integration of Small Satellites into the Terrestrial IoT Networks," in *2023 International Conference on Applied Electronics (AE)*, 2023, pp. 1-5: IEEE.
[80] H. N. Al-Anbagi and I. Vertat, "Embracing Small Satellites into Future 6G Inclusive IoT Coverage: A Deployment of Diversity-based Theoretical Framework," *IEEE Access*, vol. 11, pp. 114602-114612, 2023.

List of Student's Publications and Outputs related to the Dissertation

[A1] Al-Anbagi, H. N., & Vertat, I. (2022). Cooperative reception of multiple satellite downlinks. *Sensors*, *22*(8), 2856.

[A2] Al-Anbagi, H. N., & Vertat, I. (2022, September). Collaborative Network of Ground Stations with a Virtual Platform to Perform Diversity Combining. In *2022 International Conference on Applied Electronics (AE)* (pp. 1-6). IEEE.

[A3] Al-Anbagi, H. N., & Vertat, I. (2022, July). Pre-detection Combining of Small Satellite Downlink's Replicas. In *2022 International Conference on Electrical, Computer and Energy Technologies (ICECET)* (pp. 1-6). IEEE.

[A4] Al-Anbagi, H. N., & Vertat, I. (2023, May). Noncoherent Combining of Small Satellites Signals - Proof of Concept. Accepted for publication in *2023 3rd International Scientific Conference of Engineering Sciences (ISCES)*. IEEE.

[A5] Al-Anbagi, H. N., & Vertat, I. (2023, September). Towards Successful Integration of Small Satellites into the Terrestrial IoT Networks. In *2023 International Conference on Applied Electronics (AE)*. IEEE.

[A6] Al-Anbagi, H. N., & Vertat, I. (2023). Embracing Small Satellites into Future 6G Inclusive IoT Coverage: A Deployment of Diversity-based Theoretical Framework. *IEEE Access*, doi: 10.1109/ACCESS.2023.3324890.

Other Student's Publications and Outputs

[B1] Siahkamari, H., Jahanbakhshi, M., Al-Anbagi, H. N., Abdulhameed, A. A., Pokorny, M., & Linhart, R. (2022). Trapezoid-shaped resonators to design compact branch line coupler with harmonic suppression. *AEU-International Journal of Electronics and Communications*, *144*, 154032.

[B2] Abdulhameed, A. A., Alnahwi, F. M., Al-Anbagi, H. N., Kubík, Z., & Abdullah, A. S. (2023). Frequency reconfigurable key-shape antenna for LTE applications. *Australian Journal of Electrical and Electronics Engineering*, 1-9.

[B3] Al-Anbagi, H. N., Abdulhameed, A. A., Jasim, A. M., Jahanbakhshi, M., & Al, A. (2023). Power Efficient LNA for Satellite Communications. *Iraqi Journal for Electrical and Electronic Engineering*.

[B4] Dautov, O. S., Al-Abadi, M. S., & Al-Anbagi, H. N. (2020). New proposed spherical slotted antenna covered by the layers of dielectric material and plasma. *Journal of Electrical and Computer Engineering (IJECE), 10(2),* 1728-1735.

[B5] Salih, H. M., Al-Anbagi, H. N., & Mohammed, M. S. (2020). Design and Implementation of Investigative Committee System. *Diyala Journal of Engineering Sciences,* 84-91.

[B6] Jalalian, H., Al-Anbagi, H. N., Jahanbakhshi, M., & Abdulhameed, A. A. (2023, September). A Compact and Wideband Wilkinson Power Divider Using Lowpass Microstrip Filters. In *2023 International Conference on Applied Electronics (AE)* (pp. 1-6). IEEE.

[B7] Abdullah, A. S., Hbeeb, S. A., Al-Anbagi, H. N., & Abdulhameed, A. A. (2021, February). Power Efficient Wideband Power LNA for WSN. In *IOP Conference Series: Materials Science and Engineering* (Vol. 1076, No. 1, p. 012011). IOP Publishing.

Appendices

Appendix A: MATLAB script to simulate a reception system based on a conventional SISO structure and analze its performance versus E_b/N_o and bit rate.

Appendix B: MATLAB script to simulate a reception system based on a SIMO structure and apply the developed post-detection combining.

Appendix C: MATLAB script to simulate a reception system based on a SIMO structure and apply the developed post-detection combining along with suggested further improvement techniques.

Appendix D: MATLAB script to simulate a reception system based on a SIMO structure and apply the developed pre-detection combining.

Appendix E: MATLAB script to implement **Experiment A** to combine the best detected match of each identifier from five observations.

Appendix F: MATLAB script to implement **Experiment B** to combine all detected Sync-Words from five observations in a time manner.

Appendix G: MATLAB script to visualize the received observations in a time manner and identify the earliest and the latest ones as well as the total satellite visibility time to all GSs.

Appendix H: MATLAB script to implement **Experiments C** and **D** for combining all detected identifiers from six and nine observations, in a time manner.